Paul Langacker

The Standard Model and Beyond

Update of Section 7.7, December 17, 2014.

www.sns.ias.edu/~pgl/SMB/
www.crcpress.com/product/isbn/9781420079067/

7.7 Neutrino Mass and Mixing

Neutrinos are a unique probe of many aspects of physics, geophysics, and astrophysics on scales ranging from 10^{-33} to 10^{+28} cm. Neutrino scattering and decays involving neutrinos have been essential in establishing the Fermi theory and parity violation, determining the elements of the CKM matrix, and testing the weak neutral current predictions of the standard model, and therefore played a significant role in the precision electroweak program as described in Section 7.3.6. Deep inelastic scattering involving neutrinos and charged leptons has also been critical in establishing the existence and properties of quarks, the structure of the nucleon, and the predictions of the short distance behavior of QCD. Similarly, neutrinos are important for the physics and/or probes of the Sun, Earth, stars, core-collapse supernovae, the origins of cosmic rays, the large scale structure of the universe, big bang nucleosynthesis, and possibly baryogenesis.

Neutrinos are also interesting because their masses are so tiny and because, unlike the quarks, some of the leptonic mixing angles are large. Small neutrino masses are sensitive to new physics at scales ranging from a TeV up to the Planck scale, but because of their unusual nature there is a good chance that they are somehow connected with the latter, possibly shedding light on an underlying grand unification or superstring theory. The neutrinos are also unique in that they do not carry either color or electric charge. It is therefore possible (and many physicists think probable) that their masses are *Majorana* (lepton number violating) rather than *Dirac* (lepton number conserving, analogous to the quark and charged lepton masses). Establishing the nature of the neutrino masses, as well as understanding the origin of the small masses and large mixings, is of fundamental interest.

The original version of the $SU(2) \times U(1)$ model did not have any mechanism to generate nonzero masses at the renormalizable level. However, it is straightforward to extend the original model by the addition of $SU(2)$-singlet right-chiral neutrinos*, allowing Dirac mass terms. These could yield light Dirac neutrinos if the Yukawa couplings are extremely small, as could occur, for example, if the Yukawa couplings are forbidden at tree-level by some new symmetry. Alternatively, $SU(2)$-singlet neutrinos could lead to light Majorana neutrinos through the *seesaw* mechanism. One could also generate small Majorana masses without right-handed neutrinos via extended Higgs sectors or higher-dimension operators. Most extensions of the standard model (with the notable exception of the minimal $SU(5)$ grand unified theory) involve either $SU(2)$-singlet neutrinos or extended Higgs sectors, though they do not necessarily explain the smallness of the masses.

*Also referred to as singlet, right-handed, or sterile neutrinos.

In this Section we review the basic issues related to the neutrino masses and mixings, the major classes of models, and some of the experiments. More detailed discussions may be found in a number of books (Bahcall, 1989; Langacker, 2000; Mohapatra and Pal, 2004; Giunti and Kim, 2007; Bilenky, 2010; Xing and Zhou, 2011; Barger et al., 2012; Zuber, 2012; Valle and Romao, 2014) and review articles (Raffelt, 1999; Dolgov, 2002; Strumia and Vissani, 2006; Mohapatra et al., 2007; Gonzalez-Garcia and Maltoni, 2008; Camilleri et al., 2008; Olive et al., 2014).

7.7.1 Basic Concepts for Neutrino Mass

Active and Sterile Neutrinos

We saw in Chapter 2 that the minimal fermionic degree of freedom is a Weyl two-component field, as defined in (2.196) on page 47 and in Section 2.11. A Weyl field can be represented either in four-component notation, e.g., by $\psi_L = P_L\psi = \begin{pmatrix} \Psi_L \\ 0 \end{pmatrix}$, or in two-component notation as Ψ_L. We will use both in this section.

It is useful to first distinguish between *active* and *sterile* neutrinos. Active (a.k.a. ordinary or doublet) neutrinos are left-chiral Weyl neutrinos which transform as $SU(2)$ doublets with a charged lepton partner, and which therefore have normal weak interactions. The electron-type L doublet and its right-handed partner are

$$\ell_L \equiv \begin{pmatrix} \nu_{eL} \\ e^-_L \end{pmatrix} \xrightarrow[CP]{} \tilde{\ell}_R \equiv \begin{pmatrix} e^+_R \\ -\nu^c_{eR} \end{pmatrix}, \tag{7.326}$$

in four-component notation, where $\psi^c_R = \mathcal{C}\bar{\psi}^T_L$ is the field related by CP to ψ_L up to γ matrices and a possible CP phase, as in (2.301) on page 67 (or (2.328) in two-component notation). We have also carried out a "tilde" transformation on the $SU(2)$ doublet indices, analogous to the one for the Higgs in (7.14) on page 285, so that $\tilde{\ell}$ transforms as a 2 rather than a 2^*. We reemphasize that we define $\bar{\psi}_L \equiv (\psi_L)^\dagger \gamma^0 = (P_L\psi)^\dagger \gamma^0$, i.e., the Dirac adjoint acts on ψ_L and not on ψ.

Sterile (a.k.a. singlet or "right-handed") neutrinos, which are present in most extensions of the SM, are $SU(2)$ singlets. They do not interact except by mixing, Yukawa interactions, or beyond the SM (BSM) interactions. In four-component notation, a sterile right-chiral Weyl field will be written as ν_R and its conjugate as ν^c_L,

$$\nu_R \xrightarrow[CP]{} \nu^c_L. \tag{7.327}$$

In two-component notation, the L and R chiral fields will be written as $\mathcal{N}_L$ and $\mathcal{N}_R$, respectively, with their CP conjugates $\mathcal{N}^c_R$ and $\mathcal{N}^c_L$:

$$\mathcal{N}_L \xrightarrow[CP]{} \mathcal{N}^c_R \quad \text{(active)}, \qquad \mathcal{N}_R \xrightarrow[CP]{} \mathcal{N}^c_L \quad \text{(sterile)}. \tag{7.328}$$

Dirac Masses

A fermion mass term converts a Weyl field of one chirality into one of the opposite chirality,

$$-\mathcal{L} = m\left(\bar{\psi}_{aL}\psi_{bR} + \bar{\psi}_{bR}\psi_{aL}\right) = m\left(\Psi^{\dagger}_{aL}\Psi_{bR} + \Psi^{\dagger}_{bR}\,\Psi_{aL}\right), \tag{7.329}$$

as in (2.342) on page 74. A physical interpretation is that a massless fermion has the same helicity (chirality) in all frames of reference, while that of a massive particle depends on the reference frame and therefore can be flipped.

A *Dirac mass* connects two distinct Weyl fields, i.e., $\Psi_{bR} \neq \Psi^{c}_{aR}$. For a single type of neutrino, a Dirac mass connects an active neutrino with a sterile one[†],

$$\begin{aligned} -\mathcal{L}_D &= m_D\left(\bar{\nu}_L\nu_R + \bar{\nu}_R\nu_L\right) = m_D\bar{\nu}_D\nu_D \\ &= m_D\left(\mathcal{N}^{\dagger}_L\mathcal{N}_R + \mathcal{N}^{\dagger}_R\mathcal{N}_L\right), \end{aligned} \tag{7.330}$$

where $\nu_D = \nu_L + \nu_R$ is a Dirac field. It has four distinct components, ν_L, ν^{c}_R, ν_R and ν^{c}_L, and there is a conserved fermion number (or lepton number L in this case), corresponding to the global phase symmetry $\nu_{L,R} \to e^{i\beta}\nu_{L,R}$. This L conservation ensures that there is no mixing between ν_L and ν^{c}_L, or between ν_R and ν^{c}_R. However, when embedded in the SM context the neutrinos are chiral, so m_D violates the third component T^3_L of weak isospin by $\Delta t^3_L = \frac{1}{2}$. It can be generated by the Higgs mechanism, as described in Section 7.2.1 and illustrated in Figure 7.41, and is in principle analogous to the quark and charged lepton masses. Dirac masses can be easily generalized to three or more families. However, the tiny values of the neutrino masses require that the Higgs Yukawa couplings $h_\nu = m_\nu/\nu$ defined in (7.46) on page 295 would have to be extremely small if they are due to a simple Dirac-type Higgs coupling: $m_\nu \sim 0.1$ eV would correspond to $h_\nu \sim 10^{-12}$, for example, to be compared with the t quark coupling $h_t = \mathcal{O}(1)$ or the electron coupling $h_e \sim 10^{-5}$. Of course, we do not understand the ratio h_e/h_t either, so some caution should be taken with such statements. In any case, most particle physicists believe that either an alternative mechanism or some explanation for a small h_ν is needed, as will be discussed below.

Majorana Masses

Majorana mass terms are more economical in that they only require a single Weyl field, i.e., $\Psi_{bR} = \Psi^{c}_{aR}$ in (7.329). They are not as familiar as Dirac mass terms because they violate fermion number by two units. For the quarks

[†]There are variant forms of Dirac neutrino masses involving two distinct active or two distinct sterile neutrinos, as will be discussed below.

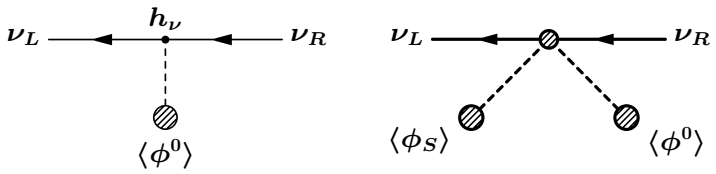

FIGURE 7.41
Mechanisms for generating a Dirac neutrino mass. Left: an elementary Yukawa coupling to the neutral Higgs doublet field ϕ^0. Right: a higher-dimensional operator leading to a suppressed Yukawa coupling.

and charged leptons such mass terms are forbidden because they would violate color and/or electric charge. However, the neutrinos do not carry any unbroken gauge quantum numbers, so Majorana masses are a possibility.

For an active neutrino, a Majorana mass term describes a transition between a left-handed neutrino and its conjugate right-handed antineutrino. In four-component language, it can be written

$$-\mathcal{L}_T = \frac{m_T}{2}\left(\bar\nu_L \nu_R^c + \bar\nu_R^c \nu_L\right) = \frac{m_T}{2}\left(\bar\nu_L \mathcal{C}\bar\nu_L^T + \nu_L^T \mathcal{C}\nu_L\right) = \frac{m_T}{2}\bar\nu_M \nu_M. \quad (7.331)$$

As is clear from the second form, $\mathcal{L}_T$ can be viewed as the annihilation or creation of two neutrinos, and therefore violates lepton number by two units, $\Delta L = 2$. In the last form in (7.331), $\nu_M \equiv \nu_L + \nu_R^c$ is a self-conjugate[‡] two-component (Majorana) field satisfying[§] $\nu_M = \nu_M^c \equiv \mathcal{C}\bar\nu_M^T$. A Majorana ν is therefore its own antiparticle and can mediate *neutrinoless double beta decay* ($\beta\beta_{0\nu}$), in which two neutrons turn into two protons and two electrons, violating lepton number by two units, as shown in Figure 7.42. A Majorana mass for an active neutrino also violates weak isospin by one unit, $\Delta t_L^3 = 1$ (hence the subscript T for triplet), and can be generated either by the VEV of a Higgs triplet or by a higher-dimensional operator involving two Higgs doublets (such as the minimal seesaw model), as in Figure 7.43. The $\frac{1}{2}$ in $\mathcal{L}_T$ is needed to yield the correct expression for the Hamiltonian. It is somewhat analogous to the extra $\frac{1}{2}$ in the free-field Lagrangian density for a Hermitian

[‡]Unlike a Hermitian scalar, a Majorana state still has two helicities, corresponding to ν_L and ν_R^c. They only mix by the Majorana mass term, so there is still an approximately conserved lepton number to the extent that m_T is small. For example, there could be a cosmological asymmetry between ν_L and ν_R^c, even for Majorana masses, if the rate for transitions between them is sufficiently slow compared to the age of the universe (Barger et al., 2003).

[§]We have taken a convention in which $\eta_\nu = 1$ for the CP phase in (2.301). More generally, $\nu_M \equiv \nu_L + \eta_\nu^* \nu_R^c = \eta_\nu^* \mathcal{C}\bar\nu_M^T$, where ν_R^c is still defined as $\mathcal{C}\bar\nu_L^T$.

scalar. This is more obvious from the kinetic energy term

$$\mathcal{L}_{KE} = \frac{1}{2}(\bar{\nu}_M i\,\partial\!\!\!/\,\nu_M) = \frac{1}{2}\left(\bar{\nu}_L i\,\partial\!\!\!/\,\nu_L + \bar{\nu}_R^c i\,\partial\!\!\!/\,\nu_R^c\right) = \bar{\nu}_L i\,\partial\!\!\!/\,\nu_L, \tag{7.332}$$

where the two terms are equal because of (2.297) on page 66. The Majorana mass term can be rewritten in two-component language using (2.326) as

$$-\mathcal{L}_T = \frac{m_T}{2}\left(\mathcal{N}_L^\dagger \mathcal{N}_R^c + \mathcal{N}_R^{c\dagger}\mathcal{N}_L\right) = \frac{m_T}{2}\left(\mathcal{N}_L^\dagger i\sigma^2 \mathcal{N}_L^* - \mathcal{N}_L^T i\sigma^2 \mathcal{N}_L\right). \tag{7.333}$$

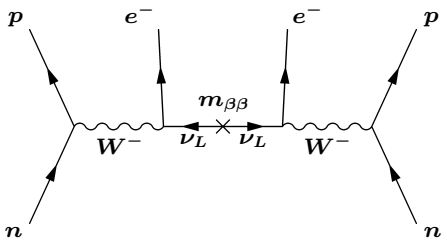

FIGURE 7.42
Diagram for neutrinoless double beta decay ($\beta\beta_{0\nu}$). For a single Majorana neutrino, $m_{\beta\beta}$ is just m_T in (7.331).

A sterile neutrino can also have a Majorana mass term of the form,

$$-\mathcal{L}_S = \frac{m_S}{2}\left(\bar{\nu}_L^c \nu_R + \bar{\nu}_R \nu_L^c\right) = \frac{m_S}{2}\left(\bar{\nu}_L^c \mathcal{C}\bar{\nu}_L^{cT} + \nu_L^{cT}\mathcal{C}\nu_L^c\right) = \frac{m_S}{2}\bar{\nu}_{M_S}\nu_{M_S}, \tag{7.334}$$

where $\nu_{M_S} \equiv \nu_L^c + \nu_R = \nu_{M_S}^c$. In this case, weak isospin is conserved, $\Delta t_L^3 = 0$, so m_S can be generated by the VEV of a Higgs singlet¶. In two-component form

$$-\mathcal{L}_S = \frac{m_S}{2}\left(\mathcal{N}_L^{c\dagger}\mathcal{N}_R + \mathcal{N}_R^\dagger \mathcal{N}_L^c\right) = \frac{m_S}{2}\left(\mathcal{N}_L^{c\dagger} i\sigma^2 \mathcal{N}_L^{c*} - \mathcal{N}_L^{cT} i\sigma^2 \mathcal{N}_L^c\right). \tag{7.335}$$

The four-component fields for Dirac and for active and sterile Majorana neutrinos can therefore be written

$$\begin{aligned} \nu_D &= \begin{pmatrix} \mathcal{N}_L \\ \mathcal{N}_R \end{pmatrix} = \begin{pmatrix} \mathcal{N}_L \\ i\sigma^2 \mathcal{N}_L^{c*} \end{pmatrix} \\ \nu_M &= \begin{pmatrix} \mathcal{N}_L \\ \mathcal{N}_R^c \end{pmatrix} = \begin{pmatrix} \mathcal{N}_L \\ i\sigma^2 \mathcal{N}_L^* \end{pmatrix}, \qquad \nu_{M_S} = \begin{pmatrix} \mathcal{N}_L^c \\ \mathcal{N}_R \end{pmatrix} = \begin{pmatrix} \mathcal{N}_L^c \\ i\sigma^2 \mathcal{N}_L^{c*} \end{pmatrix}, \end{aligned} \tag{7.336}$$

¶m_S could also be generated in principle by a bare mass, but this is usually forbidden by additional symmetries in extensions of the SM.

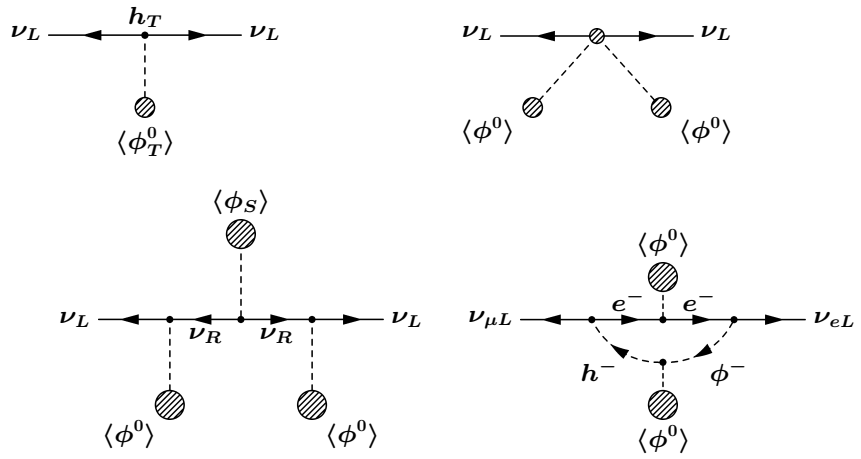

FIGURE 7.43
Mechanisms for a Majorana mass term. Top left: coupling to a neutral Higgs triplet field ϕ^0_T. Top right: a higher-dimensional operator coupling to two Higgs doublets. Botton left: the minimal seesaw mechanism (a specific implementation of the higher-dimensional operator), in which a light active neutrino mixes with a very heavy sterile Majorana neutrino. Bottom right: a loop diagram involving a charged scalar field h^-.

where two of the components are not independent in the Majorana cases.

The free-field equations of motion with a Majorana mass term obtained from the Euler-Lagrange equation (2.18) on page 10 are

$$i\,\partial\!\!\!/\nu_L - m_T\mathcal{C}\bar{\nu}_L^T = 0, \qquad i\bar{\sigma}^\mu\partial_\mu\mathcal{N}_L - m_T i\sigma^2\mathcal{N}_L^* = 0. \tag{7.337}$$

This leads to the free-field expression

$$\nu_M(x) = \int \frac{d^3\vec{p}}{(2\pi)^3 2E_p} \sum_{s=+,-} \left[u(\vec{p},s)\; a(\vec{p},s)e^{-ip\cdot x} + v(\vec{p},s)a^\dagger(\vec{p},s)e^{+ip\cdot x}\right], \tag{7.338}$$

which is of the same form as the free Dirac field in (2.155) on page 40 except that there is no distinction between a and b operators. Any spin basis can be used, but the helicity basis is usually most convenient.

A more compact notation for dealing with Majorana masses and fields will be developed in Section 8.2.2.

A Comment on Phases

We implicitly assumed that the masses m_D and m_T in (7.330) and (7.331) are real and positive. More generally, however, they can be negative or complex,

but can be made real and positive by field redefinitions. In the Dirac case for an arbitrary ψ, one has generally

$$-\mathcal{L}_D = m_D \bar{\psi}_L \psi_R + m_D^* \bar{\psi}_R \psi_L = m_D \Psi_L^\dagger \Psi_R + m_D^* \Psi_R^\dagger \Psi_L. \tag{7.339}$$

There is freedom to redefine both ψ_L and ψ_R by separate phase transformations to remove any phase in m_D and make it positive (see Section 3.3.5 and Problem 3.28). In the SM, only the WCC interactions depend on the phases of the left-chiral fermion fields, and no SM interaction involves the right chiral phases. It is therefore convenient to choose the phases of the L-chiral mass eigenstates (ψ_L in the simple example in (7.339)) by any convenient convention, and then adjust the ψ_R fields to make the mass eigenvalues real and positive. This was done in Section 7.2.2 to remove unobservable phases from the CKM matrix, and a similar procedure can be applied to the lepton mixing if there are only Dirac masses.

However, for a general Majorana mass term,

$$-\mathcal{L}_M = \frac{1}{2}\left(m_M \bar{\psi}_L \mathcal{C} \bar{\psi}_L^T + m_M^* \psi_L^T \mathcal{C} \psi_L\right) = \frac{1}{2}\left(m_M \Psi_L^\dagger i\sigma^2 \Psi_L^* - m_M^* \Psi_L^T i\sigma^2 \Psi_L\right), \tag{7.340}$$

there is only one independent field ψ_L (or Ψ_L). One usually chooses to use the phase freedom in ψ_L to make m_M real and positive, in which case there is no remaining freedom. This will imply the existence of additional *Majorana phases* in the leptonic mixing matrix V_ℓ for the WCC for the case of Majorana neutrino masses. However, such phases are only observable in processes such as $\beta\beta_{0\nu}$ which involve the phases of the neutrino masses explicitly, as can be seen by working in an alternative convention of a simple V_ℓ but leaving m_M complex.

Even after a phase redefinition we will define the conjugate fields by the same convention as for the original ones. That is, for

$$\nu_L' \equiv e^{i\beta}\nu_L, \qquad \mathcal{N}_L' = e^{i\beta}\mathcal{N}_L, \tag{7.341}$$

we define

$$\nu_R^{c\prime} \equiv \mathcal{C}\bar{\nu}_L'^T, \qquad \mathcal{N}_R^{c\prime} = i\sigma^2 \mathcal{N}_L'^*. \tag{7.342}$$

Mixed Models

When active and sterile neutrinos are both present, there can be Dirac and Majorana mass terms simultaneously. For one family, the Lagrangian density has the form

$$-\mathcal{L} = \frac{1}{2}\begin{pmatrix} \bar{\nu}_L^0 & \bar{\nu}_L^{0c} \end{pmatrix} \begin{pmatrix} m_T & m_D \\ m_D & m_S \end{pmatrix} \begin{pmatrix} \nu_R^{0c} \\ \nu_R^0 \end{pmatrix} + h.c., \tag{7.343}$$

where 0 refers to weak eigenstates, and the masses are

$$\begin{aligned} m_T: &\quad |\Delta L| = 2, &\quad \Delta t_L^3 = 1 &\quad \text{(Majorana)} \\ m_D: &\quad |\Delta L| = 0, &\quad \Delta t_L^3 = \frac{1}{2} &\quad \text{(Dirac)} \\ m_S: &\quad |\Delta L| = 2, &\quad \Delta t_L^3 = 0 &\quad \text{(Majorana).} \end{aligned} \tag{7.344}$$

The two terms involving m_D are equal since

$$\begin{aligned} \bar\psi^c_{aL}\psi^c_{bR} &= \bar\psi_{bL}\psi_{aR}, \qquad \bar\psi^c_{aR}\psi^c_{bL} = \bar\psi_{bR}\psi_{aL} \\ \bar\psi_{aL}\psi^c_{bR} &= \bar\psi_{bL}\psi^c_{aR}, \qquad \bar\psi^c_{aL}\psi_{bR} = \bar\psi^c_{bL}\psi_{aR} \end{aligned} \tag{7.345}$$

for arbitrary $\psi_{a,b}$ by (2.291) on page 65. Diagonalizing the matrix in (7.343) yields two Majorana mass eigenvalues m_i and two Majorana mass eigenstates[‖], $\nu_{iM} = \nu_{iL} + \nu^c_{iR} = \nu^c_{iM}$, with $i = 1, 2$. The weak and mass bases are related by the unitary transformations

$$\begin{pmatrix} \nu_{1L} \\ \nu_{2L} \end{pmatrix} = A_L^{\nu\dagger} \begin{pmatrix} \nu^0_L \\ \nu^{0c}_L \end{pmatrix}, \qquad \begin{pmatrix} \nu^c_{1R} \\ \nu^c_{2R} \end{pmatrix} = A_R^{\nu\dagger} \begin{pmatrix} \nu^{0c}_R \\ \nu^0_R \end{pmatrix}, \tag{7.346}$$

similar to (7.47) on page 295. A_L and A_R are generally different for Dirac mass matrices, which need not be Hermitian. However, the general 2×2 neutrino mass matrix in (7.343) on page 410 is symmetric because of (7.345). This implies that $A^\nu_L = A^{\nu*}_R K$, where K is a diagonal matrix of phases analogous to (7.52) on page 296. (There is additional freedom in K in the presence of degeneracies.) K is in general arbitrary, but our phase convention, in which $\nu^c_{iR} = \mathcal{C}\bar\nu^T_{iL}$, implies $K = I$.

There are several important special cases of the mixed model in (7.343)

(a) Majorana: $m_D = 0$ is the pure Majorana case: the mass matrix is diagonal, with $m_1 = m_T$, $m_2 = m_S$, and

$$\begin{aligned} \nu_{1L} &= \nu^0_L, \qquad \nu^c_{1R} = \nu^{0c}_R \\ \nu_{2L} &= \nu^{0c}_L, \qquad \nu^c_{2R} = \nu^0_R. \end{aligned} \tag{7.347}$$

(b) Dirac: The Dirac limit is $m_T = m_S = 0$. There are formally two Majorana mass eigenstates, with eigenvalues $m_1 = m_D$ and $m_2 = -m_D$ and eigenstates

[‖]For Majorana masses, and especially in mixed models, there is no conserved lepton number, and it is just a matter of definition to refer to the L states as particles, ν_{iL}, and the R states as antiparticles, ν^c_{iR}. Unfortunately, this becomes awkward in the Dirac limit where the Weyl states ν_R and ν^c_R are labelled as particle and antiparticle because they carry lepton number $+1$ and -1, respectively. There is no notation known to the author that is not awkward in some circumstances.

$$\begin{aligned} \nu_{1L} &= \frac{1}{\sqrt{2}}(\nu_L^0 + \nu_L^{0c}), \qquad \nu_{1R}^c = \frac{1}{\sqrt{2}}(\nu_R^{0c} + \nu_R^0) \\ \nu_{2L} &= \frac{1}{\sqrt{2}}(\nu_L^0 - \nu_L^{0c}), \qquad \nu_{2R}^c = \frac{1}{\sqrt{2}}(\nu_R^{0c} - \nu_R^0). \end{aligned} \tag{7.348}$$

Note that $\nu_{1,2}$ are degenerate in the sense that $|m_1| = |m_2|$, but the actual eigenvalues have opposite sign. To recover the Dirac limit, we will depart from our usual procedure of redefining the phase of ν_2 to make m_2 positive. Rather, let us expand the mass term

$$-\mathcal{L} = \frac{m_D}{2}(\bar{\nu}_{1L}\nu_{1R}^c - \bar{\nu}_{2L}\nu_{2R}^c) + h.c. = m_D(\bar{\nu}_L^0\nu_R^0 + \bar{\nu}_R^0\nu_L^0), \tag{7.349}$$

which clearly conserves lepton number (i.e., there is no $\nu_L^0 - \nu_L^{0c}$ or $\nu_R^{0c} - \nu_R^0$ mixing). Thus, a Dirac neutrino can be thought of as two Majorana neutrinos, with maximal (45°) mixing and with equal and opposite masses. This interpretation is useful in considering the Dirac limit of general models.

(c) Seesaw: The limit $m_S \gg m_{D,T}$ (e.g., $m_T = 0$, $m_D = \mathcal{O}(m_u, m_e, m_d)$, and $m_S = \mathcal{O}(M_X)$, where $M_X \sim 10^{14}$ GeV) is known as the *seesaw* (or *minimal seesaw*) (Minkowski, 1977; Gell-Mann et al., 1979; Yanagida, 1979; Schechter and Valle, 1980). The eigenstates and eigenvalues in the seesaw limit are

$$\begin{aligned} \nu_{1L} &\sim \nu_L^0 - \frac{m_D}{m_S}\nu_L^{0c} \sim \nu_L^0, \qquad m_1 \sim m_T - \frac{m_D^2}{m_S} \\ \nu_{2L} &\sim \frac{m_D}{m_S}\nu_L^0 + \nu_L^{0c} \sim \nu_L^{0c}, \qquad m_2 \sim m_S, \end{aligned} \tag{7.350}$$

with $|m_1| \ll m_D$ for $m_T = 0$. At energies low compared to m_S the ν_2 decouples and one obtains an effective theory involving a single active Majorana $\nu_{1M} \sim \nu_L^0 + \nu_R^{0c}$. The minimal seesaw mechanism is illustrated in Figure 7.43.

(d) Pseudo-Dirac: this is a perturbation on the Dirac case, with m_T, $m_S \ll m_D$. There is a small lepton number violation, and a small splitting between the magnitudes of the mass eigenvalues. As an example, $m_T = \epsilon$, $m_S = 0$ leads to $|m_{1,2}| = m_D \pm \epsilon/2$. The pseudo-Dirac case is also sometimes encountered for the variant Dirac forms involving two active or two sterile neutrinos.

(e) Mixing: The general case in which m_D and m_S (and/or m_T) are both small and comparable leads to non-degenerate Majorana mass eigenvalues and significant ordinary-sterile ($\nu_L^0 - \nu_L^{0c}$) mixing, such as were suggested by the LSND and some subsequent results to be described below. Only this and the pseudo-Dirac cases allow such mixings.

Extension to Two or More Families

These considerations can be generalized to two or more families, or even to the case of different numbers of active and sterile neutrinos. For $F = 3$ families, define the three-component weak eigenstate vectors

$$\nu_L^0 = \begin{pmatrix} \nu_{1L}^0 \\ \nu_{2L}^0 \\ \nu_{3L}^0 \end{pmatrix}, \ \nu_L^{0c} = \begin{pmatrix} \nu_{1L}^{0c} \\ \nu_{2L}^{0c} \\ \nu_{3L}^{0c} \end{pmatrix}, \tag{7.351}$$

and similarly for ν_R^{0c}, ν_R^0 and the two-component fields. In the Dirac case, (7.330) generalizes to

$$-\mathcal{L}_D = \left(\bar{\nu}_L^0 M_D \nu_R^0 + \bar{\nu}_R^0 M_D^\dagger \nu_L^0\right) = \left(\mathcal{N}_L^{0\dagger} M_D \mathcal{N}_R^0 + \mathcal{N}_R^{0\dagger} M_D^\dagger \mathcal{N}_L^0\right), \tag{7.352}$$

where M_D is a completely arbitrary 3×3 matrix. M_D can be diagonalized by separate left and right unitary matrices $A_{L,R}^\nu$, just as in (7.47) on page 295,

$$A_L^{\nu\dagger} M_D A_R^\nu = (M_D)_D = \begin{pmatrix} m_1 & 0 & 0 \\ 0 & m_2 & 0 \\ 0 & 0 & m_3 \end{pmatrix}, \tag{7.353}$$

with mass eigenstate fields

$$\nu_L = A_L^{\nu\dagger} \nu_L^0, \qquad \nu_R = A_R^{\nu\dagger} \nu_R^0. \tag{7.354}$$

The leptonic part of the weak charge raising current is then

$$J_W^{\ell\mu\dagger} = 2\bar{\nu}_L \gamma^\mu V_\ell e_L, \tag{7.355}$$

where

$$V_\ell = A_L^{\nu\dagger} A_L^e, \tag{7.356}$$

is the leptonic mixing matrix, analogous to the quark mixing matrix V_q in (7.61). $\mathcal{V} \equiv V_\ell^\dagger$ is also know as the PMNS matrix, after Maki, Nakagawa, and Sakata (Maki et al., 1962) and Pontecorvo (Pontecorvo, 1968). The counting of angles and phases in V_ℓ is the same as for the CKM matrix (see Eq. 7.62). One can choose the arbitrary phases in A_L^ν (i.e., the K_L^ν matrix analogous to (7.51)) to remove unobservable phases from V_ℓ (leaving 3 angles and one phase for $F = 3$), and then choose those in A_R^ν (i.e., K_R^ν) to make the mass eigenvalues real and nonnegative.

For $F_A = 3$ active and $F_S > 3$ sterile neutrinos (and only Dirac masses), three linear combinations of the sterile fields will join with the active ones to form three massive Dirac fields, leaving $F_S - 3$ massless Weyl fields. The reverse situation occurs for $F_S < F_A$.

In the Majorana case the triplet mass term (7.331) generalizes to

$$-\mathcal{L}_T = \frac{1}{2}\left(\bar{\nu}_L^0 M_T \nu_R^{0c} + \bar{\nu}_R^{0c} M_T^\dagger \nu_L^0\right) = \frac{1}{2}\left(\bar{\nu}_L^0 M_T \mathcal{C}\bar{\nu}_L^{0T} + \nu_L^{0T} \mathcal{C} M_T^\dagger \nu_L^0\right), \tag{7.357}$$

where M_T is symmetric, $M_T = M_T^T$, by (7.345). This symmetric property holds for all Majorana mass matrices. The corresponding two-component expression is

$$-\mathcal{L}_T = \frac{1}{2}\left(\mathcal{N}_L^{0\dagger} M_T i\sigma^2 \mathcal{N}_L^{0*} - \mathcal{N}_L^{0T} i\sigma^2 M_T^\dagger \mathcal{N}_L^0\right). \tag{7.358}$$

Since M_T is symmetric, it can be diagonalized by a transformation analogous to (7.353), but with $A_L^\nu = A_R^{\nu *} K$, where as usual K is an undetermined diagonal phase matrix in the absence of degeneracies. We will choose $K = I$ in order to maintain $\nu_{iR}^c = \mathcal{C}\bar{\nu}_{iL}^T$ for the eigenstates (cf (7.342)). In that case, the phases in A_L^ν are uniquely determined by the requirement that the mass eigenvalues m_i are real and positive**. Consequently, there is less freedom to remove phases from V_ℓ than in the Dirac case (or in the CKM matrix). The counting in (7.62) is modified in that one can only remove the F phases associated with the charged lepton fields from the F^2 parameters in a general unitary $F \times F$ matrix, so that there are $F(F-1)/2$ mixing angles and $F(F-1)/2$ observable CP-violating phases. The upshot is that V_ℓ can be written

$$V_\ell = K_M^\nu \hat{V}_\ell, \tag{7.359}$$

where $\hat{V}_\ell$ involves $\frac{1}{2}(F-1)(F-2)$ phases analogous to those in the CKM matrix, such as the single phase for $F = 3$ displayed in (7.211) on page 373. K_M^ν is a diagonal matrix of Majorana phases. Only the $F-1$ phase differences are observable, so one often takes it to be of the form $K_M^\nu = \mathrm{diag}(e^{-i\alpha_1}, \cdots, e^{-i\alpha_{F-1}}, 1)$. Since the Majorana phases only multiply the mass eigenstate fields, they do not enter any amplitude involving only external neutrinos or those involving an ordinary (lepton-number conserving) internal neutrino line. They do affect amplitudes involving lepton number violation, such as the $\beta\beta_{0\nu}$ amplitude in Figure 7.42.

To summarize, for $F = 3$ families, the adjoint of the leptonic mixing matrix can be parametrized by

$$V_\ell^\dagger = \begin{pmatrix} 1 & 0 & 0 \\ 0 & c_{23} & s_{23} \\ 0 & -s_{23} & c_{23} \end{pmatrix} \begin{pmatrix} c_{13} & 0 & s_{13}e^{-i\delta} \\ 0 & 1 & 0 \\ -s_{13}e^{i\delta} & 0 & c_{13} \end{pmatrix} \begin{pmatrix} c_{12} & s_{12} & 0 \\ -s_{12} & c_{12} & 0 \\ 0 & 0 & 1 \end{pmatrix} \begin{pmatrix} e^{i\alpha_1} & 0 & 0 \\ 0 & e^{i\alpha_2} & 0 \\ 0 & 0 & 1 \end{pmatrix}, \tag{7.360}$$

where $c_{ij} \equiv \cos\theta_{ij}$ and $s_{ij} \equiv \sin\theta_{ij}$ and δ are leptonic mixing angles and a CP-violating phase similar to (but numerically different from) the angles in the CKM matrix in (7.211), and $\alpha_{1,2}$ are Majorana phases. The same form holds for Dirac masses, except the last factor becomes the identity. Note that we are following the conventions in (Olive et al., 2014), and that (7.211) refers to V_q while (7.360) refers to $V_\ell^\dagger$. To conform to standard notations, we will also define the mixing matrix

$$\mathcal{V} \equiv V_\ell^\dagger. \tag{7.361}$$

**The phase would be undetermined but unobservable for a zero eigenvalue.

It is often convenient to choose a basis for the lepton doublets in which the charged lepton mass matrix is already diagonalized, i.e., $A_L^e = I$. Then, $\mathcal{V} = A_L^\nu$.

In the general multi-family case, with both Dirac and Majorana masses,

$$-\mathcal{L} = \frac{1}{2} \left(\bar{\nu}_L^0 \ \bar{\nu}_L^{0c} \right) \begin{pmatrix} M_T & M_D \\ M_D^T & M_S \end{pmatrix} \begin{pmatrix} \nu_R^{0c} \\ \nu_R^0 \end{pmatrix} + h.c., \tag{7.362}$$

where $M_T = M_T^T$ and $M_S = M_S^T$. For $F = 3$ there are six Majorana mass eigenvalues and eigenvectors. The transformation to the mass eigenstate basis is

$$\nu_L = \mathcal{A}_L^{\nu\dagger} \begin{pmatrix} \nu_L^0 \\ \nu_L^{0c} \end{pmatrix}, \tag{7.363}$$

where $\mathcal{A}_L^\nu$ is a 6×6 unitary matrix and ν_L is a six-component vector. The analogous transformation for the R fields involves $\mathcal{A}_R^\nu = \mathcal{A}_L^{\nu *} \mathcal{K}$ because the 6×6 Majorana mass matrix is symmetric. Our phase convention $\nu_R^c = \mathcal{C} \bar{\nu}_L^T$ again implies the choice $\mathcal{K} = I$.

Analogous to (7.350), the seesaw limit of (7.362) occurs when the three eigenvalues of M_S are all large compared to the elements of M_D and M_T (the latter is usually assumed to be zero). Then, one has

$$\mathcal{A}_L^{\nu\dagger} = \mathcal{A}_R^{\nu T} = \begin{pmatrix} A_L^{\nu\dagger} & 0 \\ 0 & A_L^{\nu_S\dagger} \end{pmatrix} B_L^{\nu\dagger}, \tag{7.364}$$

where A_L^ν and $A_L^{\nu_S}$ are 3×3 unitary matrices, I and 0 are respectively the 3×3 identity and zero matrices, and

$$B_L^{\nu\dagger} \sim \begin{pmatrix} I & -M_D M_S^{-1} \\ M_S^{-1\dagger} M_D^\dagger & I \end{pmatrix}. \tag{7.365}$$

One finds

$$B_L^{\nu\dagger} \begin{pmatrix} M_T & M_D \\ M_D^T & M_S \end{pmatrix} B_L^{\nu *} \sim \begin{pmatrix} M_T - M_D M_S^{-1} M_D^T & 0 \\ 0 & M_S \end{pmatrix}. \tag{7.366}$$

That is, there are three light (approximately) active neutrinos with an effective Majorana mass matrix $M_T - M_D M_S^{-1} M_D^T$, diagonalized by $A_L^\nu = A_R^{\nu *}$. There are also three heavy (approximately) sterile neutrinos with mass matrix M_S, which is diagonalized by $A_L^{\nu_S} = A_R^{\nu_S *}$. The latter decouple at energies small compared with their masses.

In the more general case in which one or more of the eigenvalues of M_S are not large, some or all of the light states will include non-negligible sterile components. In particular, the active and sterile neutrinos of the same chirality will mix significantly (as was suggested by the LSND and some other experiments) if both Majorana and Dirac masses are of the same order of magnitude or in the pseudo-Dirac case. Constructing models with these features presents

a special challenge compared to the Dirac, Majorana, and seesaw cases because one must find an explanation as to why two different types of mass terms are small. If all three sterile states remain light, the leptonic mixing matrix in the charge raising current in (7.355) becomes 6×3 dimensional, i.e.,

$$V_\ell = A_L^{\nu\dagger} P_A^\dagger A_L^e, \tag{7.367}$$

where $A_L^{\nu\dagger}$ is the 6×6 neutrino mixing matrix and $P_A = (I\ 0)$ is the 3×6 dimensional matrix that projects onto the active neutrino subspace. One can easily generalize to the case of $F_A = 3$ active neutrinos and F_S sterile neutrinos, in which case there are $3 + F_S$ Majorana mass eigenvalues and P_A becomes a $3 \times (3 + F_S)$ dimensional projection.

Our original definition of a Dirac mass term as one which couples two distinct Weyl fields and a Majorana mass as one which couples a Weyl field to itself is not very useful in the multi-family case. In the above discussion we implicitly referred to couplings between active and sterile neutrinos as Dirac, and active-active or sterile-sterile couplings as Majorana. However, an alternate definition, which we will now adopt, is to define Majorana or Dirac masses on the basis of the form of the mass eigenvalues and eigenvectors. One can then view Majorana mass terms as the generic case, and reserve the term Dirac for special or limiting cases in which there is a conserved lepton number. We already saw an example of the Dirac limit of the one family mixed model, which trivially generalizes to the F family case when $M_T = M_S = 0, M_D \neq 0$.

A less obvious example involves the two family Majorana mass matrix

$$M_T = \begin{pmatrix} 0 & m_{ZKM} \\ m_{ZKM} & 0 \end{pmatrix}. \tag{7.368}$$

This has the same form as the Dirac limit of (7.343), except that in this case the L and R components are both active. Let us be even more explicit, and assume that (7.368) holds in the basis in which the charged leptons (e and μ) are already diagonal. Then we can identify $\nu_{1L}^0 = \nu_{eL}$, $\nu_{1R}^{0c} = \nu_{eR}^c$, $\nu_{2L}^0 = \nu_{\mu L}$, and $\nu_{2R}^{0c} = \nu_{\mu R}^c$, so that

$$\begin{aligned} -\mathcal{L}_T &= \frac{m_{ZKM}}{2} \left(\bar{\nu}_{eL} \nu_{\mu R}^c + \bar{\nu}_{\mu L} \nu_{eR}^c + \bar{\nu}_{\mu R}^c \nu_{eL} + \bar{\nu}_{eR}^c \nu_{\mu L} \right) \\ &= m_{ZKM} \left(\bar{\nu}_{eL} + \bar{\nu}_{\mu R}^c \right) \left(\nu_{eL} + \nu_{\mu R}^c \right). \end{aligned} \tag{7.369}$$

This *Zeldovich-Konopinski-Mahmoud* model (Zeldovich, 1952; Konopinski and Mahmoud, 1953) involves a Dirac neutrino, in that there is a conserved quantum number ($L_e - L_\mu$, rather than $L = L_e + L_\mu$) and because two distinct Weyl neutrinos are involved. However, in many ways it is more closely related to the Majorana case, i.e., it violates weak isospin by one unit and is a limiting case of the general 2×2 Majorana matrix. Any perturbation involving nonzero diagonal elements of M_T would break the "degeneracy" $m_1 = -m_2$

of the two eigenvalues. A modern $F = 3$ version of the ZKM model involves the matrix

$$M_T = m_{ZKM} \begin{pmatrix} 0 & 1 & 1 \\ 1 & 0 & 0 \\ 1 & 0 & 0 \end{pmatrix}, \tag{7.370}$$

which leads to one massive Dirac neutrino $\nu_{eL} + \frac{1}{\sqrt{2}}(\nu^c_{\mu R} + \nu^c_{\tau R})$, and one massless Weyl neutrino $\frac{1}{\sqrt{2}}(\nu_{\mu L} - \nu_{\tau L})$, with $L_e - L_\mu - L_\tau$ conserved. This actually yields a spectrum somewhat similar to the observed one, but would require nontrivial perturbations both in M_T and the charged lepton mixing to be fully realistic. An example of a perturbation on M_T leading to a generalization of the pseudo-Dirac case is considered in Problem 7.21.

An analogous situation sometimes occurs (especially in complicated models in which $F_S > F_A$) when two sterile neutrinos pair to form a Dirac neutrino, e.g., with M_S of a form analogous to (7.368).

Let us conclude this section by reemphasizing that there is no distinction between Dirac and Majorana neutrinos except by their masses (or by new BSM interactions). As the masses go to zero, the active components reduce to standard active Weyl neutrinos in both cases. There are additional sterile Weyl neutrinos in the massless limit of the Dirac case, but these decouple from the other particles. We also repeat the comment from Section 7.2.2 that one can ignore V_ℓ in processes for which the neutrino masses are too small to be relevant. They are then effectively degenerate (with vanishing mass) and one can work in the weak basis.

7.7.2 The Propagators for Majorana Fermions

For free Dirac fields there is a conserved fermion number and therefore only a single type of propagator, given in (2.178) on page 44. For Majorana neutrinos, on the other hand, there is no conserved fermion number and there are three non-zero propagators,

$$\begin{aligned} \langle 0|\mathcal{T}[\nu_M(x), \bar{\nu}_M(x')]|0\rangle &= i \int \frac{d^4k}{(2\pi)^4} e^{-ik\cdot(x-x')} S_F(k) \\ \langle 0|\mathcal{T}[\bar{\nu}_M(x), \bar{\nu}_M(x')]|0\rangle &= i \int \frac{d^4k}{(2\pi)^4} e^{-ik\cdot(x-x')} \mathcal{C}^\dagger S_F(k) \\ \langle 0|\mathcal{T}[\nu_M(x), \nu_M(x')]|0\rangle &= i \int \frac{d^4k}{(2\pi)^4} e^{-ik\cdot(x-x')} S_F(k)(-\mathcal{C}), \end{aligned} \tag{7.371}$$

where $S_F(k)$ is the usual $\frac{\not{k}+m}{k^2-m^2+i\epsilon}$. The first Majorana propagator is analogous to the Dirac case, while the second and third can be thought of as annihilating or creating two neutrinos, respectively. They can easily be de-

rived from

$$\begin{aligned}\sum_s u(\vec{p},s)\ v(\vec{p},s)^T &= (\not{p}+m)\,(-\mathcal{C})\\ \sum_s \bar{u}(\vec{p},s)^T\ \bar{v}(\vec{p},s) &= \mathcal{C}^\dagger\,(\not{p}-m)\end{aligned} \tag{7.372}$$

and two similar identities with $u \leftrightarrow v$ and $m \to -m$, which in turn follow immediately from (2.173), (2.285), and (2.286). Similar expressions apply to the Majorana fields which occur in supersymmetry.

Expressions for amplitudes involving the second and third terms in (7.371) take an unusual form, but they can usually be rendered more familiar by use of (2.285) and (2.286) on page 65, or by the use of (2.291) along with $\nu_M = \nu_M^c$. As a simple example, consider the process $W^-W^- \to e^-e^-$, assuming that the ν_e is Majorana and ignoring all family mixing effects. This proceeds via the diagrams in Figure 7.44, which form a critical part of those for $\beta\beta_{0\nu}$ in Figure 7.42. The relevant WCC interaction is

$$\mathcal{L} = -\frac{g}{2\sqrt{2}} J_W^\mu W_\mu^-, \tag{7.373}$$

where

$$J_W^\mu = \bar{e}\gamma^\mu(1-\gamma^5)\nu_L = \bar{e}\gamma^\mu(1-\gamma^5)\nu_M, \tag{7.374}$$

since $P_L\nu_R^c = 0$. The amplitude from the t-channel diagram is therefore

$$M_t = \left(\frac{-ig}{2\sqrt{2}}\right)^2 \epsilon_{1\mu}\epsilon_{2\nu}\left[\bar{u}_3\gamma^\mu(1-\gamma^5)\right]_\alpha\left[\bar{u}_4\gamma^\nu(1-\gamma^5)\right]_\beta\left[i\frac{\not{k}+m_T}{k^2}(-\mathcal{C})\right]_{\alpha\beta}, \tag{7.375}$$

where $k = p_3 - p_1$, m_T is the Majorana neutrino mass, the propagator follows from the last expression in (7.371), and we have assumed $|k^2| \gg m_T^2$. This expression can be simplified using (2.284), (2.286), and (2.287),

$$\left[\bar{u}_4\gamma^\nu(1-\gamma^5)\right]_\beta(-\mathcal{C})_{\delta\beta} = -\left[(1-\gamma^5)\gamma^\nu v_4\right]_\delta, \tag{7.376}$$

so that

$$M_t = \left(\frac{-ig}{2\sqrt{2}}\right)^2 \epsilon_{1\mu}\epsilon_{2\nu}\left(\frac{-2im_T}{k^2}\right)\bar{u}_3\gamma^\mu(1-\gamma^5)\gamma^\nu v_4, \tag{7.377}$$

which can be evaluated in the usual way. Note that the $\bar{u}_4$ spinor has been replaced by v_4. The $\not{k}$ part of the propagator has dropped out because of the pure $V-A$ interaction, but would be allowed if there were an admixture of $V+A$. The same result can be obtained more directly by rewriting

$$J_W^\nu = \bar{e}\gamma^\nu(1-\gamma^5)\nu_M = -\bar{\nu}_M\gamma^\nu(1+\gamma^5)e^c \tag{7.378}$$

obtained from (2.291) for *one* of the vertices. Then, the first propagator in (7.371) is the relevant one, and we must use a v spinor for e_4^- since e^c is the positron field.

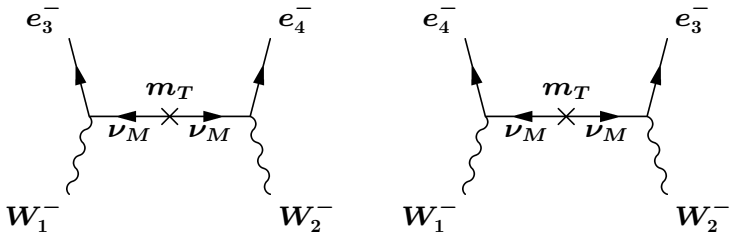

FIGURE 7.44
Diagrams for $W^-W^- \to e^-e^-$ assuming a Majorana neutrino. Left: t-channel. Right: u-channel. The cross represents a Majorana mass insertion.

7.7.3 Experiments and Observations

In this section we describe the principal laboratory and astrophysical constraints on the number of light active and sterile neutrinos, and their masses and mixings. The constraints on possible heavy Dirac or Majorana neutrinos and on neutrino decays[††] are reviewed in (Kolb and Turner, 1990; Cvetič and Langacker, 1991; Raffelt, 1999; Mohapatra and Pal, 2004; Atre et al., 2009; Olive et al., 2014; Giunti and Studenikin, 2014; Faessler et al., 2014).

Neutrino Counting

As discussed below (7.169) on page 346, the width for Z to decay invisibly implies that there are only 3 active neutrinos with masses $\lesssim M_Z/2$. More precisely, $N_\nu^{inv} = 2.990 \pm 0.007$ from the global fit to precision data[‡‡] (Olive et al., 2014), where N_ν^{inv} does not include sterile neutrinos or very heavy active neutrinos, but does include the effects of other possible invisible decay channels asssociated with new physics. Precision constraints also exclude additional heavy active neutrinos if they belong to a complete degenerate chiral family, but may be evaded, e.g., for non-chiral doublets or nondegenerate families.

Another major constraint comes from *big bang nucleosynthesis* (BBN) (e.g., Kolb and Turner, 1990; Dolgov, 2002; Steigman, 2012; Lesgourgues et al., 2013; Olive et al., 2014), which has also been a critical test of hot big bang

[††] *Radiative decays*, such as $\nu_2 \to e^+e^-\nu_1$, if kinematically allowed, or $\nu_2 \to \nu_1\gamma$, are possible in the SM. The latter is loop suppressed and extremely slow. BSM physics could allow faster $\nu_2 \to \nu_1\gamma$ or invisible decays, such as $\nu_2 \to \nu_1\nu_1\bar{\nu}_1$, $\nu_2 \to \nu_1 F$, or $\nu_2 \to \bar{\nu}_1 M$, where F is a *familon* (a Goldstone boson associated with a hypothetical broken family symmetry), and M is a *Majoron* (a Goldstone boson associated with a spontaneously broken lepton number).

[‡‡] There is also a more direct determination of the invisible width from $e^-e^+ \to \gamma +$ invisible, yielding $N_\nu^{inv} = 2.92 \pm 0.05$.

cosmology and of many possible types of nonstandard particle physics. The basic point is that the reactions

$$n + \nu_e \leftrightarrow p + e^-, \qquad n + e^+ \leftrightarrow p + \bar{\nu}_e \tag{7.379}$$

kept the ratio of neutrons to protons in thermal equilibrium $\frac{n}{p} = \exp(-\frac{E_n - E_p}{T})$ $\sim \exp(-\frac{m_n - m_p}{T})$ in the early universe as long as the reaction rate $\Gamma \sim G_F^2 T^5$ was larger than the expansion rate (Hubble parameter) $H \sim 1.66\sqrt{g_*}\, T^2/M_P$, where M_P is the Planck mass. H^2 is proportional to the energy density $\rho = g_* \pi^2 T^4/30$, where $g_* \equiv g_B + \frac{7}{8} g_F$ and $g_{B,F}$ are the number of relativistic bosonic and fermionic degrees of freedom in equilibrium at temperature T. The equilibrium was maintained until the freezeout temperature $T_f \sim (\sqrt{g_*}/G_F^2 M_P)^{1/3} = \mathcal{O}(\text{few MeV})$ when $\Gamma \sim H$, at which time the n/p ratio was frozen at the value $\exp(-\frac{m_n - m_p}{T_f})$ except for neutron decay, and most of the neutrons were eventually incorporated into ^4He. By apparent coincidence T_f is close to $m_n - m_p$, so the expected abundance depends sensitively on g_*. In the SM, one expects $g_* = 43/4$ for $m_e < T < m_\mu$ ($g_B = 2$ from two photon helicities and $g_F = 10$ from $3(\nu_L + \nu_R^c)$ + two helicities each of $e^\pm$). This leads to the prediction that the ratio of primordial ^4He to H by mass should be ∼24%, in agreement with observations*. However, any additional contribution to the energy density for $T \gtrsim$ few MeV would increase H and T_f, and therefore the predicted helium abundance. This can be parametrized by writing

$$g_F = 4 + 2N_\nu^{BBN} \tag{7.380}$$

where any deviation of the effective N_ν^{BBN} from 3.046† could indicate new light degrees of freedom in (partial) equilibrium, or such effects as neutrino masses of $\mathcal{O}$(MeV) or neutrino decay. There has long been some uncertainty and controversy in the observational primordial abundance, and therefore the limits on N_ν^{BBN}. Recent estimates include $1.8 < N_\nu^{BBN} < 4.5$ at 95% c.l. (Olive et al., 2014) and $N_\nu^{BBN} = 3.7 \pm 0.5$ (Steigman, 2012). $\Delta N_\nu^{BBN} \equiv N_\nu^{BBN} - 3.046$ constrains not only additional active neutrinos with masses $\lesssim 1$ MeV, but also light sterile neutrinos of the type suggested by the LSND experiment, which could be produced by mixing‡ with active neutrinos for a wide range of parameters (e.g., Dolgov, 2002; Cirelli et al., 2005; Lesgourgues and Pastor, 2012). However, ΔN_ν^{BBN} does *not* include the sterile ν_R components of light Dirac neutrinos, which could not (for the currently relevant mass ranges) have been produced in equilibrium numbers

*There is also a weak dependence on the baryon density relative to photons, which is determined independently by the D abundance and by the cosmic microwave background anisotropies (Steigman, 2012).

†The standard model value for N_ν^{BBN} differs slightly from 3 due to such effects as non-instantaneous neutrino decoupling.

‡For mixing angles smaller than those suggested by LSND a sterile neutrino would decouple early and contribute $\Delta N_\nu^{BBN} < 1$.

unless they have new BSM interactions or properties (Barger et al., 2003; Anchordoqui et al., 2013). Of course, other light BSM particles besides sterile neutrinos could contribute to ΔN_ν^{BBN}, such as (pseudo-)Goldstone bosons associated with some new symmetry (Weinberg, 2013).

Most new physics effects increase the predicted ^4He abundance, leading to a more stringent upper limit on ΔN_ν^{BBN}. One important counterexample is a possible large asymmetry between ν and $\bar{\nu}$, which would preferentially drive the reactions in (7.379) to the right, decreasing the n/p ratio and allowing a larger ΔN_ν^{BBN}. (Only the $\nu_e - \bar{\nu}_e$ asymmetry directly affects the reactions, but the observed neutrino mixing would probably have equilibrated the asymmetries between the families.) However, such an asymmetry would have to be enormous, $(n_\nu - n_{\bar{\nu}})/n_\gamma \sim \mathcal{O}(0.1)$, compared to the baryon or charged lepton asymmetries to have much effect. Even allowing it, the present constraints from BBN along with the cosmic microwave background (CMB) and large scale structure data imply that such asymmetries would not significantly perturb the constraints on ΔN_ν^{BBN} (Simha and Steigman, 2008). A large asymmetry could lead to important nonlinear effects in the case of active-sterile neutrino mixing, however (Foot et al., 1996).

There are also stringent constraints on the number of neutrinos and their masses from the CMB and from the distribution of galaxies (e.g., Wong, 2011; Lesgourgues and Pastor, 2012; Olive et al., 2014). For example, the CMB anisotropies depend on the number of relativistic degrees of freedom that were present at recombination, when the universe had cooled sufficiently (to $T \sim 0.26$ eV, or redshift $z \sim 1100$) for neutral atoms to form so that the photons decoupled from matter. The WMAP (Hinshaw et al., 2013) and Planck (Ade et al., 2014) collaborations have made very detailed studies of the CMB. When combined with galaxy distributions, the Planck analysis obtains $N_\nu^{CMB} = 3.30 \pm 0.27$ for the number of neutrinos (active and sterile, weighted by their abundance), as well as other BSM forms of dark radiation, that were relativistic at recombination[§]. This is consistent with 3.046, but also allows one or more additional species if they have a somewhat reduced abundance. The effects of and constraints on active or sterile neutrino masses are discussed in the the next subsection.

Neutrino Mass Constraints

A stringent kinematic limit on the effective ν_e mass-squared

$$m_{\nu_e}^2 \equiv \sum_{i=1}^{3} |\mathcal{V}_{ei}|^2 m_i^2 \tag{7.381}$$

[§]The various cosmological limits on the number and masses of neutrinos depend significantly on the data set chosen and on possible correlations with other parameters (e.g., Giusarma et al., 2014).

can be obtained from the shape of the e^- spectrum near the endpoint in tritium β decay, ${}^3H \to {}^3He\ e^-\bar{\nu}_e$ (for a review, see Drexlin et al., 2013). In (7.381) m_i is the i^{th} mass eigenvalue, independent of whether it is Dirac or Majorana, and $\mathcal{V}$ is the leptonic mixing matrix as defined in (7.361). The current limits from experiments in Troitsk and Mainz are $m_{\nu_e} < 2.05$ eV and < 2.3 eV at 90% c.l., respectively. The Karlsruhe KATRIN experiment should improve the sensitivity on m_{ν_e} down to around 0.2 eV. See Figure 7.45 for a view of the KATRIN spectrometer.

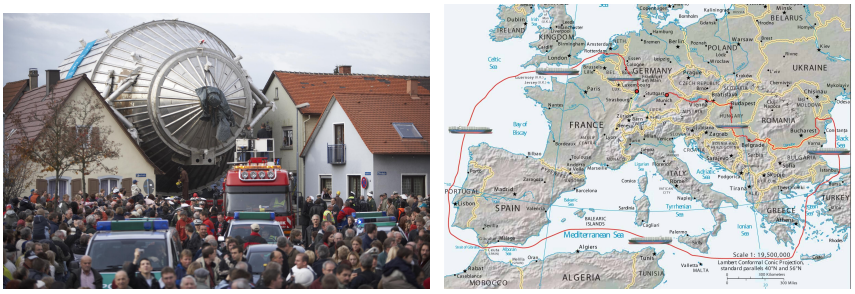

FIGURE 7.45
Left: transport of the KATRIN spectrometer through the village of Leopoldshafen near Karlsruhe. Right: the spectrometer was too large to transport 290 km from the fabrication site by road, and had travel by a roundabout 8600 km route.

The kinematic limits on the ν_μ and ν_τ masses, defined analogously to (7.381), are much weaker: $m_{\nu_\mu} < 0.19$ MeV from $\pi^+ \to \mu^+\nu_\mu$ and $m_{\nu_\tau} < 18.2$ MeV from $\tau^- \to 3\pi^\pm\nu_\tau, 5\pi^\pm(\pi^0)\nu_\tau$. These bounds are now superseded by much more stringent ones from neutrino oscillations and cosmology. However, it is interesting that the combination of this bound on m_{ν_τ} from ALEPH with the BBN constraint (which becomes relevant because an $\sim (1-20)$ MeV neutrino contributes more than 1 to N_ν^{BBN}) excluded the possibility of a stable or long-lived ν_τ above 1 MeV (e.g., Fields et al., 1997).

We also mention the historically important observation of a burst of $\mathcal{O}(20)$ neutrinos (presumably mainly $\bar{\nu}_e$'s) from the core-collapse Supernova 1987A by the Kamiokande, IMB, and Baksan collaborations, which implied (amongst many other things[¶]) that $m_{\nu_e} \lesssim 20$ eV, because otherwise the arrival times of

[¶]For example, the neutrinos arrived within a few hours of the supernova photons, whereas they would have arrived ~ 5 months sooner (after a 160,000 yr journey) if they did not share the same gravitational interactions, testing the weak equivalence principle (Longo, 1988; Krauss and Tremaine, 1988).

the detected neutrinos would have spread out more than was observed. It was hard to make the limit precise, however, because it depended on theoretical details of the neutrino emission (e.g., Bahcall, 1989; Raffelt, 1999). Core-collapse supernovae are expected to occur in our galaxy at the rate of several per century. Observation of the ν's from such a supernova in neutrino and other detectors would yield a wealth of information on neutrino properties as well as on the dynamics of the supernova explosion (e.g., Duan et al., 2010; Scholberg, 2012). The diffuse background flux of neutrinos from core-collapse supernovae in other galaxies may also be observable (Beacom, 2010).

Light massive neutrinos would contribute to the cosmological matter density, and they would close the Universe, $\Omega_\nu = 1$, for $\Sigma \sim 35$ eV, where

$$\Sigma \equiv \sum_i |m_i| \tag{7.382}$$

is the sum of the masses of the light active neutrinos. Observationally, some 25% of the matter density is dark (Olive et al., 2014), but it is most likely cold dark matter (CDM) that was non-relativistic at decoupling, such as weakly interacting massive particles (WIMPs) or axions. Light neutrinos would be hot dark matter (relativistic at decoupling), which would free-stream away from density perturbations, preventing the formation of the observed smaller scale structures during the lifetime of the universe[‖]. Smaller neutrino masses (close to the recombination temperature ~ 0.26 eV) would lead to subtle effects in the CMB and galaxy distributions (e.g., Wong, 2011; Abazajian et al., 2011; Lesgourgues and Pastor, 2012; Hinshaw et al., 2013; Ade et al., 2014). For example, the Planck collaboration (Ade et al., 2014) finds

$$\Sigma < 0.23 \text{ eV at } 95\% \text{ c.l.} \tag{7.383}$$

for the sum of the active neutrino masses (assuming $N_\nu^{CMB} = 3.046$) from the combination of CMB and galaxy data. Future cosmological observations (Abazajian et al., 2013) should be able to extend the sensitivity to Σ down to or below the minimum value 0.05 eV $\sim \sqrt{|\Delta m^2_{atm}|}$ allowed by the neutrino oscillation data.

Allowing for light sterile neutrinos as well one must take into account the extra contribution to the radiation. Furthermore, the cosmological observables depend on how the masses are distributed amongst the states, possible asymmetries, and possible non-thermal production. The Planck collaboration considered the example of one light ($m_S < 10$ eV) thermally-produced sterile neutrino. In that case, $\Delta N_\nu^{CMB} = (T_S/T_\nu)^4$, where T_S and T_ν are respectively the sterile and active neutrino termperatures (e.g., Kolb and Turner,

[‖]Warm dark matter, e.g., from keV mass sterile neutrinos, is an intermediate possibility (e.g., Kusenko, 2009). The *neutrino minimal standard model (νMSM)* and other astrophysical and cosmological implications of intermediate mass sterile neutrinos are reviewed in (Boyarsky et al., 2009), and theoretical models in (Merle, 2013).

1990). (One expects $T_S \leq T_\nu$ due to earlier decoupling.) Assuming also that $\Sigma = 0.06$ eV and no asymmetries, they obtained the correlated 95% c.l. limits

$$N_\nu^{CMB} < 3.80, \qquad m_S^{eff} < 0.42 \text{ eV}, \tag{7.384}$$

where the effective mass m_S^{eff} is m_S weighted by the sterile abundance, i.e., $m_S^{eff} = (T_S/T_\nu)^3\, m_S$.

Neutrinoless Double Beta Decay

Majorana masses can lead to $\beta\beta_{0\nu}$, i.e., $nn \to ppe^-e^-$, which violates lepton number by two units, by the diagrams in Figure 7.42 (for reviews, see Avignone et al., 2008; Rodejohann, 2011; Gomez-Cadenas et al., 2012; Vergados et al., 2012; Bilenky and Giunti, 2014). Since there is no missing energy**, events should show up as a peak of known energy in the e^-e^- spectrum from a sample of $\beta\beta_{0\nu}$-unstable nuclei. However, the process would have an extremely long half-life, so problems of backgrounds are severe.

The amplitude for $\beta\beta_{0\nu}$ is $M \sim A_{nuc}\, m_{\beta\beta}$, where A_{nuc} contains the nuclear matrix element. A_{nuc} cannot be directly measured and therefore introduces considerable uncertainty into the interpretation of any upper limit or future observation (Simkovic et al., 2008; Vogel, 2008; Vergados et al., 2012). $m_{\beta\beta}$ is the effective Majorana mass in the presence of mixing between light Majorana neutrinos,

$$m_{\beta\beta} \equiv \left| \sum_i (\mathcal{V}_{ei})^2 m_i \right|. \tag{7.385}$$

It is just the (e,e) element of m_T or of the effective Majorana mass matrix in a seesaw model (i.e., the $(1,1)$ element in the family basis in which $A_L^e = I$). It involves the square of $\mathcal{V}_{ei}$ rather than the absolute square, allowing for the possibility of cancellations between terms. Such cancellations could occur even if the original mass matrix were real because some of the eigenvalues could be negative. (In our phase convention the m_i are taken to be positive, but the signs would appear because some of the Majorana phases in (7.360) would then be $\pm i$.) This also shows why the $\beta\beta_{0\nu}$ amplitude vanishes for a Dirac neutrino, which can be viewed as two Majorana neutrinos which give equal and opposite contributions. The cancellations could in principle allow the determination of (CP-violating) Majorana phases different from 0 or $\pm i$, though this is difficult in practice because the other parameters including the matrix elements would have to be known rather well (Barger et al., 2002; Pascoli et al., 2002).

**Two-neutrino double beta decay, $\beta\beta_{2\nu}$, is the process $nn \to ppe^-e^-\bar\nu\bar\nu$, which can occur by ordinary second-order weak processes in some β-stable nuclei. It leads to a continuous e^-e^- spectrum and has been studied in a number of nuclei (Barabash, 2013). It is helpful for testing calculations of the nuclear matrix elements entering $\beta\beta_{0\nu}$. A third possibiity is Majoron decay, $nn \to ppe^-e^-M$ or $\beta\beta_{0\nu M}$, where M is a Majoron (Goldstone boson). It would lead to a spectrum intermediate between $\beta\beta_{0\nu}$ and $\beta\beta_{2\nu}$.

There are a number of existing or proposed $\beta\beta_{0\nu}$ experiments in various nuclei (Gomez-Cadenas et al., 2012; Barabash, 2014). For example, the KamLAND-ZEN (Gando et al., 2013a) and EXO-200 (Auger et al., 2012) experiments have obtained the respective 90% c.l. limits 1.9×10^{25} yr and 1.6×10^{25} yr on the $\beta\beta_{0\nu}$ half-life in ^{136}Xe. The combination corresponds to $m_{\beta\beta} < (0.12 - 0.25)$ eV, with the range due to the nuclear matrix element uncertainties. Several other experiments have results that are nearly as strong[††], and future experiments should be sensitive down to $\mathcal{O}(0.01 - 0.02$ eV) or better (e.g., Barabash, 2014). They should be sufficient to observe $\beta\beta_{0\nu}$ if the neutrinos are Majorana with masses corresponding to the inverted or degenerate spectra described in Section 7.7.5, but no scheduled experiment would be sensitive to the normal hierarchy. (See Biller, 2013, however.)

A heavy Majorana neutrino could also contribute to $m_{\beta\beta}$, but its contribution would be suppressed by finite range effects (i.e., the m_i^2 in the denominator of the propagator would be important),

$$m_{\beta\beta} \to \left| \sum_i (\mathcal{V}_{ei})^2 m_i F(m_i, A) \right|, \qquad F(m_i, A) \equiv \frac{\langle e^{-m_i r}/r \rangle}{\langle 1/r \rangle}, \tag{7.386}$$

where A is the nucleon number. $F(m_i, A)$ is ~ 1 for $m_i \ll 10$ MeV, but falls rapidly for larger values (e.g., Vergados et al., 2012; Faessler et al., 2014). Lepton-number violating effects other than Majorana neutrino masses can also lead to $\beta\beta_{0\nu}$ (although the existence of a $\beta\beta_{0\nu}$ amplitude implies the existence of a Majorana mass at some level (Schechter and Valle, 1982)). For example, models involving both $V - A$ and $V + A$ interactions as well as lepton number violation can induce $\beta\beta_{0\nu}$ amplitudes not directly proportional to neutrino masses (Problem 7.22). There could also be effects from new interactions such as leptoquarks or R-parity violation in supersymmetry. If $\beta\beta_{0\nu}$ is observed, it would be useful to study it in several different nuclei, both to help control nuclear matrix element uncertainties and to shed some light on the underlying mechanism.

Relic Neutrinos

The BBN and CMB constraints on the cosmological neutrinos are indirect. Following their decoupling at $T \sim$ few MeV the neutrino wavelengths were redshifted so that their momentum distribution should at present have a thermal form, characterized by an effective temperature $T_\nu = (4/11)^{1/3} T_\gamma \sim 1.9\,\mathrm{K}$, where $T_\gamma \sim 2.73\,\mathrm{K}$ is the CMB temperature and the $(4/11)^{1/3}$ factor is because the γ's but not the neutrinos were reheated by $e^- e^+$ annihilation at

[††] An observation of $\beta\beta_{0\nu}$ in ^{76}Ge with a half-life $\sim 2 \times 10^{25}$ yr has been claimed (Klapdor-Kleingrothaus and Krivosheina, 2006) by members of the Heidelberg-Moscow experiment. This would correspond to $m_{\beta\beta} \sim (0.25 - 0.60)$ eV. However, the result has not been confirmed by other experiments, and is apparently excluded by the ^{136}Xe results for plausible nuclear matrix elements (Gando et al., 2013a).

$T \lesssim m_e$ (Steigman, 1979; Kolb and Turner, 1990; Weinberg, 2008). This corresponds to a number density of $\sim 50/\mathrm{cm}^3$ for each neutrino degree of freedom, i.e., $\sim 300/\mathrm{cm}^3$ for 3 flavors with two helicity states. Local clustering and modifications of the momentum distribution are not expected to be large unless the masses are $\gtrsim 0.1$ eV (e.g., Ringwald and Wong, 2004). Direct detection of these *relic neutrinos* appears extremely difficult. Effects involving macroscopic torques or forces (Stodolsky, 1975; Cabibbo and Maiani, 1982; Langacker et al., 1983) are tiny. Another possibility are *Z bursts*, in which ultra high energy cosmic ray neutrinos annihilate on relic neutrinos to produce Z's (Weiler, 1982; Eberle et al., 2004), which could be observed through their decay products or as absorption dips in the cosmic ray ν spectrum. However, this would only be feasible if there were some unexpected intense source of such high energy neutrinos. More promising are ν-induced $e^{\pm}$ emission by nuclei (e.g., Weinberg, 1962; Cocco et al., 2007; Lazauskas et al., 2008), which would show up as $e^{\pm}$ emission above the β decay endpoint. For example, the recent PTOLEMY proposal for tritium decay involving a graphene source (Betts et al., 2013) might be sensitive to relic neutrinos for a degenerate spectrum with $m_i \gtrsim 0.1$ eV, with a larger rate for Majorana than Dirac neutrinos (Long et al., 2014). Such experiments would also have sensitivity to heavier sterile neutrinos and to $\nu - \bar{\nu}$ asymmetries. For reviews of relic neutrinos, see (Gelmini, 2005; Strumia and Vissani, 2006; Ringwald, 2009).

Electromagnetic Form Factors

Neutrinos have no electric charge, but they can acquire magnetic and electric dipole moments by diagrams analogous to the weak corrections to the muon magnetic moment in Figure 2.20 on page 85 or from new physics. These lead to effective electromagnetic interactions

$$\mathcal{H}_{\nu Q} = \frac{1}{2}\mu_{ij}\bar{n}_j\sigma^{\mu\nu}n_iF_{\mu\nu} + \frac{i}{2}d_{ij}\bar{n}_j\sigma^{\mu\nu}\gamma^5 n_iF_{\mu\nu}, \tag{7.387}$$

where n_i can represent either a Dirac (ν_{iD}) or Majorana (ν_{iM}) mass eigenstate field. The first (second) terms are magnetic (electric) dipole interactions, as can be seen from (2.353), (7.320), and Problem 2.22. The flavor-diagonal terms $i = j$ are known as *direct or intrinsic moments*, while those for $i \neq j$ are *transition moments*.

The magnetic and electric dipoles flip chirality. In the Majorana case, $\nu_{iM} = \nu_{iL} + \nu^c_{iR}$, so that

$$\bar{\nu}_{jM}\sigma^{\mu\nu}\nu_{iM} = \bar{\nu}_{jL}\sigma^{\mu\nu}\nu^c_{iR} + \bar{\nu}^c_{jR}\sigma^{\mu\nu}\nu_{iL}. \tag{7.388}$$

However, using $\nu^c_{iR} = \mathcal{C}\bar{\nu}^T_{iL}$,

$$\bar{\nu}_{jL}\sigma^{\mu\nu}\nu^c_{iR} = \nu^{cT}_{jR}\mathcal{C}\sigma^{\mu\nu}\mathcal{C}\bar{\nu}^T_{iL} = -\bar{\nu}_{iL}\sigma^{\mu\nu}\nu^c_{jR}, \tag{7.389}$$

so that $\mu_{ij} = -\mu_{ji}$. (This can also be seen from (2.298) on page 66.) Majorana neutrinos therefore cannot have direct magnetic moments, but can have

transition moments $\mu_{ij} \neq 0$ for $i \neq j$, which can mediate decays such as $\nu_{iM} \to \nu_{jM}\gamma$. Similar statements apply to electric dipole moments.

Both direct and transition moments are possible for Dirac neutrinos $\nu_{iD} = \nu_{iL} + \nu_{iR}$. For a single flavor

$$\bar{\nu}_D \sigma^{\mu\nu} \nu_D = \bar{\nu}_L \sigma^{\mu\nu} \nu_R + \bar{\nu}_R \sigma^{\mu\nu} \nu_L. \tag{7.390}$$

One can write ν_L and ν_R in terms of two degenerate Majorana neutrinos using (7.348),

$$\nu_L = \frac{1}{\sqrt{2}}(\nu_{1L} + \nu_{2L}), \qquad \nu_R = \frac{1}{\sqrt{2}}(\nu^c_{1R} - \nu^c_{2R}), \tag{7.391}$$

where the unnecessary superscript 0 has been dropped. Then

$$\bar{\nu}_L \sigma^{\mu\nu} \nu_R = -\frac{1}{\sqrt{2}} \bar{\nu}_{1L} \sigma^{\mu\nu} \nu^c_{2R} + \frac{1}{\sqrt{2}} \bar{\nu}_{2L} \sigma^{\mu\nu} \nu^c_{1R}. \tag{7.392}$$

That is, a direct Dirac magnetic (or electric) moment is an antisymmetric combination of transition moments between degenerate Majorana states.

In the simplest extension of the SM with a small Dirac mass m_i, the direct neutrino magnetic moment is (Marciano and Sanda, 1977; Lee and Shrock, 1977)

$$\mu_i \sim \frac{3eG_F m_i}{8\sqrt{2}\pi^2} \sim 3.2 \times 10^{-19} \left(\frac{m_i}{1\text{ eV}}\right) \mu_B, \tag{7.393}$$

where μ_B is the Bohr magneton. This is negligibly small compared with laboratory limits $\lesssim 10^{-10}\mu_B$ (Vogel and Engel, 1989; Olive et al., 2014; Giunti and Studenikin, 2014), and various astrophysical limits, e.g., from stellar cooling, $\mu_\nu \lesssim$ few $\times 10^{-12}$ (Raffelt, 1999; Giunti and Studenikin, 2014). The latter often applies to electric dipole moments as well, and to both Dirac and Majorana transition moments.

One can construct models with magnetic moments that are much larger than (7.393), as was motivated by an alternative solution to the Solar neutrino problem involving resonant spin-flavor precession in an assumed strong Solar magnetic field (Akhmedov, 1988; Lim and Marciano, 1988; Gonzalez-Garcia and Maltoni, 2008). However, there is a limit as to how large they can be. For Dirac neutrinos, higher-dimensional operators that can generate a magnetic dipole moment μ^D_ν also contribute to m_ν (Bell et al., 2005). If the operators are generated by new physics at a scale $\gtrsim 1$ TeV then there is an upper limit on μ^D_ν of around $10^{-15}\mu_B$ for $m_\nu < 0.3$ eV. The corresponding limits in the Majorana case are much weaker because of Yukawa suppressions to the Majorana mass (Bell et al., 2006). Thus, observation of a dipole moment above $\sim 10^{-15}\mu_B$ would imply that the mass is Majorana (or that there are fine-tuned cancellations between contributions to m_ν).

7.7.4 Neutrino Oscillations

Neutrino oscillations are analogous to the neutral K and B meson oscillations described in Sections 7.6.3 and 7.6.4, and occur due to the mismatch between

weak and mass eigenstates. They do not mix the neutrino helicities, and are therefore independent of whether the masses are Majorana or Dirac. First consider two neutrino flavors, ν_e and ν_μ, related to the mass eigenstates by

$$|\nu_e\rangle = |\nu_1\rangle \cos\theta + |\nu_2\rangle \sin\theta, \qquad |\nu_\mu\rangle = -|\nu_1\rangle \sin\theta + |\nu_2\rangle \cos\theta, \tag{7.394}$$

where θ, which corresponds to θ_{12} in (7.360), is the neutrino mixing angle. Suppose that one starts at time $t = 0$ with a pure state $|\nu(0)\rangle = |\nu_\mu\rangle$ of definite momentum[‡‡] $|\vec{p}|$ from the decay $\pi^+ \to \mu^+\nu_\mu$. The two mass eigenstate components each develop with their own time dependence, so that

$$\begin{aligned} |\nu(t)\rangle &= -|\nu_1\rangle \sin\theta e^{-iE_1 t} + |\nu_2\rangle \cos\theta e^{-iE_2 t} \\ &\sim \left[-|\nu_1\rangle \sin\theta e^{-i\frac{m_1^2 t}{2E}} + |\nu_2\rangle \cos\theta e^{-i\frac{m_2^2 t}{2E}} \right] e^{-iEt}, \end{aligned} \tag{7.395}$$

at a later time t, where we have assumed that the neutrinos are extremely relativistic, so that $E_i = \sqrt{|\vec{p}|^2 + m_i^2} \sim E + m_i^2/2E$ where $E \sim |\vec{p}|$. After traveling a distance L there is a probability

$$\begin{aligned} P_{\nu_\mu \to \nu_e}(L) = |\langle \nu_e | \nu(t) \rangle|^2 &= \sin^2\theta \cos^2\theta \left| -e^{-i\frac{m_1^2 t}{2E}} + e^{-i\frac{m_2^2 t}{2E}} \right|^2 \\ &= \sin^2 2\theta \sin^2\left(\frac{\Delta m^2 L}{4E}\right) \\ &= \sin^2 2\theta \sin^2\left[\frac{1.27 \Delta m^2(\mathrm{eV}^2) L(\mathrm{km})}{E(\mathrm{GeV})}\right], \end{aligned} \tag{7.396}$$

for the neutrino to have oscillated into a ν_e, where $\Delta m^2 = m_2^2 - m_1^2$ and $L \sim t$. The ν_e could be detected, e.g., by the reaction $\nu_e n \to e^- p$. The *oscillation length* is defined as

$$L_{osc} = \frac{4\pi E}{\Delta m^2}. \tag{7.397}$$

Such *vacuum oscillations* depend only on $|\Delta m^2|$ and not on the absolute mass scale or on the hierarchy (which mass is larger). In *appearance experiments* one searches for the production of a different neutrino flavor than one started from, such as by the production of an e^- or τ^- in an initial ν_μ beam. In an ideal experiment with definite L and E one observes not only the appearance of the new flavor, but the characteristic L/E dependence. However, for large $\Delta m^2 L/E$ the oscillations are averaged by the spread in neutrino energy E and by finite detector/source sizes, so that

$$P_{\nu_\mu \to \nu_e}(L) \to \frac{1}{2} \sin^2 2\theta, \tag{7.398}$$

[‡‡]This simple approximation yields the correct result. However, a complete treatment requires consideration of the coherence of the initial and final wave packets, the relation between t and the location L of the detector, entanglement with other particles, etc. For recent discussions, see, e.g., (Akhmedov and Smirnov, 2009; Cohen et al., 2009; Kayser et al., 2010).

which is the same result one would have obtained from an incoherent superposition of ν_1 and ν_2. In a *disappearance experiment*, one searches for the reduction in the flux of the initial ν_μ (or other flavor) as a function of L and E, making use of the *survival probability* $P_{\nu_\mu\to\nu_\mu}(L) = 1 - P_{\nu_\mu\to\nu_e}(L)$ for the state to remain a ν_μ. For both types of experiments, careful attention has to be paid to the initial flux and spectrum (obtained from other measurements, theory, or by an initial calibration detector) and to backgrounds.

Even with more than two types of neutrino, it is sometimes a good approximation to use the two-neutrino formalism in the analysis of a given experiment, e.g., if some of the mixings are small or if some of the $\Delta_{ij} \equiv m_i^2 - m_j^2$ are small compared to E/L (see below), and most results are presented in terms of allowed or excluded regions in the $\sin^2 2\theta - \Delta m^2$ plane or the $\tan^2\theta - \Delta m^2$ plane*, whether or not that is really valid. However, a more precise or general analysis should take all three neutrinos into account. It is straightforward to show that the oscillation probability for $\nu_a \to \nu_b$ after a distance L is

$$\begin{aligned} P_{\nu_a\to\nu_b}(L) =& \delta_{ab} - 4\sum_{i<j} \Re e\big(\mathcal{V}_{ai}^*\mathcal{V}_{bi}\mathcal{V}_{aj}\mathcal{V}_{bj}^*\big)\sin^2\left(\frac{\Delta_{ij}L}{4E}\right) \\ &+ 2\sum_{i<j} \Im m\big(\mathcal{V}_{ai}^*\mathcal{V}_{bi}\mathcal{V}_{aj}\mathcal{V}_{bj}^*\big)\sin\left(\frac{\Delta_{ij}L}{2E}\right), \end{aligned} \tag{7.399}$$

where ν_a and ν_b are weak (flavor) eigenstates and $\mathcal{V}$ is the leptonic mixing matrix in (7.360). For antineutrinos, $P_{\bar\nu_a\to\bar\nu_b}(L)$ is given by the same formula, except the sign of the last term is reversed†. It is apparent from (7.399) that $P_{\nu_b\to\nu_a}(L)$ is the same as $P_{\nu_a\to\nu_b}(L)$ except that $\mathcal{V}\to\mathcal{V}^*$, and that any difference between them is due to CP-violating phases in $\mathcal{V}$. The combination $\mathcal{V}_{ai}^*\mathcal{V}_{bi}\mathcal{V}_{aj}\mathcal{V}_{bj}^*$ is a Jarlskog invariant, i.e., independent of phase conventions. The Majorana phases do not enter, so CP-violation in neutrino oscillations requires mixing between at least 3 families, just as in the CKM matrix. For $F = 3$, it is given by the phase δ in (7.360), and all CP-violating effects would vanish for $s_{13} = 0$. In practice, it is extremely difficult to compare $P_{\nu_a\to\nu_b}(L)$ and $P_{\nu_b\to\nu_a}(L)$ directly, because, e.g., $\bar\nu_e$ are mainly produced at reactors, and $\nu_\mu(\bar\nu_\mu)$ at accelerators. However, CPT, which is built into the expressions above, implies that $P_{\nu_b\to\nu_a}(L) = P_{\bar\nu_a\to\bar\nu_b}(L)$. Thus,

$$P_{\nu_a\to\nu_b}(L) \xrightarrow[\mathcal{V}\to\mathcal{V}^*]{} P_{\bar\nu_a\to\bar\nu_b}(L). \tag{7.400}$$

*One usually labels the mass eigenstates so that $\Delta m^2 \geq 0$. The cases $0 \leq \theta \leq \pi/4$ and $\pi/4 \leq \theta \leq \pi/2$ are physically different. However, they cannot be distinguished by vacuum oscillation experiments, so it was traditional to use the variable $\sin^2 2\theta$ to describe the results. Matter effects, however, *can* distinguish the two cases (de Gouvea et al., 2000), so it is better to use $\tan^2\theta$ instead. The region $\tan^2\theta > 1$ is sometimes known as the "dark side". The cases $\theta <$ or $> \pi/4$ also differ by subleading effects for more than two flavors.

†ν_a and $\bar\nu_a$ are respectively the left and right-chiral states annihilated by ν_{aL} and ν_{aR}^c.

The oscillation rates for ν_a vs $\bar{\nu}_a$ can be compared, e.g., by using ν_μ ($\bar{\nu}_\mu$) beams from $\pi^+ \to \mu^+\nu_\mu$ ($\pi^- \to \mu^-\bar{\nu}_\mu$), and any difference must be due to leptonic CP violation. From (7.399) and (7.400) the survival probabilities in vacuum must be equal, $P_{\nu_a\to\nu_a}(L) = P_{\bar{\nu}_a\to\bar{\nu}_a}(L)$; CP violation in vacuum can therefore only occur in appearance experiments. The discussion above assumes the validity of CPT. Possible CPT violation in the neutrino sector is discussed in (Diaz and Kostelecky, 2012).

Oscillations between active neutrinos of different flavors are known as *first class (flavor) oscillations*. The results in (7.399) and (7.400) generalize to *second class oscillations* (Barger et al., 1980) between light active and sterile neutrinos of the same helicity, which can occur when there are both Majorana and Dirac mass terms. For example, mixing between 3 active and 3 sterile neutrinos would still be described by (7.399), except $\mathcal{V}$ is now a 6×6 unitary matrix. Other phenomena, which can sometimes mimic neutrino oscillations, include non-standard interactions in the source or detector (e.g., Gavela et al., 2009; Ohlsson, 2013), neutrino-antineutrino transitions (involving new interactions to flip helicity) (Langacker and Wang, 1998), and massless neutrinos that are non-orthogonal due to mixing with heavy states (Langacker and London, 1988a). The latter can be generalized to massive oscillating neutrinos with an effectively non-unitary mixing matrix, again due to neglecting the mixing with heavier neutrinos (Antusch et al., 2006; Antusch and Fischer, 2014).

An important special case of (7.399) occurs when the mass eigenstates can be divided into two sets, each of which is nearly degenerate compared to the E/L of the experiment. That is, consider F mass eigenstates, in which $\nu_i,\ i = 1\cdots n$ are close in mass, as are $\nu_j,\ j = n+1\cdots F$. If L/E is such that $\Delta_{kl}L/E$ can be neglected when k and l are in the same set, then it is straightforward to show that

$$P_{\nu_a\to\nu_b}(L) = P_{\bar{\nu}_a\to\bar{\nu}_b}(L) = \sin^2 2\theta_{ab}\sin^2\left(\frac{\Delta m^2 L}{4E}\right), \tag{7.401}$$

for $a \neq b$, where

$$\sin^2 2\theta_{ab} \equiv 4\left|\sum_{i=1}^{n}\mathcal{V}_{ai}^*\mathcal{V}_{bi}\right|^2 = 4\left|\sum_{j=n+1}^{F}\mathcal{V}_{aj}^*\mathcal{V}_{bj}\right|^2, \tag{7.402}$$

and $\Delta \equiv m_j^2 - m_i^2$ for $i \leq n < j$. The last form in (7.402) follows from unitarity. Thus, if one can neglect all but one mass splitting the two-neutrino formula holds, although the effective mixing angle may be a complicated function of the elements of $\mathcal{V}$. In particular, there are no CP-violating effects in this limit. Similarly, the survival probabilities are given by

$$P_{\nu_a\to\nu_a}(L) = P_{\bar{\nu}_a\to\bar{\nu}_a}(L) = 1 - \sin^2 2\theta_{aa}\sin^2\left(\frac{\Delta m^2 L}{4E}\right), \tag{7.403}$$

with

$$\sin^2 2\theta_{aa} = \sum_{b\neq a} \sin^2 2\theta_{ab} = 4\sum_{i=1}^{n} |\mathcal{V}_{ai}|^2 \left(1 - \sum_{k=1}^{n} |\mathcal{V}_{ak}|^2\right), \tag{7.404}$$

which implies

$$\sin^2 \theta_{aa} \equiv \sum_{j=n+1}^{F} |\mathcal{V}_{aj}|^2 = 1 - \sum_{i=1}^{n} |\mathcal{V}_{ai}|^2 . \tag{7.405}$$

Examples will be given below for oscillations involving atmospheric and sterile neutrinos.

The Mikheyev-Smirnov-Wolfenstein (MSW) Effect

Eq. 7.395 or its generalization to 3 or more flavors describes the time evolution of an (initial) weak eigenstate in vacuum. However, for propagation through matter, such as the Sun or Earth, one must take into account the phase changes associated with the coherent forward scattering of the neutrinos with the matter, very much like index of refraction effects in optics (Wolfenstein, 1978). Under appropriate conditions, the matter effects can combine with the neutrino masses to yield an effective degeneracy and therefore an enhanced transition probability, the MSW resonance (Mikheyev and Smirnov, 1985).

To see how this works, consider the time evolution of a neutrino state

$$|\nu(t)\rangle = \sum_a c_a(t)|\nu_a\rangle, \tag{7.406}$$

in vacuum. The weak eigenstates $|\nu_a\rangle$ are related to the mass eigenstates $|\nu_i\rangle$ by

$$|\nu_a\rangle = \sum_i |\nu_i\rangle\langle\nu_i|\nu_a\rangle = \sum_i \mathcal{V}^*_{ai}|\nu_i\rangle. \tag{7.407}$$

(In (7.407) and the following, we ignore the momentum integrals and delta functions, as well as the $(2\pi)^3 2E$ normalization factors, all of which cancel between the matrix elements and the sums over intermediate states.) Evolving the mass eigenstates analogously to (7.395), one finds that the coefficients satisfy the Schrödinger-like equation

$$i\frac{d}{dt}c_a(t) = \langle\nu_a|H_V|\nu_b\rangle\, c_b(t), \tag{7.408}$$

where the vacuum Hamiltonian (due to the masses) is

$$\langle\nu_a|H_V|\nu_b\rangle = \sum_i \mathcal{V}_{ai}E_i\mathcal{V}^*_{bi} \sim \sum_i \mathcal{V}_{ai}\frac{m_i^2}{2E}\mathcal{V}^*_{bi} + E\delta_{ab}. \tag{7.409}$$

The last term only affects the irrelevant overall phase of the state. This and similar multiples of the identity can be dropped in what follows. For two

flavors, H_V becomes

$$H_V = \frac{\Delta m^2}{4E} \begin{pmatrix} -\cos 2\theta & \sin 2\theta \\ \sin 2\theta & \cos 2\theta \end{pmatrix} \tag{7.410}$$

using the conventions in (7.394), with $\Delta m^2 = m_2^2 - m_1^2$.

In the presence of matter, (7.408) must be modified by the addition of the effective (matter) Hamiltonian

$$H_M = \int d^3\vec{x} \sum_a \frac{2G_F}{\sqrt{2}} \bar{\nu}_{aL}\gamma^\mu \nu_{aL} \sum_r \langle \bar{\psi}_r \gamma_\mu (g_V^{ar} - g_A^{ar}\gamma^5)\psi_r \rangle, \tag{7.411}$$

which describes the scattering of ν_a from fermions $r = e, p, n$, where $g_{V,A}^{ar}$ are the effective vector and axial couplings which receive contributions from Z exchange and (in the case of $r = e$) from W exchange, as in (7.93) on page 309. The brackets on the last term indicate an expectation value in the static medium. Assuming the medium is unpolarized,

$$\langle \bar{\psi}_r \gamma_\mu (g_V^{ar} - g_A^{ar}\gamma^5)\psi_r \rangle = g_V^{ar} n_r \delta_\mu^0, \tag{7.412}$$

where n_r is the number density of particle r (cf., Eq. A.19 on page 545). Using also that $\int d^3\vec{x}\, \nu_{aL}^\dagger \nu_{aL}$ is the ν_a number operator, $N_{\nu_{aL}} - N_{\nu_{aR}^c}$, we obtain the propagation equation[‡]

$$i\frac{d}{dt}c_a(t) = \langle \nu_a | H_V | \nu_b \rangle\, c_b(t) + \sqrt{2}G_F \left(\sum_{r=e,p,n} g_V^{ar} n_r \right) c_a(t). \tag{7.413}$$

The vector coefficients are

$$\begin{aligned} g_V^{ee} &= +\frac{1}{2} + 2\sin^2\theta_W, \qquad g_V^{ep} = +\frac{1}{2} - 2\sin^2\theta_W, \qquad g_V^{en} = -\frac{1}{2} \\ g_V^{\mu e} &= -\frac{1}{2} + 2\sin^2\theta_W, \qquad g_V^{\mu p} = +\frac{1}{2} - 2\sin^2\theta_W, \qquad g_V^{\mu n} = -\frac{1}{2} \\ g_V^{sr} &= 0, \end{aligned} \tag{7.414}$$

for ν_{eL}, $\nu_{\mu,\tau L}$, and sterile ν_{sL}, respectively. The signs are reversed for ν_R^c, as can be seen from the number operator or from (2.297) on page 66. g_V^{ee} contains an extra $+1$ from the WCC, which makes the effect important for $\nu_e \leftrightarrow \nu_{\mu,\tau}$.

Specializing to two families,

$$i\frac{d}{dt}\begin{pmatrix} c_a(t) \\ c_b(t) \end{pmatrix} = \begin{pmatrix} -\frac{\Delta m^2}{4E}\cos 2\theta + \frac{G_F}{\sqrt{2}}n & \frac{\Delta m^2}{4E}\sin 2\theta \\ \frac{\Delta m^2}{4E}\sin 2\theta & \frac{\Delta m^2}{4E}\cos 2\theta - \frac{G_F}{\sqrt{2}}n \end{pmatrix} \begin{pmatrix} c_a(t) \\ c_b(t) \end{pmatrix}, \tag{7.415}$$

[‡]The numerical factor and sign for the matter term were derived in (Barger et al., 1980) and (Langacker et al., 1983), respectively.

where

$$n = n_a - n_b, \qquad n_a \equiv \sum_{r=e,p,n} g_V^{ar} n_r, \tag{7.416}$$

and we have symmetrized the diagonal elements by subtracting the common term $\sqrt{2}G_F\, n/2$. For an electrically neutral medium, i.e., $n_e = n_p$, this yields

$$n = \begin{cases} n_e & \text{for} \quad \nu_{eL} \leftrightarrow \nu_{\mu L}, \nu_{\tau L} \\ n_e - \frac{1}{2} n_n & \text{for} \quad \nu_{eL} \leftrightarrow \nu_{sL} \\ -\frac{1}{2} n_n & \text{for} \quad \nu_{\mu L}, \nu_{\tau L} \leftrightarrow \nu_{sL} \end{cases}, \tag{7.417}$$

with the signs reversed for ν_R^c.

Under the right conditions, the matter effect can greatly enhance the transitions. In particular, if the Mikheyev-Smirnov-Wolfenstein (MSW) resonance condition $\frac{\Delta m^2}{2E} \cos 2\theta = \sqrt{2} G_F n$ is satisfied, the diagonal elements vanish and even small vacuum mixing angles lead to a maximal effective mixing angle. Because of the sign switch, an enhancement for ν_L corresponds to a suppression for ν_R^c and vice-versa (i.e., the presence of matter effectively breaks CPT). The matter effect breaks the sign degeneracy for vacuum oscillations, and allows a determination of the sign of Δm^2. Because of the E dependence it can lead to a distortion in the final neutrino spectra. Finally, if the matter density varies significantly along the neutrino path, as is the case for Solar neutrinos produced near the Solar core, one may encounter a level-crossing at the position for which the resonance condition is satisfied (for a given E), as illustrated in Figure 7.46. If the density varies sufficiently gradually, the transition is adiabatic, i.e., the neutrino remains on one level, with a maximal flavor transition probability. A more abrupt (non-adiabatic) transition will have a non-negligible probability to jump from one level to another, reducing the flavor transition probability (see e.g., Kuo and Pantaleone, 1989; Gonzalez-Garcia and Nir, 2003; Strumia and Vissani, 2006; Gonzalez-Garcia and Maltoni, 2008; Blennow and Smirnov, 2013; Gonzalez-Garcia and Maltoni, 2013).

Oscillation Experiments

There have been many experimental searches for and observations of neutrino oscillations and transitions (for recent reviews, see Gonzalez-Garcia and Maltoni, 2008; Olive et al., 2014), including experiments at accelerators and reactors, and those involving Solar neutrinos and atmospheric neutrinos (from the decay products of particles produced by cosmic ray interactions in the atmosphere). Major observation and exclusion regions are plotted in the two-neutrino formalism in Figure 7.47.

Solar Neutrinos

Neutrinos (ν_e) are produced by fusion reactions in main sequence stars by the pp and CNO chains, which ultimately lead to $4p \rightarrow \alpha + 2e^+ + 2\nu_e$. The

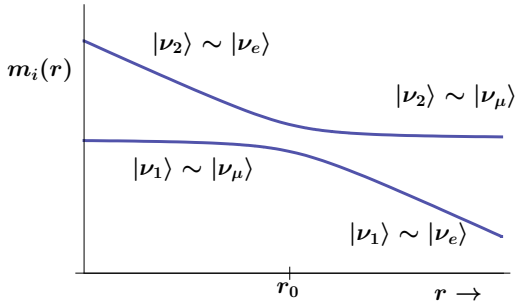

FIGURE 7.46
A level-crossing (resonance) at r_0 in the presence of matter density that decreases with distance r from the neutrino source. The $m_i(r)$ are the eigenvalues of the matrix in (7.415). (In the full three-neutrino case the state orthogonal to ν_e is actually a linear combination of ν_μ and ν_τ.)

standard solar model (SSM) (Bahcall, 1989; Bahcall et al., 2006; Turck-Chieze and Couvidat, 2011; Haxton et al., 2013), which is well tested and constrained by helioseismology and other Solar observations[§], and by the properties of other stars, is dominated by the *pp* chain and leads to the predicted Solar ν_e spectrum in Figure 7.48. The most important reactions are

$$p + p \rightarrow\ D + e^+ + \nu_e, \qquad D + p \rightarrow\ {}^3He + \gamma, \qquad 2\ {}^3He \rightarrow\ \alpha + 2p. \quad (7.418)$$

The first step leads to the most abundant (*pp*) neutrinos, which however, have low energy and are hard to detect. About 15% of the time, however,

$${}^3He + \alpha \rightarrow\ {}^7Be + \gamma, \qquad {}^7Be + e^- \rightarrow\ {}^7Li + \nu_e, \quad (7.419)$$

for one of the ${}^3He$, leading to the two intermediate energy discrete ${}^7Be$ lines in the ν_e spectrum. Approximately 0.02% of the chains involve the sequence

$${}^7Be + p \rightarrow\ {}^8B + \gamma, \qquad {}^8B \rightarrow\ {}^8Be^* + e^+ + \nu_e, \quad (7.420)$$

which leads to the ${}^8B$ neutrinos. These are insignificant numerically, but because of their much higher energy are easiest to detect. The flux of *pp* neutrinos is well constrained by the observed Solar luminosity, but the predicted ${}^7Be$ and (especially) ${}^8B$ fluxes are much more uncertain because of their strong dependence on the temperature of the Solar core, low energy cross sections, and the Solar composition.

[§]Recent observations of heavy element abundances yield lower values than earlier (less precise) determinations, creating some tension with helioseismology (e.g., Haxton et al., 2013).

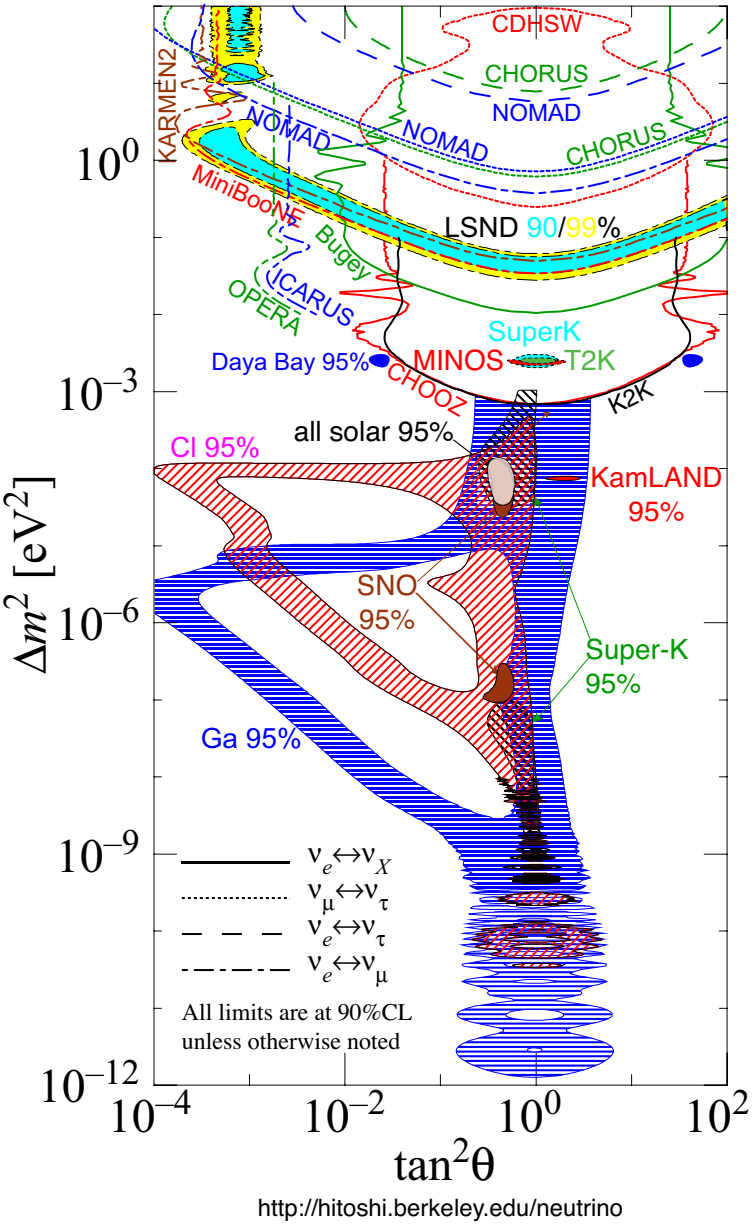

FIGURE 7.47
Neutrino oscillation results, showing the Solar/KamLAND and atmospheric neutrino oscillation regions, the LSND and MiniBooNE regions, and various exclusion regions. Plot courtesy of H. Murayama.

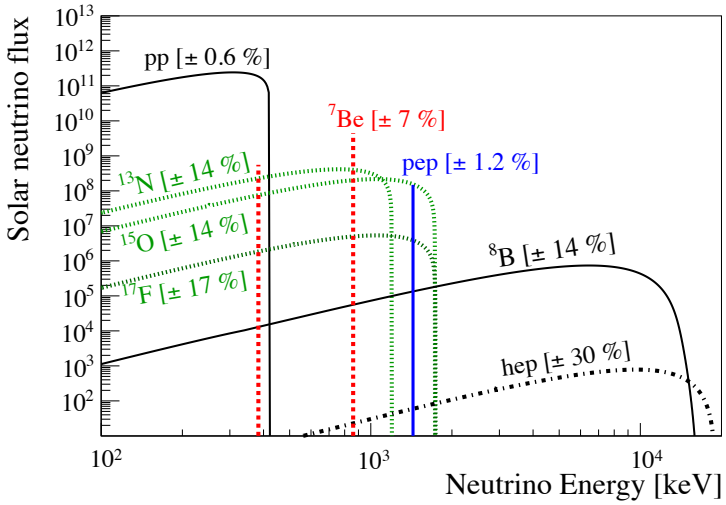

FIGURE 7.48
Spectrum of Solar neutrinos predicted by the standard solar model, from (Bellini et al., 2014a). The gallium and liquid scintillator experiments are sensitive to the *pp* and higher energy neutrinos, the Homestake chlorine experiment to the higher energy ^{7}Be line and above, and the water Cherenkov experiments to the ^{8}B neutrinos. The other (minor) reactions, i.e., the *hep*, *pp*, and *CNO* neutrinos, are described in (Bahcall, 1989).

The first Solar neutrino experiment was the radiochemical ^{37}Cl experiment, which used a 10^5 gallon tank of cleaning fluid placed deep underground in the Homestake gold mine in South Dakota to shield from cosmic rays. Ray Davis and collaborators observed the decays of the ^{37}Ar atoms produced in the reaction $\nu_e + ^{37}Cl \rightarrow e^- + {}^{37}Ar$ and separated chemically from the tank. The original goal was to probe the Solar interior, but by the early 1970s it was apparent that they were only observing $\sim 1/3$ of the expected flux, beginning a 30-year enterprise that ultimately explored both Solar and neutrino physics.

The Homestake results were confirmed in the late 1980s by the Kamiokande II water Cherenkov experiment in Japan, which also searched for proton decay and observed neutrinos from Supernova 1987A and atmospheric neutrinos. The reaction $\nu e^- \rightarrow \nu e^-$ was mainly sensitive to ν_e's, but because of WNC scattering had about 1/7 sensitivity to $\nu_{\mu,\tau}$, which could be produced if the ν_e's oscillated. They observed about 1/2 of the expected (without oscillations) Solar flux, and also confirmed that the ν's actually came from the Sun because the e^- direction was correlated with that of the neutrino. These results were later confirmed and improved by the successor SuperKamiokande experiment (Abe et al., 2011b; Sekiya, 2013), which extended the analysis to

lower energies.

The water Cherenkov experiments were only sensitive to the upper part of the ^8B spectrum and the much rarer *hep* neutrinos. The Homestake experiment had a lower threshold and was sensitive to more of the ^8B spectrum and to some extent the ^7Be and *pep* neutrinos. The reduced fluxes that they observed could have been due to uncertainties in the standard solar model (e.g., by a 5% reduction in the temperature of the core) or other astrophysical effects, or to neutrino oscillations/transitions into ν_μ, ν_τ, or sterile neutrinos. To distinguish these possibilities, radiochemical experiments on gallium, using the reaction $\nu_e + {}^{71}Ga \rightarrow \ e^- + \ {}^{71}Ge$, were carried out in the 1990s. This has a much lower threshold (233 keV) than the chlorine reaction (814 keV), allowing detection of the much more numerous *pp* neutrinos. An observation comparable to the SSM prediction would have suggested that the Homestake and (Super)Kamiokande deficits were due to astrophysical effects, while a reduction comparable to that for ^8B would have indicated neutrino oscillations. Eventually three gallium experiments, GALLEX and GNO in the Gran Sasso and SAGE in the Baksan lab in Russia, were carried out, indicating $\gtrsim 50\%$ of the predicted SSM flux.

No one type of these experiments by itself could definitively exclude an astrophysical explanation, especially allowing for large modifications of the SSM, but the three types together constituted a rough measurement of the distortion of the neutrino energy spectrum. Including the Solar luminosity constraint and assuming that plausible astrophysical effects would not significantly modify the shape of the ^8B spectrum, it was found that the ^7Be neutrinos would have had to be suppressed much more than the ^8B ones (Hata et al., 1994). Because the ^8B is made from ^7Be, this effectively excluded astrophysical explanations, but allowed neutrino oscillations or transitions (which *could* modify the shape of the ^8B spectrum).

The case was clinched a decade later by the SNO (Sudbury Neutrino Observatory) heavy water experiment in Canada (Aharmim et al., 2005, 2013). SNO observed Cherenkov radiation from electrons and photons from neutron capture, allowing then to measure both WCC and WNC scattering from deuterium by

$$\nu_e + D \rightarrow e^- + p + p, \qquad \nu_x + D \rightarrow \nu_x + p + n, \tag{7.421}$$

where ν_x is any active neutrino. They also measured the electron scattering reaction $\nu e^- \rightarrow \nu e^-$, consistent with but less precisely than SuperKamiokande. The combination of these measurements allowed the SNO collaboration to separately determine the fluxes of ν_e and of $\nu_\mu + \nu_\tau$ arriving at the Earth, as shown in Figure 7.49. The result was that the sum of the three was consistent with the SSM flux prediction, and that about 2/3 had oscillated or been converted into $\nu_{\mu,\tau}$ (assuming that there are no sterile neutrinos involved), confirming both the SSM and neutrino oscillations.

More recently, the Borexino experiment (Bellini et al., 2014a,b) has studied Solar neutrinos to much lower energy by observing $\nu e^- \rightarrow \nu e^-$ in a liquid

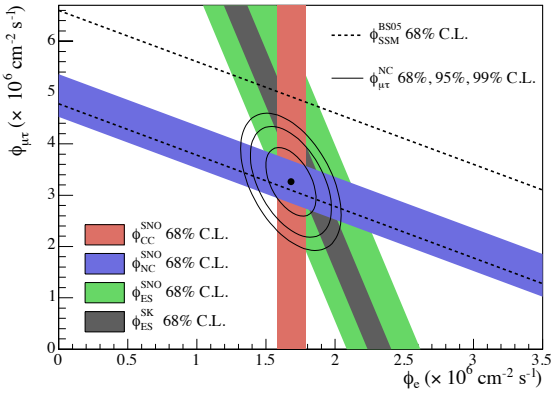

FIGURE 7.49
Fluxes from the WCC and WNC reactions in the SNO heavy water experiment, and on electron scattering (ES) from SuperKamiokande and SNO, compared with the standard solar model expectation. Plot reproduced with permission from (Aharmim et al., 2005).

scintillator detector in the Gran Sasso Laboratory. Borexino has measured the rates for the upper ^7Be neutrino line, *pp* neutrinos, and ^8B neutrinos at lower energy than the water Cherenkov experiments. They also measured the rare *pep* neutrinos and set limits on neutrinos from the CNO cycle.

The survival probabilities $P_{\nu_e \to \nu_e}$ as measured by Borexino and the other experiments are shown as a function of neutrino energy in Figure 7.50.

At various stages the Solar neutrino experiments allowed a number of solutions for neutrino oscillation parameters. These included the $\Delta m^2 \sim 10^{-10}$ eV^2 vacuum oscillation solutions, for which the Earth-Sun distance was of $\mathcal{O}(L_{osc})$. The matter effects were unimportant for these solutions and oscillations during the propagation between the Sun and Earth dominated. There were also several solutions with higher Δm^2, for which matter effects were significant. Eventually, the combination of the observed rates from the different reactions, as well as limits on the distortion of the ^8B spectrum and constraints (Bellini et al., 2014a) on or observation (Renshaw et al., 2014) of energy-dependent day-night asymmetries (due to reconversion to ν_e in the Earth), established the large mixing angle (LMA) solution characterized by (Bellini et al., 2014a)

$$\Delta m^2_\odot = 5.4^{+1.7}_{-1.1} \times 10^{-5} \text{ eV}^2, \qquad \tan^2\theta_\odot = 0.468^{+0.031}_{-0.044}. \tag{7.422}$$

A more detailed analysis would involve all three neutrinos. However, it will turn out that θ_{13} in (7.360) is small. This justifies the two-neutrino formalism

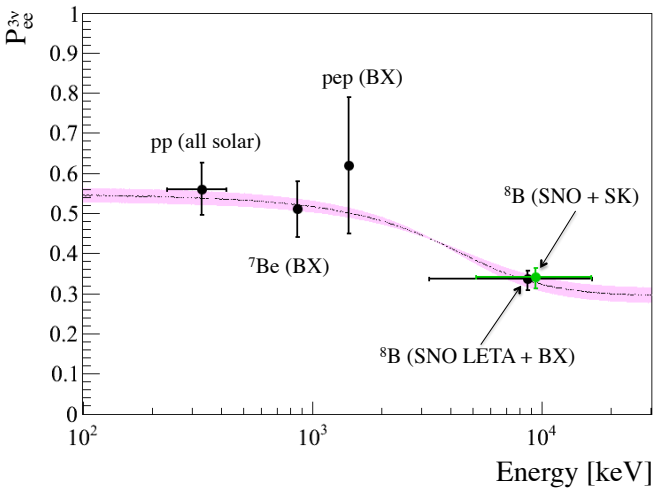

FIGURE 7.50
Survival probabilities $P_{\nu_e \to \nu_e}$ as a function of energy, compared with the predictions of the large mixing angle (LMA) solution. From (Bellini et al., 2014a). Not included is the recent direct measurement of the *pp* flux from the Phase 2 of Borexino (Bellini et al., 2014b).

to a good approximation, and allows the identification $\Delta m^2_\odot \sim \Delta m^2_{21}$ and $\theta_\odot \sim \theta_{12}$.

The Solar angle $\theta_\odot$ is large but not maximal, i.e., $\theta_\odot \neq \pi/4$, so the ν_e is predominantly ν_1, while ν_2 consists mainly of a linear combination of ν_μ and ν_τ. The characteristics of the LMA solution are that a higher energy ν_e encounters an adiabatic MSW resonance, emerging from the Sun in an essentially pure ν_2 mass eigenstate. This does not oscillate, and has a probability $\sin^2\theta_\odot \sim 0.32$ of interacting as a ν_e. The density is too low for a resonance for the lower energy neutrinos, so they emerge from the Sun as a ν_e, arriving at the Earth with an average survival probability $\sim 1 - \frac{1}{2}\sin^2 2\theta_\odot \sim 0.57$. The sign of $\Delta m^2_\odot > 0$ is determined from the matter effect. Subsequently, the LMA solution was dramatically confirmed by the KamLAND reactor experiment in Japan (see below), which yielded a more precise (but slightly higher) $\Delta m^2_\odot$.

A number of other particle physics interpretations for the Solar neutrino deficits and other observations have been advanced, including oscillations into sterile neutrinos (Cirelli et al., 2005); resonant spin-flavor transitions involving a large magnetic moment (Pulido, 1992; Shi et al., 1993; Giunti and Studenikin, 2014); neutrino decay (Beacom and Bell, 2002); new flavor changing or conserving interactions (Friedland et al., 2004; Miranda et al.,

2006; Ohlsson, 2013); mass varying neutrinos due to interactions with the environment (Kaplan et al., 2004); Lorentz, CPT, or equivalence principle violations (Glashow et al., 1997; Gonzalez-Garcia and Maltoni, 2008; Diaz and Kostelecky, 2012); or CPT-violating decoherence between the quantum components of the wave function (Barenboim and Mavromatos, 2005). All of these are now excluded as the dominant effect for Solar neutrinos, although they could still exist as perturbations on the basic picture.

Atmospheric Neutrinos

Although the first indications of neutrino oscillations involved the Solar neutrinos, the first unambiguous evidence came from the oscillations of atmospheric neutrinos. Atmospheric neutrinos result from pion and muon decays, which are produced in the upper layers of the atmosphere due to the interaction of primary cosmic rays. The data from the Kamiokande and SuperKamiokande water Cherenkov detectors indicated the disappearance of ν_μ and $\bar{\nu}_\mu$ (which will not be further distinguished in this paragraph). This was first seen in the ratio of the ν_μ/ν_e fluxes, and later confirmed dramatically by the zenith angle distribution of ν_μ events, with SuperKamiokande officially announcing their results in 1998 (Fukuda et al., 1998). Results from other experiments such as IMB, MACRO, and Soudan confirmed the results. The details of the SuperKamiokande ν_e and ν_μ events (Abe et al., 2013a) as well as constraints from other experiments show that the dominant effect is the oscillations of ν_μ into ν_τ, and not ν_e or a sterile ν_S. SuperKamiokande obtained (Abe et al., 2011a) the 90% c.l. ranges

$$|\Delta m^2_{atm}| \sim (1.7 - 3.0) \times 10^{-3}\ \text{eV}^2, \qquad \tan^2\theta_{atm} \sim (0.58 - 1.72). \quad (7.423)$$

To a good approximation, $\Delta m^2_\odot$ can be neglected for the atmospheric neutrinos, justifying the two-neutrino formalism with $\Delta m^2_{atm} \sim \Delta m^2_{32}$. From (7.405) and (7.360) the effective angle for ν_μ survival is

$$\sin^2\theta_{atm} = |\mathcal{V}_{\mu 3}|^2 = s^2_{23}c^2_{13}, \quad (7.424)$$

so that $\theta_{atm} \sim \theta_{23}$ for small θ_{13}.

The $\tan^2\theta_{atm}$ range corresponds to $\sin^2 2\theta_{atm} > 0.93$. The data is consistent with maximal mixing ($\theta_{atm} = \pi/4$), and in fact the best fit is for that value. There are no Earth matter effects for $\nu_\mu \to \nu_\tau$, so the sign of Δm^2_{atm} is not determined. The atmospheric neutrino fluxes were subsequently measured in the MINOS detector (Adamson et al., 2012), which is the steel-scintillator far detector for the NuMI-MINOS long-baseline facility described below. MINOS obtained results consistent with SuperKamiokande.

Both experiments also showed that the ν_μ and $\bar{\nu}_\mu$ disappearance parameters are the same within uncertainties, consistent with CPT. This was done by MINOS on an event by event basis by exploiting the magnetization of the detector, while SuperKamiokande utilized the differences in the distortions of

the zenith angle distributions. The recent long-baseline experiments further confirm the atmospheric neutrino results.

Comments similar to those for Solar neutrinos concerning alternatives to neutrino oscillations apply to the atmospheric results. It is interesting that the atmospheric neutrino oscillations are a quantum mechanical coherence effect on the size scale of the Earth.

Accelerator Neutrinos

Early *short-baseline* accelerator experiments included ν_μ (or $\bar{\nu}_\mu$) disappearance experiments and searches for ν_e or ν_τ appearance at CERN, Brookhaven, and Fermilab (e.g., Gonzalez-Garcia and Maltoni, 2008). These typically involved energies in the $1 - 100$ GeV range and distances $100 - 1000$ m, with sensitivities to $\Delta m^2 \gtrsim 10^{-1} - 1$ eV^2 for large mixing. No evidence for oscillations was found (but see the discussion of possible sterile neutrinos below).

More recently, there have been *long-baseline* experiments involving beams from KEK (K2K) and J-PARC (T2K) to SuperKamiokande, Fermilab to the Soudan mine (NuMI/MINOS), and CERN (CNGS) to the OPERA and ICARUS detectors in the Gran Sasso Laboratory (for a review, see Feldman et al., 2013). These experiments monitor the initial neutrino fluxes by their interactions in a near detector close to the accelerator (or by detailed simulations of the neutrino beam in CNGS). The K2K and T2K experiments have baselines $L \lesssim 300$ km, while those using the Fermilab and CERN beams have $L \sim 735$ km. These are sensitive to much lower Δm^2 than the traditional short-baseline accelerator experiments, down into the atmospheric neutrino region $\sim 10^{-3}$ eV^2. The K2K, MINOS (Adamson et al., 2014), and T2K (Abe et al., 2013b) results have confirmed the SuperKamiokande and MINOS atmospheric oscillation results. They have significantly reduced the uncertainty in $|\Delta m^2_{32}|$, as can be seen in Figure 7.51, and also suggest that θ_{23} may be non-maximal. The results are consistent with dominantly $\nu_\mu \to \nu_\tau$ oscillations[¶], and that the ν_μ and $\bar{\nu}_\mu$ survival probabilities are the same. They have also observed evidence for sub-dominant oscillations into ν_e, which is associated with the (small) angle θ_{13}, and obtained strong constraints on possible sterile neutrinos.

In the future it should be possible to search for leptonic CP violation and determine the type of neutrino hierarchy via matter effects in long-baseline ν_e and $\bar{\nu}_e$ appearance experiments. These include the *off-axis*[‖] T2K and NOνA (810 km, with a beam from Fermilab to Ash River, Minnesota) experiments, both of which will benefit from planned upgrades to the intensity of the neutrino beams. There are also proposals for next generation experiments, including LBNE (Adams et al., 2013) (1300 km, from Fermilab to the

[¶]The OPERA hybrid emulsion experiment has directly observed several ν_τ appearance events (Agafonova et al., 2014).

[‖]The neutrino energy spectrum is narrower away from the center of the beam.

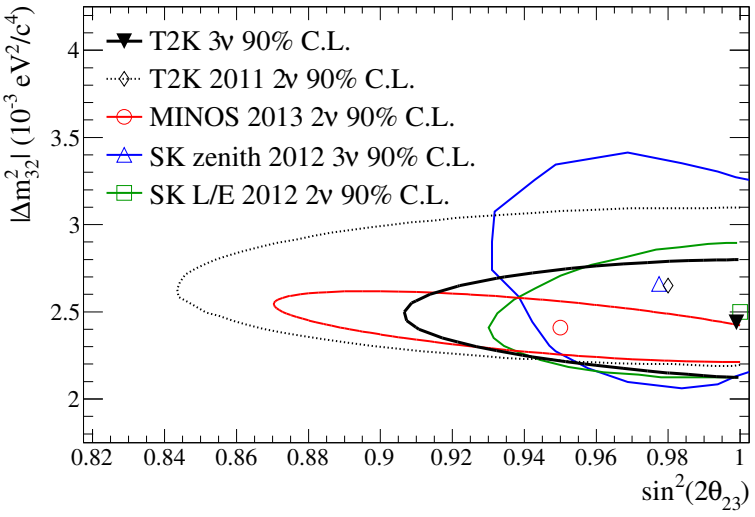

FIGURE 7.51
90% c.l. regions for the atmospheric neutrino oscillation parameters from atmospheric and long-baseline data, from (Abe et al., 2013b).

Sanford Laborary in Homestake) and LBNO (Agarwalla et al., 2014) (2300 km, from CERN to Pyhäsalmi, Finland). Both would feature liquid argon far detectors. Another proposal is Hyper-Kamiokande (Kearns et al., 2013), a megaton water Cherenkov detector near SuperKamiokande. These detectors would also be sensitive to proton decay, and to supernova, Solar, and atmospheric neutrinos.

Reactor Neutrinos

There were a number of early reactor disappearance experiments, which compared the flux of $\bar{\nu}_e$ at short distances, $L \sim (10 - 100)$ m, with the theoretical expectations based on the known reactor energy output (see, e.g., Gonzalez-Garcia and Maltoni, 2008). These were sensitive down to $|\Delta m^2| \gtrsim 10^{-2}$ eV^2 for large mixing. They did not report any evidence for oscillations at the time, although a recent reanalysis of the expected fluxes (Mention et al., 2011) has suggested the possibilitiy of disappearance into sterile neutrinos, as described below.

The subsequent (around 2000) Palo Verde and Chooz experiments had longer baselines of $\mathcal{O}(1$ km), and were able to exclude significant $\bar{\nu}_e$ mixing for $|\Delta m^2| \gtrsim 10^{-3}$ eV^2 (e.g., Qian and Wang, 2014). Since the atmospheric neutrino results already established $|\Delta m^2_{32}| >$ few $\times 10^{-3}$ eV^2, this implied that $\sin^2 2\theta_{13} < 0.12$ ($\tan^2 \theta_{13} < 0.032$) at 90% c.l., which is small compared to the other leptonic mixing angles but comparable to quark mixings. The

value of θ_{13} is critical: the small value motivated models of neutrino mass in which θ_{13} vanishes or is tiny (Section 7.7.6). Furthermore, the possibility of observing leptonic CP violation (and significant matter effects in terrestrial experiments) depends on having a sufficiently large θ_{13}.

For these reasons, an intensive effort was undertaken to observe or constrain θ_{13} for $|\Delta m^2|$ in the atmospheric neutrino range (Qian and Wang, 2014). Hints of a nonzero value were obtained from a global analysis of existing data (Fogli et al., 2008), but the first direct experimental evidence was obtained around 2011 by the MINOS and T2K long-baseline accelerator experiments, which observed $\nu_\mu \to \nu_e$ appearance at the several σ level. Subsequently, the Double Chooz** reactor experiment reported evidence for $\bar{\nu}_e$ disappearance. Finally, the Daya Bay†† reactor experiment in China observed $\bar{\nu}_e$ disappearance at greater than 5σ, establishing that $\theta_{13} \neq 0$. RENO in South Korea also observed disappearance at nearly 5σ. Currently, The Daya Bay value (An et al., 2014) is

$$\sin^2 2\theta_{13} = 0.090^{+0.008}_{-0.009} \quad \Rightarrow \quad \tan^2 \theta_{13} = 0.024^{+0.002}_{-0.003}, \tag{7.425}$$

which is 10σ away from zero, and also close to the earlier upper limits.

Because of the characteristic $\Delta m^2 L/E$ dependence of neutrino oscillations, long-baseline ($L \sim$ hundreds of km) experiments can probe to much lower Δm^2 than the traditional short-baseline ones. The KamLAND experiment was a liquid scintillator detector at the location of the original Kamiokande detector (Araki et al., 2005). It observed a $\bar{\nu}_e$ flux from a number of Japanese reactors, at a typical distance $L \sim 200$ km, which allows one to probe down into the region of the LMA Solar neutrino solution. The KamLAND results dramatically confirmed the LMA interpretation of the Solar neutrino deficit and gave a much more precise value for $\Delta m^2_\odot$ around 7.5×10^{-5} eV^2. There is some tension between subsequent Solar neutrino observations and KamLAND, as can be seen in Figure 7.52, but the basic correctness of the picture is likely to remain. KamLAND was also able to directly observe the L/E dependence expected from neutrino oscillations, and to observe $8B$ and ^7Be Solar neutrinos.

Geoneutrinos

Low-energy antineutrinos from radioactive decays in the Earth were initially an important background for the liquid scintillator experiments. Both KamLAND and Borexino were eventually able to measure the flux of these geoneutrinos from the decay chains of ^{232}Th and ^{238}U (but not those from ^{40}K),

**Double Chooz is a follow up to the Chooz experiment, which will have near and far detectors. The initial result on $\bar{\nu}_e$ disappearance was obtained with only the far detector.

††The Daya Bay experiment consists of a number of near ($L \sim 0.5$ km) and far ($L \sim 1.5$ km) detectors relative to a reactor complex. Comparison of the fluxes in the near and far detectors essentially eliminates the uncertainties from the initial reactor flux. RENO is configured analogously.

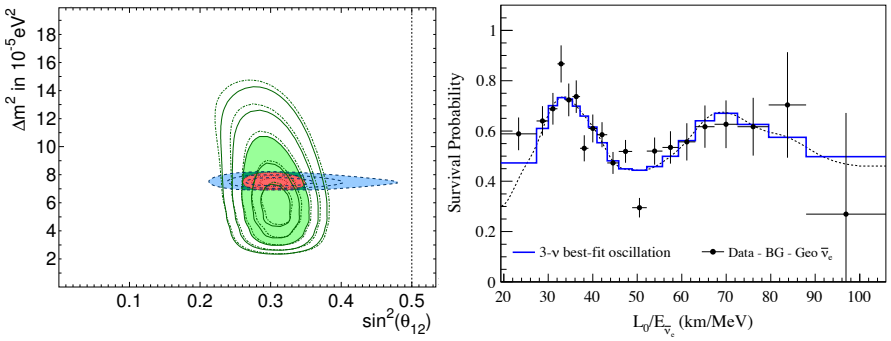

FIGURE 7.52
Left: Oscillation parameters determined from SuperKamiokande Solar neutrino data at 1-5σ for 2 d.f. (green solid contours), or the combination of SuperKamiokande and SNO (dot-dashed), compared with the KamLAND results at 1-3σ (blue dashed contours), and the combined fit (red dotted). From (Sekiya, 2013). Right: L/E dependence of the $\bar{\nu}_e$ survival probability as determined by KamLAND. From (Gando et al., 2013b).

constraining models of the element abundances and interior heating of the Earth (for a review, see Ludhova and Zavatarelli, 2013).

High Energy Neutrinos

Ultra-high energy neutrinos, e.g., produced by pion decay, are potentially an extremely useful probe of violent astrophysical events. They are not significantly absorbed in interstellar/intergalactic media, and (unlike cosmic ray protons or nuclei) they are not deflected in magnetic fields and therefore point back to their sources. Neutrino telescopes are large detectors with good ability to measure the direction of the incoming neutrino. These typically involve strings of photomultiplier tubes deployed deep underwater (such as the ANTARES array in the Mediterranean) or under ice (such as the km^3 IceCube array at the South Pole). The expected cross sections for ultra-high energy neutrinos are reviewed in (Gandhi et al., 1998), and the experiments in (Katz and Spiering, 2012; Gaisser and Halzen, 2014).

The IceCube collaboration has recently observed (Aartsen et al., 2013) two events with energies above 1 PeV (10^6 GeV), the highest energy neutrinos ever observed, as well as 26 additional events with energies above 30 TeV. These are most likely extra-terrestrial, and could be due to galactic or extra-galactic astrophysical events, or to exotic particle physics such as super-heavy dark matter decays (see Anchordoqui et al., 2014). IceCube has also observed atmospheric oscillations at much lower energies (but still higher energy than the other atmospheric experiments).

In the future, IceCube may sensitive to the *Glashow resonance* (Glashow,

1960), in which the cross section for $\bar{\nu}_e$ scattering is greatly enhanced at 6.3 PeV due to the resonant scattering $\bar{\nu}_e e^- \to W^- \to X$ off of electrons in the atmosphere. It may also be able to observe neutrino flavor ratios[‡‡], constrain oscillations into sterile states, and may be sensitive to the hierarchy. It would also be sensitive to nonstandard interactions and could observe galactic supernova neutrinos.

Proposed upgrades and future neutrino telescopes are reviewed in (Katz and Spiering, 2012).

Possible Sterile Neutrinos

There are several indications of mixing between active and light (eV scale) sterile neutrinos, as well as many null experiments. For reviews, see, for example, (Abazajian et al., 2012; Palazzo, 2013; Kopp et al., 2013).

The LSND experiment at Los Alamos observed a 3.8σ excess of $\bar{\nu}_e p \to e^+ n$ events in a $\bar{\nu}_\mu$ beam obtained from μ^+ decay at rest (Aguilar-Arevalo et al., 2001). This suggested $\bar{\nu}_\mu \to \bar{\nu}_e$ oscillations* with $L \sim 30$ m and $L/E \sim (0.4 - 1.5)$ m/MeV, corresponding to $|\Delta m^2_{LSND}| \sim (0.2 - 10)$ eV^2 and small mixing. This was not confirmed by the KARMEN2 experiment at Rutherford, but there was a small parameter region allowed by both. The LSND result, along with the Solar and atmospheric oscillations, would imply three or more distinct Δm^2's, and therefore at least four light neutrinos that mix with each other. The extra neutrinos would have to be sterile because the invisible Z width result $N_\nu^{inv} = 2.990 \pm 0.007$ does not allow a fourth light active neutrino.

Subsequently, the Fermilab MiniBooNE experiment searched for ν_e appearance in a ν_μ beam with $L \sim 541$ m and $E_\nu \sim (20 - 1250)$ MeV, and later for $\bar{\nu}_e$ appearance in a $\bar{\nu}_\mu$ beam. The final MiniBooNE results[†] (Aguilar-Arevalo et al., 2013) showed excesses in both ν_e and $\bar{\nu}_e$-like events. The $\bar{\nu}_e$ excess was consistent with the LSND oscillation signal, though with a lower statistical significance. The energy dependence of the ν_e excess was only marginally consistent with the other results, however, at least within the framework of a single sterile neutrino.

[‡‡]Stable neutrinos produced by pion decay in distant sources should arrive at the Earth in the ratio $\nu_e/\nu_\mu/\nu_\tau = 1/1/1$ when oscillations are taken into account, while different ratios are expected from other sources, e.g., unstable neutrino decays (e.g., Baerwald et al., 2012).

*Other possibilities to account for LSND, e.g., involving CPT violation, decoherence, new interactions, extra dimensions, mass-varying neutrinos, and hybrids, are surveyed in (Gonzalez-Garcia and Maltoni, 2008).

[†]The initial MiniBooNE $\nu_\mu \to \nu_e$ analysis was restricted to $E_\nu > 475$ MeV so as to coincide with the LSND L/E range. No excess was observed in this range, although there was an anomalous excess of ν_e events at lower energies. The excess observed in the subsequent $\bar{\nu}_\mu$ runs stimulated considerable discussion of possible CP violation to account for the $\nu - \bar{\nu}$ difference. However, the final MiniBooNE ν_e analysis included events with E_ν down to 200 MeV. The resulting excess was mainly due to (but did not fully account for) the low energy anomaly. The LSND and MiniBooNE experiments are reviewed in (Conrad et al., 2013).

$|\Delta m^2_{LSND}|$ and the associated E/L are large compared to $|\Delta m^2_{atm}|$ and $\Delta m^2_{\odot}$. Assuming the existence of a single sterile neutrino ν_S, one can therefore treat the three largely-active states as degenerate and use the effective two-neutrino formalism in Eqs. 7.401-7.405, with $|\Delta| = |m^2_4 - m^2_{1,2,3}| = |\Delta m^2_{LSND}| \sim (0.2 - 10)$ eV^2, where m_4 is the mass of the additional (largely sterile) mass eigenstate. The effective mixing for $\bar{\nu}_\mu \to \bar{\nu}_e$ and $\nu_\mu \to \nu_e$ appearance is therefore

$$\sin^2 2\theta_{\mu e} = 4 \sin^2 \theta_{\mu\mu} \sin^2 \theta_{ee} \sim \frac{1}{4} \sin^2 2\theta_{\mu\mu} \sin^2 2\theta_{ee}, \tag{7.426}$$

where $\sin^2 \theta_{\mu\mu} = |\mathcal{V}_{\mu 4}|^2$, $\sin^2 \theta_{ee} = |\mathcal{V}_{e4}|^2$, and the last expression assumes small mixing. But $\sin^2 \theta_{\mu\mu}$ and $\sin^2 \theta_{ee}$ respectively control the ν_μ and ν_e survival probabilities; e.g., the the mixing for ν_e disappearance into ν_S is $\sin^2 2\theta_{eS} = 4|\mathcal{V}^*_{e4}\mathcal{V}_{S4}|^2 \sim 4 \sin^2 \theta_{ee}$. Thus, sterile-induced oscillations $\nu_\mu \to \nu_e$ necessarily imply disappearance of both ν_μ and ν_e into ν_S, and also the absence of any CP-violating difference between ν and $\bar{\nu}$, as long as the effective two-neutrino approximation is valid. For additional sterile neutrinos one can still usually treat the (mainly) active states as degenerate. The LSND-MiniBooNE signal still typically leads to ν_μ and ν_e disappearance, although the additional parameters would allow for cancellations and for observable differences between ν and $\bar{\nu}$.

Short-baseline ($L \lesssim 100$ m) reactor experiments should be sensitive to $\bar{\nu}_e$ disappearance into a sterile neutrino for Δm^2 in the LSND range. However, in existing experiments the measured fluxes must be compared with theoretical $\bar{\nu}_e$ spectra obtained from detailed modeling of the relevant fission decay chains in the reactors. A recent reanalysis (Mention et al., 2011) obtained a predicted flux about 3% higher than earlier estimates (see also Huber, 2011), leading to the *reactor anomaly*: whereas the previous measurements were consistent with no $\bar{\nu}_e$ disappearance ($P_{\bar{\nu}_e \to \bar{\nu}_e} = 0.976 \pm 0.024$), the new theoretical spectrum suggested a 2.5σ deficit (0.943 ± 0.023), which could be due to oscillations into sterile neutrinos. Some caution is required, however, since a later analysis (Zhang et al., 2013) that took the longer-distance experiments and $\theta_{13} \neq 0$ into account[‡] found a smaller discrepancy (0.959 ± 0.029), and a later study (Hayes et al., 2014) argued that the systematic uncertainties in the flux are as large as the anomaly.

Additional evidence for sterile neutrino oscillations comes from the *gallium anomaly*. The SAGE and GALLEX Solar neutrino experiments each used intense radioactive ν_e sources (^{51}Cr, ^{37}Ar) of known intensity as a cross check on their efficiencies and on the theoretical estimate of the cross section for $\nu_e + {}^{71}Ga \to e^- + {}^{71}Ge$. The observed rates were around 2.8σ below the expectation (Giunti and Laveder, 2011), suggesting $P_{\nu_e \to \nu_e} = 0.86 \pm 0.05$ (or that the other uncertainties are underestimated).

[‡]The value of θ_{13} is insensitive to the sterile mixing (Gonzalez-Garcia et al., 2014).

The parameters obtained from a global fit (Kopp et al., 2013) to the LSND, MiniBooNE, short-baseline reactor, and gallium data for one sterile neutrino are shown in Figure 7.53. There are several solutions, with central values for $|\Delta m^2|$ around 0.3, 0.9, and 5 eV^2, all with small mixing.

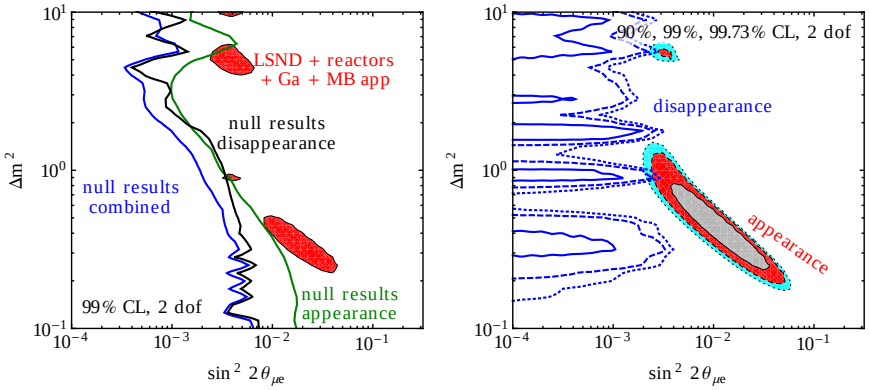

FIGURE 7.53
Left: 90% c.l. allowed regions for sterile neutrino oscillations in the two-neutrino approximation from the positive experiments, contrasted with the exclusion regions (to the right) from null experiments. Right: preferred parameter region from appearance experiments and the exclusion regions from disappearance experiments. Both plots from (Kopp et al., 2013).

There have also many negative searches for oscillations involving sterile neutrinos (for reviews, see Abazajian et al., 2012; Conrad and Shaevitz, 2012; Kopp et al., 2013). These include searches for ν_e or $\bar{\nu}_e$ disappearance in accelerator and longer-distance reactor experiments, and global analyses of the Solar neutrinos. Similarly, there are many null results on ν_μ and $\bar{\nu}_\mu$ disappearance[§] from short and long-baseline accelerator experiments and atmospheric neutrinos, as well as searches for $\nu_\mu \to \nu_e$ appearance (above the three flavor expectations) by ICARUS and OPERA in the CNGS beam. These experiments collectively are in strong tension with the positive results in the case of one sterile neutrino (Conrad et al., 2013; Kopp et al., 2013), as can be seen in Figure 7.53. Somewhat more positive conclusions were obtained in (Giunti et al., 2013). Better agreement can be obtained if there are more parameters, such as a total of three sterile neutrinos.

[§]ν_μ oscillations into ν_τ can be distinguished from ν_S statistically by neutral current scattering, matter effects, and τ production.

As discussed in the sections on Neutrino Counting (page 419) and Neutrino Mass (page 421) there are cosmological implications for both the numbers and masses of sterile neutrinos, which could have been produced by mixing for the relevant parameters unless some new suppression mechanism is present. The actual constraints are dependent on the cosmological data set and priors. However, recent analyses (e.g., Gariazzo et al., 2013; Giusarma et al., 2014; Mirizzi et al., 2013) are broadly consistent with the Planck limits in (7.384) on page 423, with a modest preference over the case of no sterile neutrino. This would be consistent with $m_4 \sim 1$ eV (see Figure 7.53) for a moderately suppressed sterile density ($T_S < T_\nu$). However, schemes with two or more sterile states that fit the experimental data better typically involve one or more masses well above 1 eV. These would be difficult to accomodate with the cosmological data unless their production was strongly suppressed (e.g., Cirelli et al., 2005; Langacker, 2005; Hamann et al., 2010).

The situation concerning possible light sterile neutrinos and their mixing with active ones is confusing, and no compelling picture has emerged. Definitive experiments, e.g., involving intense radioactive sources, experiments very close to reactors, or specially-configured accelerator experiments, are needed to resolve the situation (for a review, see Lasserre, 2014). It is also challenging to construct a theory in which active and sterile neutrinos mix, as will be discussed in Section 7.7.6.

7.7.5 The Spectrum

Three Active Neutrinos

Most data other than the LSND results can be accommodated by three active neutrinos. The Solar and atmospheric mass-squared differences in (7.422) and (7.423) allow several possible patterns for the spectrum. Assuming that the absolute masses are comparable to the mass splittings, the sign ambiguity in Δm^2_{32} allows either the *normal hierarchy* (NH) or the *inverted hierarchy* (IH), as illustrated in Figure 7.54. The normal hierarchy is most similar to the quark spectrum, but the analogy is poor since the CKM mixing angles are all small. In both cases, the data is compatible with $m_0 = 0$, where m_0 is the lowest mass, i.e., $m_0 = m_1$ (m_3) for the normal (inverted) hierarchy.

It is also possible that the absolute masses are larger than the mass differences (the *degenerate spectrum*), perhaps as large as a few tenths of an eV each if one stretches the cosmological limits on $\Sigma = \sum_i |m_i|$ in (7.383). Either sign for Δm^2_{32} is still allowed, and both the NH and the IH smoothly merge into the degenerate spectrum as m_0 increases.

A recent global three-neutrino analysis (Gonzalez-Garcia et al., 2014) obtained

$$\Delta m^2_{21} \sim 7.50(18) \times 10^{-5}\ \text{eV}^2, \qquad |\Delta m^2_{31}| \sim 2.46(5) \times 10^{-3}\ \text{eV}^2 \quad (7.427)$$
$$\sin^2\theta_{12} \sim 0.30(1), \qquad \sin^2\theta_{23} \sim 0.45^{+0.05}_{-0.03}, \qquad \sin^2\theta_{13} = 0.022(1),$$

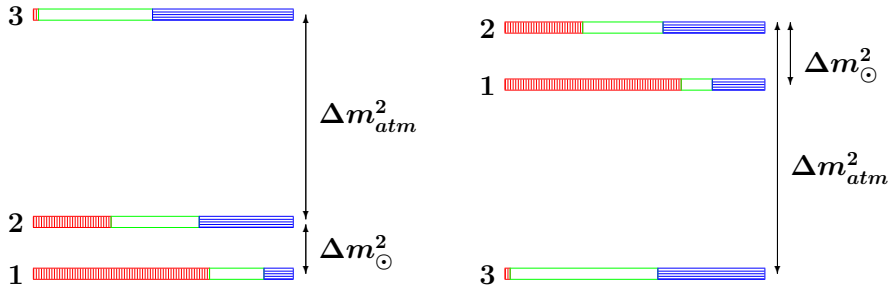

FIGURE 7.54
Left: the normal hierarchy for three neutrinos. Right: the inverted hierarchy. The red-vertical-dashed, green-open, and blue-horizontal-ruled regions indicate the central values of $|\mathcal{V}_{ei}|^2$, $|\mathcal{V}_{\mu i}|^2$, and $|\mathcal{V}_{\tau i}|^2$, respectively, using the best fit parameters. The degenerate case corresponds to adding a large common mass to each state. In this context ν_3 is usually defined as the isolated state rather than heaviest.

assuming the normal hierarchy ($\Delta m^2_{31} \gtrsim \Delta m^2_{32} > 0$). The results are similar for the inverted hierarchy except $\Delta m^2_{32} = -2.45(5) \times 10^{-3}$ eV$^2 \lesssim \Delta m^2_{31}$ and $\sin^2\theta_{23} \sim 0.58^{+0.03}_{-0.04}$. The χ^2 distributions for the parameters are shown in Figure 7.55. The analysis in (Capozzi et al., 2014) obtains similar results.

From these results it is apparent that

- There is no significant preference for either hierarchy.
- θ_{13} is nonzero but small.
- The Solar angle θ_{12} is large but non-maximal.
- There is a slight preference for non-maximal θ_{23}, as can be seen from the MINOS data in Figure 7.51, but maximal mixing ($\theta_{23} = \pi/4$) is still allowed at 90% c.l.
- The first (second) octant for θ_{23} is preferred for the normal (inverted) hierarchy.
- There is a preference for the Dirac CP phase δ to be nonzero and to lie between π and 2π. However, $\delta = \pi$ and 2π (i.e., no CP violation) are allowed at 2σ, and the entire range $0 - 2\pi$ at 3σ.

For $m_1 = 0$ in the normal hierarchy one finds $m_2 \sim 0.009$ eV and $m_3 \sim 0.050$ eV, with $m_2/m_3 \sim 0.17$, which is quite large compared to the analogous quark and charged lepton mass ratios. For the inverted hierarchy, $m_3 = 0$ implies $m_1 \sim 0.049$ eV and $m_2 \sim 0.050$ eV.

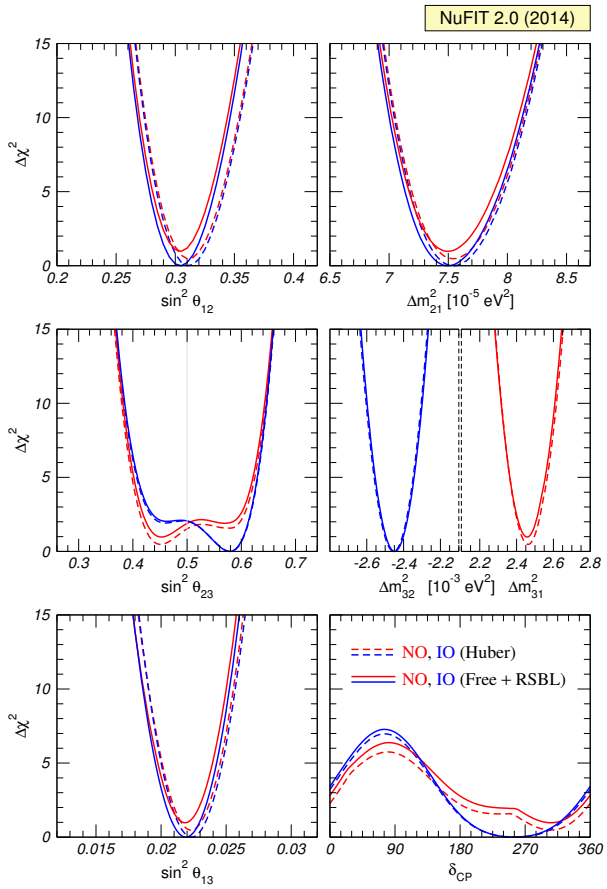

FIGURE 7.55
$\Delta\chi^2$ distributions (with repect to the best fit) from (Gonzalez-Garcia et al., 2014) for the normal (red) and inverted (blue) hierarchies, for two assumptions concerning reactor fluxes.

The predicted values for Σ are shown as functions of the lightest mass m_0 and compared with existing and projected experimental constraints in Figure 7.56. The existing cosmological limits on Σ (which, however, have a large theoretical uncertainty) are somewhat weaker than the expected values for three neutrinos except for a degenerate spectrum with $m_0 \gtrsim 0.05$ eV. Future observations may be sensitive to the entire mass range.

For three neutrinos, the effective $\beta\beta_{0\nu}$ mass is

$$m_{\beta\beta} = \left|\sum_i (\mathcal{V}_{ei})^2 m_i\right| \sim \left|e^{2i\alpha_1} c_{12}^2\, m_1 + e^{2i\alpha_2} s_{12}^2\, m_2 + e^{-2i\delta} s_{13}^2\, m_3\right|, \quad (7.428)$$

where $c_{13} \sim 1$ in the last expression. The predicted range is shown and compared with experiment in Figure 7.56. For the normal hierarchy the predicted range is very small, $m_{\beta\beta} \lesssim$ few $\times 10^{-3}$ eV, because of the small s_{13}^2, and it could even vanish due to cancellations for nonzero m_1. The range is below the sensitivity of the next generation of experiments. $m_{\beta\beta}$ is much larger for the inverted hierarchy, however. Up to small corrections from the last term, it is given by $\left|c_{12}^2\, m_1 + e^{2i(\alpha_2-\alpha_1)} s_{12}^2\, m_2\right|$, which can vary from $\sim (c_{12}^2 - s_{12}^2)\,|\Delta m_{32}^2|^{1/2}$ to $|\Delta m_{32}^2|^{1/2}$, i.e., $(0.02 - 0.05)$ eV, depending on the relative Majorana phases $(\alpha_2 - \alpha_1)$. This should be within the reach of existing and planned $\beta\beta_{0\nu}$ experiments, at least in their later phases. Both hierarchies smoothly merge in the degenerate region, where $m_{\beta\beta}$ ranges approximately from $(c_{12}^2 - s_{12}^2)\, m_0 \sim 0.4\, m_0$ to m_0.

Existing and projected β decay experiments are only sensitive to three-neutrino masses in the degenerate region, as can be seen in Figure 7.56. There, the effective β decay mass $m_{\nu_e} = \left(\sum_{i=1}^3 |\mathcal{V}_{ei}|^2 m_i^2\right)^{1/2} \sim m_0$.

Additional Sterile Neutrinos

The LSND, MiniBooNE, and reactor and gallium anomaly results, if interpreted in the context of neutrino oscillations, require the existence of one or more light sterile neutrinos that mix significantly with active neutrinos of the same helicity. One additional sterile neutrino could be accomodated in either the $2+2$ or the $3+1$ patterns, illustrated in Figure 7.57. The $2+2$ case would require that the Solar and/or atmospheric results involve a significant admixture of oscillations into the sterile neutrino. However, it is well established that neither the Solar nor the atmospheric oscillations are predominantly into sterile states, and this scheme is excluded. In the $3+1$ schemes a predominantly sterile state is separated from the others by $\sim |\Delta m_{LSND}^2|^{1/2}$. However, as mentioned in the section on Possible Sterile Neutrinos starting on page 445 any scheme with just one relevant sterile neutrino is in strong tension with other experiments. One can generalize to $3+2$, $3+3$, or $3+n$ schemes with additional sterile states heavier than the three active ones, obtaining better agreement with the other experiments, but at the expense of increased tension with the cosmological limits. One can also consider schemes in which the

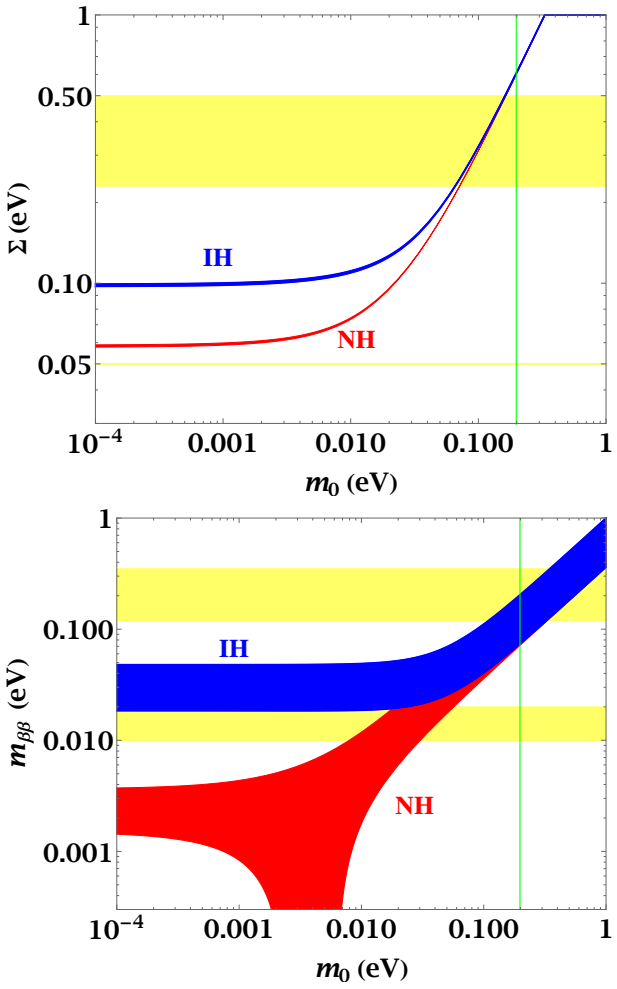

FIGURE 7.56
Predictions for the total mass Σ (top) and the effective $\beta\beta_{0\nu}$ mass $m_{\beta\beta}$ (bottom) for three neutrinos, as a function of the lightest mass m_0, for the normal hierarchy (red) and the inverted hierarchy (blue). The angles and masses are allowed to vary over their 1σ ranges, while the phases $\alpha_{1,2}$ and δ vary from 0 to 2π. In the upper figure the light yellow band is an approximate spread of upper limits from cosmology, corresponding to different data sets and priors. The lower yellow line is an estimate of future sensitivity. The vertical green line is the upper limit on $m_{\nu_e} \sim m_0$ anticipated from tritium β decay. The upper (lower) yellow bands represent the existing experimental upper limit (anticipated future sensitivity), with the widths of the bands due to uncertainties in the nuclear matrix elements.

sterile neutrinos are lighter than the active ones, or in which some are lighter and some heavier. However, these are even more difficult to reconcile with the cosmological limit on Σ, since each of the three active states must be heavier than $|\Delta m^2_{LSND}|^{1/2}$.

Sterile neutrinos can give significant contributions to the effective masses for β decay and $\beta\beta_{0\nu}$ in (7.381) and (7.385), especially if there are more than one (e.g., Barry et al., 2011). However, $m_{\beta\beta}$ can also vanish due to cancellations (i.e., if the (e, e) element of the Majorana mass matrix vanishes).

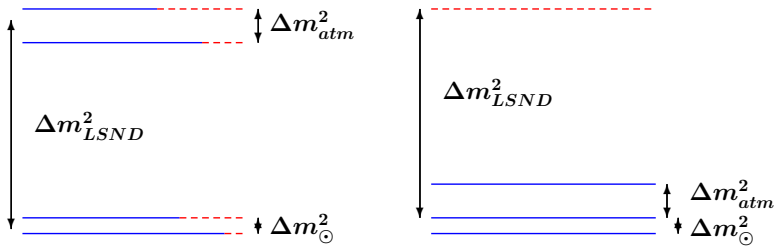

FIGURE 7.57
Left: an example of a $2 + 2$ pattern. Right: a $3 + 1$ pattern. The red-dashed (blue-solid) lines indicate qualitatively the fractions of sterile (active) neutrinos prior to small mixings. Other patterns correspond to the inverted hierarchy for the atmospheric neutrinos or to placing the largely sterile state in the $3 + 1$ case on the bottom.

7.7.6 Models of Neutrino Mass

There is an enormous number of models of neutrino mass and mixing, as reviewed in (King, 2004; Mohapatra and Smirnov, 2006; Mohapatra et al., 2007; Strumia and Vissani, 2006; Albright, 2009; Ma, 2009; Altarelli and Feruglio, 2004, 2010; Langacker, 2005, 2012; Barger et al., 2012; Antusch, 2013). Here we mention the major issues and possibilities.

General Considerations

There are a number of general issues concerning neutrino mass, including

- Are the masses Dirac or Majorana?

  The only distinction between Dirac or Majorana neutrinos in the standard model is the type of mass term and associated Yukawa interac-

tions[¶]. That is, both active and sterile neutrinos are described by Weyl two-component spinors, and in the massless limit any sterile spinors decouple.

Majorana masses have several advantages: they are not forbidden by any unbroken gauge symmetry, the active Majorana masses can be naturally small by the seesaw mechanism, and they may be connected to the leptogenesis mechanism for the baryon asymmetry. However, Dirac masses cannot be excluded: Majorana masses can be forbidden in a field theory by a conserved global lepton number symmetry[‖], there are a number of possible mechanisms for small Dirac masses, and there are alternative mechanisms for the baryon asymmetry (Chapter 8).

- Why are the masses so small compared with those of the quarks and charged leptons?

  One possibility is that the neutrinos masses are associated with higher-dimensional operators in the fundamental or effective low-energy theory, i.e., they are suppressed by powers of S/M, where M is a large new-physics scale and $S \ll M$. Usually, S is associated with a symmetry breaking scale, such as the $SU(2)$-breaking scale for the seesaw model or the scale of a new symmetry which forbids the lowest-order Dirac Yukawa coupling. The latter possibility generally implies the existence of new physics around S.

  Another mechanism involves exponential suppressions. These can occur, for example, in some superstring theories in which underlying $U(1)$ gauge symmetries are broken at the string scale. These can re-emerge as global symmetries at the perturbative level of the low-energy theory, broken by exponentially-small *D instantons* (e.g., Blumenhagen et al., 2009; Cvetič and Halverson, 2011).

  Other possibilities include small wave function overlaps in extra dimensions, couplings which only occur at loop level, and anthropic arguments (Tegmark et al., 2005).

- Why are the masses (or at least the mass-squared differences) in a hierarchical structure?

  Mass hierarchies may arise from the *Froggatt-Nielsen mechanism* (Froggatt and Nielsen, 1979), i.e., different elements of a Dirac or Majorana

[¶]There could also be a distinction if there are BSM interactions.

[‖]It is generally believed that conserved global symmetries are not possible in string theory or other theories of quantum gravity (Banks and Dixon, 1988; Witten, 2001). However, models descended from string constructions may suppress Majorana masses because of underlying symmetries and selection rules. In particular, gravitationally-induced Majorana mass terms for the active neutrinos may be of $\mathcal{O}(\nu^2/M_P) \lesssim 10^{-5}$ eV, and perhaps very much smaller, i.e., they may be too small to be relevant.

mass matrix are suppressed by different powers of a discrete or continuous symmetry-breaking parameter. This parameter is often regarded as the vacuum expectation value of a scalar field known as a *flavon*[**]. An alternative possibility involves wave function overlaps or particle locations in extra dimensions. For example, three-point vertices in intersecting brane string constructions, can be large for particles close to each other or exponentially suppressed if they are well separated. Both possibilities are similar in spirit to (and can occur simultaneously with) mechanisms for the small overall neutrino mass scale mentioned above, though they may differ in detail.

In fact, the neutrino mass hierarchies are not particularly large compared to those for the quarks and charged leptons ($\left|\Delta m^2_{31}/\Delta m^2_{21}\right|^{1/2} \sim 5.7$), and it is possible that their masses are essentially random numbers (*anarchy*)(Hall et al., 2000; de Gouvea and Murayama, 2012; Lu and Murayama, 2014).

- Why do the leptonic mixings have the observed pattern, and are they related to the (apparently different) pattern of quark mixings?

  The large mass hierarchies and small mixing angles in the quark sector suggest that the two are closely related, e.g., they may both be associated with different orders of family symmetry breaking, or with geometrical effects in extra dimensions.

  The situation is less clear for the neutrinos, for which there are two large and one small mixing angle, and only moderate hierarchies. Most theoretical work assumes that the structure of the leptonic mixing can be described by an underlying (probably broken) continuous or discrete symmetry, and in many but not all models the same symmetries account for the mass hierarchies. However, the observations are also consistent with random (anarchical) values for the parameters. In practice, an anarchical spectrum could be associated with superstring theory, which may have an enormous *landscape* of possible vacua, each with different values of the parameters.

  The general issues of the fermion spectrum and mixings are further ciscussed in Chapter 8.

- Is there leptonic CP violation?

  CP violation in the quark sector was surprising when it was first observed, and it leads to the question of whether similar effects are present in the leptonic sector. CP violation is also necessary for leptogenesis,

[**]Another possibility is that the Yukawa couplings are actually the vacuum expectation values of a number of flavons, determined by the minimization of a potential (Alonso et al., 2013).

though not necessarily in the PMNS matrix. With the benefit of hindsight, however, CP breaking might have been anticipated: many parameters in field theory are complex numbers, and CP violation is expected if the system is sufficiently complicated that the complex phases cannot all be absorbed by field redefinitions. It is now understood that no such phases are possible in QCD[††], QED, or in the weak neutral current. However, there *can be* observable phases in the quark and lepton mixings. Almost any model of neutrino masses and mixings can lead to CP violation unless CP is explicitly imposed.

We now turn to specific classes of models.

Dirac Masses

There are several possibilities for suppressing h_ν in the Yukawa interaction

$$-\mathcal{L}_{Yuk} = \sqrt{2} h_\nu \left(\bar{\ell}_L \tilde{\phi} \nu_R + \bar{\nu}_R \tilde{\phi}^\dagger \ell_L \right) \tag{7.429}$$

(cf., Eq. 7.13 on on page 285) to obtain a small Dirac mass. Usually one assumes that h_ν is forced to vanish at tree-level by some additional symmetry, such as an extra $U(1)'$ gauge symmetry and/or due to an underlying superstring construction. It is possible, however, that higher-dimensional operators of the form

$$-\mathcal{L}_{HDO} = \sqrt{2} \frac{\Gamma_D}{M^p} \left(\phi_S^p \bar{\ell}_L \tilde{\phi} \nu_R + \phi_S^{\dagger p} \bar{\nu}_R \tilde{\phi}^\dagger \ell_L \right) \tag{7.430}$$

are allowed by the symmetries (e.g., Cleaver et al., 1998; Langacker, 2012), where ϕ_S is some SM-singlet spin-0 field and M is a new physics scale, such as the Planck mass. This is illustrated for $p = 1$ in Figure 7.41. If ϕ_S acquires a VEV $\langle \phi_S \rangle \equiv S$, an effective Yukawa coupling $h_{\nu_{eff}} = \Gamma_D (S/M)^p$ will be generated, which can be very small for $S \ll M$. For example, $\Gamma_D = 1$, $M = M_P$, $p = 1$, and S at an intermediate scale $\sim 10^7$ GeV yields $m_\nu \sim 0.1$ eV. Another possibility is that $h_{\nu_{eff}}$ is only generated at loop level, e.g., in a theory with an extended Higgs sector, or in a supersymmetric theory with heavy exotic quarks (Masiero et al., 1986) or with non-holomorphic soft scalar interactions (Demir et al., 2008). Small Dirac masses may also emerge in higher-dimensional theories, e.g., in which ν_L is confined to our 4-d brane, but ν_R is free to propagate in the extra dimensions, in which case h_ν is determined by the (possibly very small) overlap of their wave functions (Dienes et al., 1999b; Arkani-Hamed et al., 2002). Related string-inspired possibilities involve large intersection areas in intersecting brane constructions (Blumenhagen et al., 2005, 2007) or string instantons (Cvetič and Langacker, 2008), both of which yield exponential suppressions[‡‡].

[††]However, the small value of the strong CP parameter discussed in Chapter 8 is not understood.

[‡‡]For a review of superstring phenomenology, see (Ibanez and Uranga, 2012). Implications of string theory for neutrino mass are reviewed in (Langacker, 2012).

It is possible that a dominant Dirac mass term is perturbed by a much smaller Majorana mass term for the active and/or sterile spinor. This is the pseudo-Dirac case mentioned on page 412. It implies that the Dirac neutrino splits into two Majorana neutrinos, each approximately half active and half sterile, with a small mass difference given by the perturbing Majorana mass. However, this would lead to an additional mass-squared difference that would have been observed by Solar neutrinos oscillating into the sterile component unless the Majorana mass is smaller than $\mathcal{O}(10^{-9}$ eV) (de Gouvea et al., 2009).

Majorana Masses

Majorana masses for active neutrinos violate weak isospin by one unit. A simple way to generate them at the renormalizable level is to extend the SM by the addition of a complex Higgs triplet $\vec{\phi}_T = (\phi_T^0,\ \phi_T^-,\ \phi_T^{--})^T$, with $t_T = 1$, and $y_T = -1$. The Yukawa couplings of ϕ_T to the leptons are

$$\begin{aligned} -\mathcal{L}_{\phi_T} &= \frac{1}{2} h_T\, \bar{\ell}_L \vec{\tau} \cdot \vec{\phi}_T\, \tilde{\ell}_R + h.c. \\ &= \frac{1}{2} h_T\, (\bar{\nu}_L\ \bar{e}_L) \begin{pmatrix} \phi_T^- & \sqrt{2}\phi_T^0 \\ \sqrt{2}\phi_T^{--} & -\phi_T^- \end{pmatrix} \begin{pmatrix} e_R^c \\ -\nu_R^c \end{pmatrix} + h.c., \end{aligned} \tag{7.431}$$

with $\phi_T^- = \phi_T^3$, $\phi_T^0 = \frac{1}{\sqrt{2}}(\phi_T^1 - i\phi_T^2)$, and $\phi_T^{--} = \frac{1}{\sqrt{2}}(\phi_T^1 + i\phi_T^2)$, and where $\tilde{\ell}_R$ is defined in (7.326) on page 405. This yields a Majorana mass $m_T = -h_T \nu_{\phi_T}$ if ϕ_T^0 acquires a VEV $\nu_{\phi_T}/\sqrt{2}$, as illustrated in Figure 7.43. The constraints on h_T are less stringent than those for a Dirac mass since one can have $|\nu_{\phi_T}| \ll \nu \sim 246$ GeV (the parameter $\rho_0 \equiv M_W^2/(M_Z^2 \cos^2\theta_W)$ requires $|\nu_{\phi_T}| \lesssim \mathcal{O}(10^{-2})\nu$ (Problem 7.1)). The original version of the model (Gelmini and Roncadelli, 1981; Georgi et al., 1981) involved a global lepton number symmetry (the coupling in (7.431) is invariant since ϕ_T can be defined to have $L = 2$). Therefore, the spontaneous breaking implies a massless Goldstone boson, known as the *triplet Majoron*. Astrophysical constraints (see, e.g., Raffelt, 1999) on stellar cooling from Majoron emission required $|\nu_{\phi_T}| < \mathcal{O}(10)$ keV, consistent with small neutrino mass. However, there was no special reason for ν_{ϕ_T} to actually be that small. The triplet Majoron model was eventually excluded by the invisible Z width, as already discussed below (7.169) on page 346, because the decay into a Majoron and light scalar would have a partial width equal to that of two additional active neutrinos. The triplet model could survive, however, by adding a coupling

$$-\mathcal{L}_{\phi\phi_T} = V_{\phi\phi_T} = \kappa\, \tilde{\phi}^\dagger \vec{\tau} \cdot \vec{\phi}_T\, \phi + h.c. \tag{7.432}$$

between ϕ_T and the Higgs doublet ϕ, where κ has dimensions of mass. The clash between (7.432) and (7.431) implies that the lepton number is explicitly violated, yielding a mass for the Majoron which can be taken large enough to evade observational bounds. A currently popular version (the *type II seesaw* (Ma and Sarkar, 1998; Hambye et al., 2001)) includes a mass term

$\frac{1}{2}\mu_T^2 \vec{\phi}_T^\dagger \cdot \vec{\phi}_T$ for the triplet, where μ_T^2 is very large and positive and associated with a new physics scale. Substituting $\phi^0 \to \nu/\sqrt{2}$ in (7.432)*, $V_{\phi\phi_T}$ becomes linear in ϕ_T^0, so that it is forced to acquire a VEV

$$\nu_{\phi_T} = -\frac{\kappa\nu^2}{\mu_T^2}, \qquad m_T = h_T \frac{\kappa\nu^2}{\mu_T^2}. \tag{7.433}$$

This is very small in the seesaw limit, $\mu_T^2/\kappa \gg \nu$.

Instead of a Higgs triplet, a Majorana mass for active neutrinos can be generated by the *Weinberg operator* (Weinberg, 1980), which is a higher-dimensional operator† in which two Higgs doublets are combined as an isospin triplet, as illustrated in Figure 7.43. The form of the interactions can be obtained from (7.431) if we identify ϕ_T^i with $\phi^\dagger \tau^i \tilde{\phi}$, where the Higgs doublet ϕ and its tilde form $\tilde{\phi}$ are $\phi = (\phi^+ \; \phi^0)^T$ and $\tilde{\phi} = (\phi^{0\dagger} \; -\phi^-)^T$ as defined in (7.14) on page 285. Then,

$$\begin{aligned} -\mathcal{L}_{\phi\phi} &= \frac{C}{2M}\left(\bar{\ell}_L \vec{\tau}\, \tilde{\ell}_R\right) \cdot \left(\phi^\dagger \vec{\tau} \tilde{\phi}\right) + h.c. = \frac{C}{M}\left(\bar{\ell}_L\, \tilde{\phi}\right)\left(\phi^\dagger\, \tilde{\ell}_R\right) + h.c. \\ &= \frac{C}{M}\bar{\ell}_L \begin{pmatrix} \phi^{0\dagger}\phi^- & \phi^{0\dagger}\phi^{0\dagger} \\ -\phi^-\phi^- & -\phi^-\phi^{0\dagger} \end{pmatrix} \tilde{\ell}_R + h.c., \end{aligned} \tag{7.434}$$

where M is the relevant new physics scale and C is a coefficient which can be absorbed into M if desired. The second form is obtained using the $SU(2)$ Fierz identity in Problem 1.1. (The second term in the Fierz identity vanishes for a single Higgs doublet.) Thus, the Majorana mass is $m_T = -C\nu^2/M$. For example, $M \sim 10^{19}$ GeV (the Planck scale) and $C \sim 1$ implies $m_T \sim 10^{-5}$ eV. $\mathcal{L}_{\phi\phi}$ describes an effective theory that can be generated by many different underlying models, including the type II seesaw mentioned above. It is easily generalized to three families, and is considered by many to be the favored description of small neutrino masses. The scale of M/C (around 10^{14} GeV for $m_T \sim 0.1$ eV) is suggestive of, though a few orders of magnitude below, a grand unification or superstring scale.

The most familiar implementation of (7.434) is in the *minimal* or *type I seesaw* (Minkowski, 1977; Gell-Mann et al., 1979; Yanagida, 1979; Schechter and Valle, 1980)‡, in which the active neutrinos mix with heavy sterile Majorana neutrinos, as in (7.350) or (7.366) and Figure 7.43, leading to Majorana masses

*One should in principle minimize V w.r.t ν and ν_{ϕ_T} simultaneously. In practice the modification to ν from the coupling in (7.432) is usually negligible in the seesaw limit, and one can always adjust the other Higgs parameters to maintain the observed value of ν.

†The Weinberg operator, with dimension $k = 5$ (i.e., the coefficient has mass dimension $4-k$), is the lowest-dimensional extension of the standard model (with no ν_R) that is consistent with the gauge and Lorentz symmetries. Higher-dimensional SM operators relevant to neutrino mass are classified in (Babu and Leung, 2001; de Gouvea and Jenkins, 2008).

‡Some authors reserve the term "seesaw" for the type I version, but we will use the term to refer to any model which leads to a small Majorana or Dirac neutrino mass suppressed by one or more powers of a large new physics scale.

of $\mathcal{O}(m_D^2/m_S)$. In some versions there is a spontaneously broken global lepton number, leading to a very weakly coupled Goldstone boson, the *singlet Majoron* (Chikashige et al., 1981). Type I seesaw models have been constructed with many different scales[§], depending on m_D. For example, choosing m_D comparable to the electron mass and $m_\nu \sim 0.1$ eV implies $m_S \sim$ few TeV. However, most popular are those based on grand unified theories, where the masses in the Dirac matrix M_D are typically of $\mathcal{O}(m_{u,c,t})$. The sterile masses in M_S may be generated by large Higgs multiplets (e.g., the 126 of $SO(10)$) or by higher-dimensional operators, and must typically be several orders of magnitude below the grand unification scale M_X, which is $\gtrsim 10^{16}$ GeV in the supersymmetric case (Section 8.4). Such constructions are usually combined with family symmetries which restrict and relate the elements of M_D, M_S, and the quark and charged lepton mass matrices, and sometimes combine the type I and II seesaws (using the Higgs triplets in the 126). Generating the large observed leptonic mixings in the same GUT context which yields small quark mixings is a challenge, which requires carefully chosen family symmetries, and/or non-symmetric (*lopsided*) mass matrices (Albright et al., 1998), which lead to large mixing in the unobservable A_R^d and in the observable A_L^e mixing matrices. One especially attractive aspect of the minimal seesaw is that it opens the possibility of the *leptogenesis* (Fukugita and Yanagida, 1986; Davidson et al., 2008; Hambye, 2012; Fong et al., 2012) scenario for generating the observed baryon asymmetry of the Universe (Section 8.1).

Most of these GUT type models are hard to embed in known classes of superstring constructions, where any underlying grand unification is frequently broken in the higher-dimensional theory, and in any case it is difficult or impossible to obtain large representations like the 126. More promising is that the Majorana mass terms in M_S are generated by higher-dimensional operators in the superpotential[¶] of the form $(\phi_S/M_P)^k\, \bar{\nu}_L^c \nu_R$, in which k SM singlet fields ϕ_S (which need not be the same) acquire VEVs somewhat below the Planck scale M_P. This mechanism can lead to a sufficiently suppressed M_S, but is likely to lose the GUT and family symmetry structure of the $SO(10)$ models. String constraints sometimes forbid the simultaneous existence of such operators and those needed for M_D (Giedt et al., 2005). However, there are a few successful examples (Lebedev et al., 2008) in which both M_D and M_S emerge at high order and there are $\mathcal{O}(100)$ sterile neutrinos. Other possibilities for generating M_S involve higher-dimensional operators in the Kähler potential (Arkani-Hamed et al., 2001) or string instanton effects (Blumen-

[§]The heavy sterile neutrino aggravates the Higgs/hierarchy problem (Section 8.1) unless $m_S \lesssim 10^7$ GeV (Vissani, 1998). It also tends to destabilize the electroweak vacuum (Elias-Miro et al., 2012), but the effect is small for $M_H \sim 125$ GeV.

[¶]The Weinberg operator could also emerge directly in a superstring construction. However, C/M would typically be $\sim 1/M_P$, which is too small. This difficulty could be avoided if some of the extra dimensions are large compared to the inverse of the string scale (Conlon and Cremades, 2007; Cvetič et al., 2010).

hagen et al., 2007; Ibanez and Uranga, 2007).

Seesaw models with lower scales have also been considered. For example, in some gauge extensions of the SM (e.g., with an extra $U(1)'$ (Kang et al., 2005)) the "sterile" neutrinos are charged under the extended group, so any Majorana masses for them cannot be much larger than the symmetry breaking scale. There are also various *extended seesaw* models, which involve additional $SU(2)$ singlets. For example, in the *double seesaw* (Mohapatra and Valle, 1986) one introduces a sterile n_L with a Majorana mass μ and a Dirac mass $\mathcal{M}_D$ coupling to ν_R:

$$-\mathcal{L} = \frac{1}{2}\left(\,\bar{\nu}_L\;\bar{\nu}_L^c\;n_L\,\right)\begin{pmatrix} 0 & m_D & 0 \\ m_D & 0 & \mathcal{M}_D \\ 0 & \mathcal{M}_D & \mu \end{pmatrix}\begin{pmatrix} \nu_R^c \\ \nu_R \\ n_R^c \end{pmatrix} + h.c., \tag{7.435}$$

where we have taken the other masses to vanish. For $\mu = 0$ there is one massless Weyl neutrino and one Dirac neutrino, given approximately by ν_L and $n_L + \nu_R$ respectively for $\mathcal{M}_D \gg m_D$. For $\mu \ll m_D \ll \mathcal{M}_D$ the ν_L acquires a Majorana mass $m_\nu \sim \mu(m_D/\mathcal{M}_D)^2$. This *inverse seesaw* is actually driven by a small Majorana sterile mass μ rather than a large one, e.g., $\mu = 1$ keV, $m_D = 100$ GeV, and $\mathcal{M}_D = 10$ TeV corresponds to $m_\nu \sim 0.1$ eV. This model generalizes to three families. Variations of the doublet seesaw with larger μ and related models with small Dirac masses are also possible. Low-scale models may also have implications for LHC physics. They are reviewed in (Chen and Huang, 2011; Boucenna et al., 2014).

We briefly mention two other classes of models which lead to Majorana masses. One involves masses that are only induced at loop level, e.g., associated with an extended scalar sector. In one well-known example (Zee, 1980) an $SU(2)$-singlet charged scalar field h^- is introduced which couples to both leptons and Higgs doublets, leading to a loop-induced Majorana mass as shown in Figure 7.43 on page 409. This example actually leads to off-diagonal masses such as $\bar{\nu}_{eL}\nu_{\mu R}^c$, i.e, the ZKM model of (7.369) on page 416, and also requires a second Higgs doublet, because the h^- coupling is antisymmetric in lepton and Higgs family indices. Another possibility occurs in supersymmetric theories with R-parity violation (Section 8.2), which allows mixing and a type of seesaw between active neutrinos and neutralinos. The mixing can generate one small neutrino mass at tree level, with the other two masses entering at loop level (e.g., Grossman and Rakshit, 2004; Rakshit, 2004).

Mixed Mass Models

As discussed in Section 7.7.4 there are several experimental suggestions of possible mixing between active and light sterile neutrinos. Neutrino oscillations conserve helicity, so the mixing must be between states of the same chirality. Most extensions of the standard model involving neutrino mass introduce sterile neutrinos, which could in principle have mass at any scale. However, generating significant mixing is much more difficult. For example,

in the model with one active and one sterile neutrino in (7.343) on page 410 the appropriate $\nu_L^0 - \nu_L^{0c}$ or $\nu_R^{0c} - \nu_R^0$ mixing only occurs in the general case in which both Dirac and Majorana mass terms are present. Furthermore, for eV-scale sterile neutrinos with small mixing both the Dirac and Majorana mass terms must be tiny and not too different in magnitude. Similar statements apply to the multi-family case in (7.362) on page 415. More generally, LSND-type active-sterile mixing requires two distinct types of mass terms to be simultaneously extremely small. These could be Majorana and Dirac, or, alternatively, two distinct types of Dirac masses, such as one connecting active and sterile states, and another connecting distinct steriles. Confirmation of such mixing would therefore require a major change in the paradigm, especially from the usual seesaw model.

There have been many models for such mixing, including higher-dimensional operators associated with an intermediate scale, sterile neutrinos from a *mirror world*, supersymmetry, extra dimensions, and dynamical symmetry breaking (see, e.g., Langacker, 2012, for a list of references). Especially promising is the (minimal) *mini-seesaw* model. This is just the ordinary seesaw model in (7.350) on page 412 or in (7.366) (with m_T or $M_T = 0$), except that all of the Dirac and Majorana masses are assumed to be very small, e.g., $\lesssim \mathcal{O}(\text{eV})$. The minimal mini-seesaw has the advantage that the masses and mixings are related in a way that is roughly consistent with the LSND and other observations. For example, for one family one has

$$|m_1| \sim \frac{m_D^2}{m_S}, \qquad m_2 \sim m_S, \qquad |\theta| \sim \frac{m_D}{m_S} \tag{7.436}$$

from (7.350), e.g., $|m_1| \sim 0.04$ eV and $|\theta| \sim 0.2$ for $m_D = 0.2$ eV and $m_S = 1$ eV. There have been extensive studies of the minimal mini-seesaw for two or three families[‖] (e.g., de Gouvea and Huang, 2012; Donini et al., 2012), yielding qualitative agreement with the data. The minimal mini-seesaw predicts $m_{\beta\beta} = 0$ for the effective $\beta\beta_{0\nu}$ mass in (7.385) on page 424, because for mass eigenvalues $\ll$ MeV it is just the (vanishing) (e, e) element of the mass matrix in (7.362).

The minimal mini-seesaw model parametrizes the mixing but does not explain the small values for m_D and m_S. Just as in the discussion of small Dirac masses, it suggests that both the Dirac Yukawa couplings and m_S are forbidden at the renormalizable level by some new discrete, global, or gauge symmetry, and only generated by symmetry-breaking (and possibly loop) corrections (e.g., Langacker, 1998, 2012; Sayre et al., 2005). For example, consider the case of one active and one sterile neutrino in which the lowest-order

[‖] From (7.365) on page 415 the leading approximation to the active-sterile mixing for both the ordinary type I and mini seesaws is $-M_D M_S^{-1}$. M_D can be expressed in terms of the mass eigenvalues and PMNS matrix up to a complex orthogonal matrix (Casas and Ibarra, 2001).

allowed mass terms are

$$-\mathcal{L}_{mini} = \sqrt{2}\,\Gamma_D \frac{\phi_S^p}{M^p}\bar{\ell}_L\tilde{\phi}\nu_R + \Gamma_S\,\frac{\phi_S^{q+1}}{2M^q}\bar{\nu}_L^c\nu_R + \Gamma_T\,\frac{\phi_S^{r-1}}{2M^r}\left(\bar{\ell}_L\vec{\tau}\,\tilde{\ell}_R\right)\cdot\left(\phi^\dagger\vec{\tau}\tilde{\phi}\right) + h.c., \tag{7.437}$$

rather than those in (7.429), (7.334) and (7.434). The new symmetry is broken by $\langle\phi_S\rangle \equiv S$, and M is a new physics scale**. Neglecting the last term, (7.437) yields a minimal mini-seesaw for $p, q \geq 1$. Taking $p = q = 1$ and $\Gamma_D = \Gamma_S = 1$, for example, one finds $m_D = S\nu/M$ and $m_S = S^2/M$, so that $|\theta| \sim \nu/S$ and $|m_1| \sim \nu^2/M$. Comparing with numerical example above, one expects S in the TeV range and $S/M \sim 10^{-12}$. In general, one should not neglect the last term in (7.437). Any multiplicative symmetry of $\mathcal{L}_{mini}$ that allows the first two terms will also allow the third, with $r = 2p - q$. This corresponds to $r = 1$ in the $p = q = 1$ case, i.e, the new physics should be able to generate a contribution to m_1 directly that is of the same order as the mixing-induced term. This would modify the details of the minimal mini-seesaw model (and would allow $m_{\beta\beta} \neq 0$), but the general idea remains.

Textures and Family Symmetries

There are also many *texture models*, involving specific ansätze about the form of the 3×3 neutrino mass matrix, or of the Dirac and Majorana mass matrices entering seesaw models. These are often studied in connection with models also involving quark and charged-lepton mass matrices, such as family symmetries, left-right symmetry, or grand unification (e.g., Raby, 2009, and Chapter 8). A major complication is that the form of a mass matrix depends on the basis chosen, e.g., whether the charged-lepton mass matrix is diagonal, and any underlying family symmetries may take a different form depending on the basis. Family symmetries may be continuous (global or gauged) or discrete. There has been considerable recent interest in discrete symmetries (for reviews, see Altarelli and Feruglio, 2010; Ishimori et al., 2010; King et al., 2014) because they more naturally lead to the large mixing angles observed in the neutrino sector. Also, they are free of the unwanted Goldstone bosons associated with spontaneously broken global continuous symmetries. Family symmetries are in principle symmetries of the underlying Lagrangian, but in practice the models are often very complicated, so studies are often restricted to the symmetry and its breaking pattern.

The observed values of $\theta_{23} \sim \pi/4$ and $\theta_{13} \sim 0$ suggest that the leptonic

**An explicit example of an *ultraviolet completion*, i.e., a renormalizable model of the underlying physics that leads to the effective operators in $\mathcal{L}_{mini}$, is given in (Heeck and Zhang, 2013).

mixing matrix is close to

$$V_\ell^\dagger = \mathcal{V} = \begin{pmatrix} c_{12} & s_{12} & 0 \\ -\frac{s_{12}}{\sqrt{2}} & \frac{c_{12}}{\sqrt{2}} & \frac{1}{\sqrt{2}} \\ \frac{s_{12}}{\sqrt{2}} & -\frac{c_{12}}{\sqrt{2}} & \frac{1}{\sqrt{2}} \end{pmatrix} \tag{7.438}$$

up to field redefinitions and possible Majorana phases that are irrelevant for oscillations. The motivation for (7.438) is somewhat weakened by the observation of nonzero θ_{13} and possible deviation of θ_{23} from maximal mixing, but it may still be useful as a starting point in model building. The special case of $s_{12}^2 = 1/3$, known as *tri-bimaximal mixing* (Harrison et al., 2002; Ma, 2004), is consistent with but slightly above the current value in (7.427). Alternatively, the *golden ratio* prediction $s_{12}^2 = \frac{2}{5+\sqrt{5}} \sim 0.276$ (Kajiyama et al., 2007; Feruglio and Paris, 2011; Ding et al., 2012), is slightly below. *Bimaximal mixing*, $c_{12}^2 = s_{12}^2 = 1/2$ was also at one time a serious possibility. These and similar patterns may well be associated with underlying permutation symmetries, such as S_4, or groups of even permutations, such as A_4 or (for the golden ratio) the icosahedral group A_5.

In practice, small deviations from any specific form such as tri-bimaximal mixing are possible. For example, they may be associated with broken discrete symmetries, and/or they could apply only to the neutrino mixing, with additional small mixing comparable to the CKM angles induced by the charged leptons (*Cabibbo haze* (Datta et al., 2005; Everett, 2006)). It has been observed that θ_{12} is close to the quark-lepton complementarity (Raidal, 2004; Minakata and Smirnov, 2004) value $\theta_{12} + \theta_c = \pi/4$, where θ_c is the Cabibbo angle, reopening the possibility of bimaximal mixing in the neutrino sector. Similarlly, θ_{13} is close to the value $\theta_c/\sqrt{2}$ that has been motivated in several schemes (Minakata and Smirnov, 2004; Antusch, 2013). Renormalization group evolution of couplings is another complication, since one might expect underlying symmetries to apply at a large GUT or string scale rather than at low energies, and mass degeneracies (in sign as well as magnitude) at a high scale may be destabilized by the running (e.g., Antusch et al., 2005).

In most quark texture models the small mixing angles are associated with the small ratios of mass eigenvalues, as in Problem 7.26. Two of the neutrino mixings are large, however, suggesting the possibility that the mixings and mass eigenvalues are decoupled. This can easily occur. In particular, any Dirac, triplet Majorana, or seesaw-induced 3×3 neutrino mass matrix of the form

$$M_\nu = \begin{pmatrix} A & B & -B \\ B & C & -D \\ -B & -D & C \end{pmatrix} \tag{7.439}$$

will lead (e.g., Altarelli and Feruglio, 2010) to the leptonic mixing matrix in (7.438), corresponding to $s_{13} = 0$ and $s_{23} = c_{23} = 1/\sqrt{2}$, with

$$\sin^2 2\theta_{12} = \frac{8B^2}{[A - (C + D)]^2 + 8B^2}. \tag{7.440}$$

The mass eigenvalues are related by

$$A = c_{12}^2\, m_1 + s_{12}^2\, m_2, \qquad C+D = s_{12}^2\, m_1 + c_{12}^2\, m_2, \qquad C-D = m_3, \tag{7.441}$$

which because of the phase conventions chosen in (7.438) may be negative or complex. Clearly, the parameters can be chosen to yield any of the types of mass hierarchy. Tri-bimaximal mixing occurs whenever

$$A + B = C + D, \tag{7.442}$$

implying

$$\begin{aligned} &s_{12}^2 = \frac{1}{3}, \qquad c_{12}^2 = \frac{2}{3} \\ &m_1 = A - B, \qquad m_2 = A + 2B, \qquad m_3 = C - D. \end{aligned} \tag{7.443}$$

Bimaximal mixing corresponds to

$$A = C + D, \tag{7.444}$$

so that

$$s_{12}^2 = c_{12}^2 = \frac{1}{2}, \qquad m_{1,2} = A \mp \sqrt{2}B, \qquad m_3 = C - D. \tag{7.445}$$

The golden ratio occurs for

$$A = C + D - \sqrt{2}B. \tag{7.446}$$

The form of (7.438) and (7.439) exhibits an obvious $\nu_\mu \leftrightarrow \nu_\tau$ interchange symmetry (up to signs depending on our phase convention).

7.7.7 Implications of Neutrino Mass

Most extensions of the SM predict non-zero neutrino masses at some level, so it is difficult to determine their origin. Many of the promising mechanisms, such as the minimal seesaw, involve very short distance scales, e.g., associated with grand unification or string theories, and are therefore difficult to verify directly. Some models lead to other predictions. For example, lepton flavor violating processes[††] like $\mu \to e\gamma$, $\mu N \to eN$, or $\mu \to 3e$, by the exchange of sneutrinos $\tilde{\nu}$ in supersymmetry or other mechanisms (e.g., Hisano et al., 1996; Casas and Ibarra, 2001; Masiero et al., 2004; Alonso et al., 2013), may be observable, but their connection to the neutrino mass generation mechanism is model dependent. TeV-scale models for neutrino mass, on the other hand, are more likely to lead to consequences observable at the LHC (e.g., Atre et al., 2009).

There are many unanswered questions. These include:

[††]The nonzero neutrino masses and mixings themselves violate lepton flavor, but their effects are negligible except for neutrino oscillations.

- Are the neutrinos Dirac or Majorana? Majorana masses, especially if associated with a type I or II seesaw, would allow the possibility of leptogenesis. The observation of $\beta\beta_{0\nu}$ would establish Majorana masses (or at least L violation), but foreseeable experiments will only be sensitive to the inverted or degenerate hierarchies. If the neutrinos are Dirac, this would suggest that additional TeV scale symmetries or string symmetries/selection rules are forbidding Majorana mass terms.

- What is the absolute mass scale (with implications for cosmology)? This is very difficult, but ordinary and double beta decay experiments, as well as future cosmological observations, may be able to establish the scale.

- Is there leptonic CP violation? What is δ? Is the hierarchy normal or inverted? Is θ_{23} maximal? Leptonic CP violation is a necessary ingredient in leptogenesis. The CP phases in $\mathcal{V}$ are different from the ones relevant to leptogenesis, though they are often related in specific models. For three families, the phase δ in (7.360) may be observable, e.g., in differences between the $\nu_\mu \to \nu_e$ and $\bar{\nu}_\mu \to \bar{\nu}_e$ oscillation rates in long-baseline experiments such as T2K or NOνA, or in future experiments with even longer baselines (for reviews, see Nunokawa et al., 2008; Feldman et al., 2013; de Gouvea et al., 2013). However, such effects are proportional to θ_{13}, and also depend on the sign of Δm^2_{23} because of matter effects in the Earth. Fortunately, θ_{13} has now been measured in reactor experiments. The nature of the hierarchy may be determined simultaneously with CP breaking in long-baseline experiments, or in other matter effects involving atmospheric or supernova neutrinos. The hierarchy may also be determined in future high precision reactor experiments, in the observation of $\beta\beta_{0\nu}$ if the neutrinos are Majorana, or by cosmological determinations of $\Sigma = \sum_i |m_i|$ (see Cahn et al., 2013, for a review). On a longer time scale, CP violation, the hierarchy, and related issues may also be addressed at a dedicated neutrino factory (from a muon storage ring), or in *beta beams* involving e^- or e^+ emission from accelerated heavy ions. All of these possibilities are reviewed in (Camilleri et al., 2008). Ultra-high energy neutrinos from violent astrophysical events can be observed in large detectors in ice or water, such as IceCube and ANTARES, and in fact IceCube has already detected a number of events in the 30 TeV-PeV range. These may possibly shed light on neutrino oscillations or decay, nonstandard high energy effects, and on the astrophysical sources.

- If the LSND, MiniBooNe, reactor, and gallium results are confirmed, it will suggest mixing between ordinary and sterile neutrinos, presenting a serious challenge both to particle physics and cosmology, or imply something even more bizarre, such as CPT violation.

- Are there any new ν interactions or anomalous properties such as large magnetic moments? Most such ideas are excluded as the dominant

effect for the Solar and atmospheric neutrinos, but could still appear as subleading effects.

7.8 New References

Aartsen, M. et al. (2013). Evidence for High-Energy Extraterrestrial Neutrinos at the IceCube Detector. *Science 342*, 1242856, arXiv:1311.5238 [astro-ph.HE].

Abazajian, K., M. Acero, S. Agarwalla, A. Aguilar-Arevalo, C. Albright, et al. (2012). Light Sterile Neutrinos: A White Paper. arXiv:1204.5379 [hep-ph].

Abazajian, K., K. Arnold, J. Austermann, B. Benson, C. Bischoff, et al. (2013). Neutrino Physics from the Cosmic Microwave Background and Large Scale Structure. arXiv:1309.5383 [astro-ph.CO].

Abazajian, K., E. Calabrese, A. Cooray, F. De Bernardis, S. Dodelson, et al. (2011). Cosmological and Astrophysical Neutrino Mass Measurements. *Astropart.Phys. 35*, 177–184, arXiv:1103.5083 [astro-ph.CO].

Abe, K. et al. (2011a). Search for Differences in Oscillation Parameters for Atmospheric Neutrinos and Antineutrinos at Super-Kamiokande. *Phys.Rev.Lett. 107*, 241801, arXiv:1109.1621 [hep-ex].

Abe, K. et al. (2011b). Solar neutrino results in Super-Kamiokande-III. *Phys.Rev. D83*, 052010, arXiv:1010.0118 [hep-ex].

Abe, K. et al. (2013a). A Measurement of the Appearance of Atmospheric Tau Neutrinos by Super-Kamiokande. *Phys.Rev.Lett. 110*, 181802, arXiv:1206.0328 [hep-ex].

Abe, K. et al. (2013b). Measurement of Neutrino Oscillation Parameters from Muon Neutrino Disappearance with an Off-axis Beam. *Phys.Rev.Lett. 111*(21), 211803, arXiv:1308.0465 [hep-ex].

Adams, C. et al. (2013). The Long-Baseline Neutrino Experiment: Exploring Fundamental Symmetries of the Universe. arXiv:1307.7335 [hep-ex].

Adamson, P. et al. (2012). Measurements of atmospheric neutrinos and antineutrinos in the MINOS Far Detector. *Phys.Rev. D86*, 052007, arXiv:1208.2915 [hep-ex].

Adamson, P. et al. (2014). Combined analysis of ν_μ disappearance and $\nu_\mu \to \nu_e$ appearance in MINOS using accelerator and atmospheric neutrinos. *Phys.Rev.Lett. 112*, 191801, arXiv:1403.0867 [hep-ex].

Ade, P. et al. (2014). Planck 2013 results. XVI. Cosmological parameters. *Astron.Astrophys.*, arXiv:1303.5076 [astro-ph.CO].

Agafonova, N. et al. (2014). Observation of ν_τ appearance in the CNGS beam with the OPERA experiment. arXiv:1407.3513 [hep-ex].

Agarwalla, S. et al. (2014). The mass-hierarchy and CP-violation discovery reach of the LBNO long-baseline neutrino experiment. *JHEP 1405*, 094, arXiv:1312.6520 [hep-ph].

Aguilar-Arevalo, A. et al. (2001). Evidence for neutrino oscillations from the observation of anti-neutrino(electron) appearance in a anti-neutrino(muon) beam. *Phys.Rev. D64*, 112007, arXiv:hep-ex/0104049 [hep-ex].

Aguilar-Arevalo, A. et al. (2013). Improved Search for $\bar{\nu}_\mu \to \bar{\nu}_e$ Oscillations in the MiniBooNE Experiment. *Phys.Rev.Lett. 110*, 161801, arXiv:1207.4809 [hep-ex].

Aharmim, B. et al. (2013). Combined Analysis of all Three Phases of Solar Neutrino Data from the Sudbury Neutrino Observatory. *Phys.Rev. C88*, 025501, arXiv:1109.0763 [nucl-ex].

Akhmedov, E. K. and A. Y. Smirnov (2009). Paradoxes of neutrino oscillations. *Phys.Atom.Nucl. 72*, 1363–1381, arXiv:0905.1903 [hep-ph].

Albright, C. H. (2009). Overview of Neutrino Mixing Models and Ways to Differentiate among Them. pp. 91–109, arXiv:0905.0146 [hep-ph].

Alonso, R., M. Dhen, M. Gavela, and T. Hambye (2013). Muon conversion to electron in nuclei in type-I seesaw models. *JHEP 1301*, 118, arXiv:1209.2679 [hep-ph].

Alonso, R., M. Gavela, D. Hernandez, L. Merlo, and S. Rigolin (2013). Neutrino and Charged Lepton Flavour Today. arXiv:1311.1724 [hep-ph].

Altarelli, G. and F. Feruglio (2010). Discrete Flavor Symmetries and Models of Neutrino Mixing. *Rev.Mod.Phys. 82*, 2701–2729, arXiv:1002.0211 [hep-ph].

An, F. et al. (2014). Spectral measurement of electron antineutrino oscillation amplitude and frequency at Daya Bay. *Phys.Rev.Lett. 112*, 061801, arXiv:1310.6732 [hep-ex].

Anchordoqui, L. A., V. Barger, I. Cholis, H. Goldberg, D. Hooper, et al. (2014). Cosmic Neutrino Pevatrons: A Brand New Pathway to Astronomy, Astrophysics, and Particle Physics. *Journal of High Energy Astrophysics 1-2*, 1–30, arXiv:1312.6587 [astro-ph.HE].

Anchordoqui, L. A., H. Goldberg, and G. Steigman (2013). Right-Handed Neutrinos as the Dark Radiation: Status and Forecasts for the LHC. *Phys.Lett. B718*, 1162–1165, arXiv:1211.0186 [hep-ph].

Antusch, S. (2013). Models for Neutrino Masses and Mixings. *Nucl.Phys.Proc.Suppl. 235-236*, 303–309, arXiv:1301.5511 [hep-ph].

Antusch, S., C. Biggio, E. Fernandez-Martinez, M. Gavela, and J. Lopez-Pavon (2006). Unitarity of the Leptonic Mixing Matrix. *JHEP 0610*, 084, arXiv:hep-ph/0607020 [hep-ph].

Antusch, S. and O. Fischer (2014). Non-unitarity of the leptonic mixing matrix: Present bounds and future sensitivities. arXiv:1407.6607 [hep-ph].

Auger, M. et al. (2012). Search for Neutrinoless Double-Beta Decay in ^{136}Xe with EXO-200. *Phys.Rev.Lett. 109*, 032505, arXiv:1205.5608 [hep-ex].

Babu, K. and C. N. Leung (2001). Classification of effective neutrino mass operators. *Nucl.Phys. B619*, 667–689, arXiv:hep-ph/0106054 [hep-ph].

Baerwald, P., M. Bustamante, and W. Winter (2012). Neutrino Decays over Cosmological Distances and the Implications for Neutrino Telescopes. *JCAP 1210*, 020, arXiv:1208.4600 [astro-ph.CO].

Bahcall, J. N., A. M. Serenelli, and S. Basu (2006). 10,000 standard solar models: a Monte Carlo simulation. *Astrophys.J.Suppl. 165*, 400–431, arXiv:astro-ph/0511337 [astro-ph].

Banks, T. and L. J. Dixon (1988). Constraints on String Vacua with Space-Time Supersymmetry. *Nucl.Phys. B307*, 93–108.

Barabash, A. (2013). Average and recommended half-life values for two neutrino double beta decay: upgrade-2013. *AIP Conf.Proc. 1572*, 11–15, arXiv:1311.2421 [nucl-ex].

Barabash, A. (2014). Review of double beta decay experiments. arXiv:1403.2870 [nucl-ex].

Barger, V., D. Marfatia, and K. Whisnant (2012). *The physics of neutrinos*. Princeton, NJ: Princeton Univ. Press.

Barry, J., W. Rodejohann, and H. Zhang (2011). Light Sterile Neutrinos: Models and Phenomenology. *JHEP 1107*, 091, arXiv:1105.3911 [hep-ph].

Beacom, J. F. (2010). The Diffuse Supernova Neutrino Background. *Ann.Rev.Nucl.Part.Sci. 60*, 439–462, arXiv:1004.3311 [astro-ph.HE].

Bell, N. F., V. Cirigliano, M. J. Ramsey-Musolf, P. Vogel, and M. B. Wise (2005). How magnetic is the Dirac neutrino? *Phys.Rev.Lett. 95*, 151802, arXiv:hep-ph/0504134 [hep-ph].

Bell, N. F., M. Gorchtein, M. J. Ramsey-Musolf, P. Vogel, and P. Wang (2006). Model independent bounds on magnetic moments of Majorana neutrinos. *Phys.Lett. B642*, 377–383, arXiv:hep-ph/0606248 [hep-ph].

Bellini, G. et al. (2014a). Final results of Borexino Phase-I on low energy solar

neutrino spectroscopy. *Phys.Rev. D89*, 112007, arXiv:1308.0443 [hep-ex].

Bellini, G. et al. (2014b). Neutrinos from the primary protonproton fusion process in the Sun. *Nature 512*(7515), 383–386.

Betts, S., W. Blanchard, R. Carnevale, C. Chang, C. Chen, et al. (2013). Development of a Relic Neutrino Detection Experiment at PTOLEMY: Princeton Tritium Observatory for Light, Early-Universe, Massive-Neutrino Yield. arXiv:1307.4738 [astro-ph.IM].

Bilenky, S. (2010). *Introduction to the Physics of Massive and Mixed Neutrinos*. Lecture Notes in Physics. Berlin, Heidelberg: Springer.

Bilenky, S. and C. Giunti (2014). Neutrinoless Double-Beta Decay: a Probe of Physics Beyond the Standard Model. arXiv:1411.4791 [hep-ph].

Biller, S. D. (2013). Probing Majorana neutrinos in the regime of the normal mass hierarchy. *Phys.Rev. D87*(7), 071301, arXiv:1306.5654 [physics.ins-det].

Blennow, M. and A. Y. Smirnov (2013). Neutrino propagation in matter. *Adv.High Energy Phys. 2013*, 972485, arXiv:1306.2903 [hep-ph].

Blumenhagen, R., M. Cvetič, S. Kachru, and T. Weigand (2009). D-Brane Instantons in Type II Orientifolds. *Ann.Rev.Nucl.Part.Sci. 59*, 269–296, arXiv:0902.3251 [hep-th].

Blumenhagen, R., B. Kors, D. Lust, and S. Stieberger (2007). Four-dimensional String Compactifications with D-Branes, Orientifolds and Fluxes. *Phys.Rept. 445*, 1–193, arXiv:hep-th/0610327 [hep-th].

Boucenna, S. M., S. Morisi, and J. W. Valle (2014). The low-scale approach to neutrino masses. *Adv.High Energy Phys. 2014*, 831598, arXiv:1404.3751 [hep-ph].

Boyarsky, A., O. Ruchayskiy, and M. Shaposhnikov (2009). The Role of sterile neutrinos in cosmology and astrophysics. *Ann.Rev.Nucl.Part.Sci. 59*, 191–214, arXiv:0901.0011 [hep-ph].

Cahn, R., D. Dwyer, S. Freedman, W. Haxton, R. Kadel, et al. (2013). White Paper: Measuring the Neutrino Mass Hierarchy. arXiv:1307.5487 [hep-ex].

Capozzi, F., G. Fogli, E. Lisi, A. Marrone, D. Montanino, et al. (2014). Status of three-neutrino oscillation parameters, circa 2013. *Phys.Rev. D89*, 093018, arXiv:1312.2878 [hep-ph].

Casas, J. and A. Ibarra (2001). Oscillating neutrinos and $\mu \to e, \gamma$. *Nucl.Phys. B618*, 171–204, arXiv:hep-ph/0103065 [hep-ph].

Chen, M.-C. and J. Huang (2011). TeV Scale Models of Neutrino

Masses and Their Phenomenology. *Mod.Phys.Lett. A26*, 1147–1167, arXiv:1105.3188 [hep-ph].

Cocco, A. G., G. Mangano, and M. Messina (2007). Probing low energy neutrino backgrounds with neutrino capture on beta decaying nuclei. *JCAP 0706*, 015, arXiv:hep-ph/0703075 [hep-ph].

Cohen, A. G., S. L. Glashow, and Z. Ligeti (2009). Disentangling Neutrino Oscillations. *Phys.Lett. B678*, 191–196, arXiv:0810.4602 [hep-ph].

Conrad, J., C. Ignarra, G. Karagiorgi, M. Shaevitz, and J. Spitz (2013). Sterile Neutrino Fits to Short Baseline Neutrino Oscillation Measurements. *Adv.High Energy Phys. 2013*, 163897, arXiv:1207.4765 [hep-ex].

Conrad, J. and M. Shaevitz (2012). Limits on Electron Neutrino Disappearance from the KARMEN and LSND ν_e - Carbon Cross Section Data. *Phys.Rev. D85*, 013017, arXiv:1106.5552 [hep-ex].

Conrad, J. M., W. C. Louis, and M. H. Shaevitz (2013). The LSND and MiniBooNE Oscillation Searches at High Δm^2. *Ann.Rev.Nucl.Part.Sci. 63*, 45–67, arXiv:1306.6494 [hep-ex].

Cvetič, M. and J. Halverson (2011). TASI Lectures: Particle Physics from Perturbative and Non-perturbative Effects in D-braneworlds. pp. 245–292, arXiv:1101.2907 [hep-th].

Cvetič, M., J. Halverson, P. Langacker, and R. Richter (2010). The Weinberg Operator and a Lower String Scale in Orientifold Compactifications. *JHEP 1010*, 094, arXiv:1001.3148 [hep-th].

de Gouvea, A. et al. (2013). Working Group Report: Neutrinos. arXiv:1310.4340 [hep-ex].

de Gouvea, A., A. Friedland, and H. Murayama (2000). The Dark side of the solar neutrino parameter space. *Phys.Lett. B490*, 125–130, arXiv:hep-ph/0002064 [hep-ph].

de Gouvea, A. and W.-C. Huang (2012). Constraining the (Low-Energy) Type-I Seesaw. *Phys.Rev. D85*, 053006, arXiv:1110.6122 [hep-ph].

de Gouvea, A., W.-C. Huang, and J. Jenkins (2009). Pseudo-Dirac Neutrinos in the New Standard Model. *Phys.Rev. D80*, 073007, arXiv:0906.1611 [hep-ph].

de Gouvea, A. and J. Jenkins (2008). A Survey of Lepton Number Violation Via Effective Operators. *Phys.Rev. D77*, 013008, arXiv:0708.1344 [hep-ph].

de Gouvea, A. and H. Murayama (2012). Neutrino Mixing Anarchy: Alive and Kicking. arXiv:1204.1249 [hep-ph].

Diaz, J. S. and A. Kostelecky (2012). Lorentz- and CPT-violating models for neutrino oscillations. *Phys.Rev. D85*, 016013, arXiv:1108.1799 [hep-ph].

Ding, G.-J., L. L. Everett, and A. J. Stuart (2012). Golden Ratio Neutrino Mixing and A_5 Flavor Symmetry. *Nucl.Phys. B857*, 219–253, arXiv:1110.1688 [hep-ph].

Donini, A., P. Hernandez, J. Lopez-Pavon, M. Maltoni, and T. Schwetz (2012). The minimal 3+2 neutrino model versus oscillation anomalies. *JHEP 1207*, 161, arXiv:1205.5230 [hep-ph].

Drexlin, G., V. Hannen, S. Mertens, and C. Weinheimer (2013). Current direct neutrino mass experiments. *Adv.High Energy Phys. 2013*, 293986, arXiv:1307.0101 [physics.ins-det].

Duan, H., G. M. Fuller, and Y.-Z. Qian (2010). Collective Neutrino Oscillations. *Ann.Rev.Nucl.Part.Sci. 60*, 569–594, arXiv:1001.2799 [hep-ph].

Elias-Miro, J., J. R. Espinosa, G. F. Giudice, G. Isidori, A. Riotto, et al. (2012). Higgs mass implications on the stability of the electroweak vacuum. *Phys.Lett. B709*, 222–228, arXiv:1112.3022 [hep-ph].

Everett, L. L. (2006). Viewing lepton mixing through the Cabibbo haze. *Phys.Rev. D73*, 013011, arXiv:hep-ph/0510256 [hep-ph].

Faessler, A., M. Gonzalez, S. Kovalenko, and F. Simkovic (2014). Arbitrary mass Majorana neutrinos in neutrinoless double beta decay. *Phys.Rev. D90*, 096010, arXiv:1408.6077 [hep-ph].

Feldman, G., J. Hartnell, and T. Kobayashi (2013). Long-baseline neutrino oscillation experiments. *Adv.High Energy Phys. 2013*, 475749, arXiv:1210.1778 [hep-ex].

Feruglio, F. and A. Paris (2011). The Golden Ratio Prediction for the Solar Angle from a Natural Model with A5 Flavour Symmetry. *JHEP 1103*, 101, arXiv:1101.0393 [hep-ph].

Fogli, G., E. Lisi, A. Marrone, A. Palazzo, and A. Rotunno (2008). Hints of $\theta_{13} > 0$ from global neutrino data analysis. *Phys.Rev.Lett. 101*, 141801, arXiv:0806.2649 [hep-ph].

Fong, C. S., E. Nardi, and A. Riotto (2012). Leptogenesis in the Universe. *Adv.High Energy Phys. 2012*, 158303, arXiv:1301.3062 [hep-ph].

Foot, R., M. J. Thomson, and R. Volkas (1996). Large neutrino asymmetries from neutrino oscillations. *Phys.Rev. D53*, 5349–5353, arXiv:hep-ph/9509327 [hep-ph].

Gaisser, T. and F. Halzen (2014). IceCube. *Ann. Rev. Nucl. Part. Sci. 64*, 101–123.

Gandhi, R., C. Quigg, M. H. Reno, and I. Sarcevic (1998). Neutrino interactions at ultrahigh-energies. *Phys.Rev. D58*, 093009, arXiv:hep-ph/9807264 [hep-ph].

Gando, A. et al. (2013a). Limit on Neutrinoless $\beta\beta$ Decay of Xe-136 from the First Phase of KamLAND-Zen and Comparison with the Positive Claim in Ge-76. *Phys.Rev.Lett. 110*(6), 062502, arXiv:1211.3863 [hep-ex].

Gando, A. et al. (2013b). Reactor On-Off Antineutrino Measurement with KamLAND. *Phys.Rev. D88*(3), 033001, arXiv:1303.4667 [hep-ex].

Gariazzo, S., C. Giunti, and M. Laveder (2013). Light Sterile Neutrinos in Cosmology and Short-Baseline Oscillation Experiments. *JHEP 1311*, 211, arXiv:1309.3192 [hep-ph].

Gavela, M., D. Hernandez, T. Ota, and W. Winter (2009). Large gauge invariant non-standard neutrino interactions. *Phys.Rev. D79*, 013007, arXiv:0809.3451 [hep-ph].

Giunti, C. and M. Laveder (2011). Statistical Significance of the Gallium Anomaly. *Phys.Rev. C83*, 065504, arXiv:1006.3244 [hep-ph].

Giunti, C., M. Laveder, Y. Li, and H. Long (2013). Pragmatic View of Short-Baseline Neutrino Oscillations. *Phys.Rev. D88*, 073008, arXiv:1308.5288 [hep-ph].

Giunti, C. and A. Studenikin (2014). Neutrino electromagnetic interactions: a window to new physics. arXiv:1403.6344 [hep-ph].

Giusarma, E., E. Di Valentino, M. Lattanzi, A. Melchiorri, and O. Mena (2014). Relic Neutrinos, thermal axions and cosmology in early 2014. *Phys.Rev. D90*, 043507, arXiv:1403.4852 [astro-ph.CO].

Glashow, S. L. (1960). Resonant Scattering of Antineutrinos. *Phys.Rev. 118*, 316–317.

Gomez-Cadenas, J., J. Martin-Albo, M. Mezzetto, F. Monrabal, and M. Sorel (2012). The Search for neutrinoless double beta decay. *Riv.Nuovo Cim. 35*, 29–98, arXiv:1109.5515 [hep-ex].

Gonzalez-Garcia, M. and M. Maltoni (2013). Determination of matter potential from global analysis of neutrino oscillation data. *JHEP 1309*, 152, arXiv:1307.3092.

Gonzalez-Garcia, M., M. Maltoni, and T. Schwetz (2014). Updated fit to three neutrino mixing: status of leptonic CP violation. *JHEP 1411*, 052, arXiv:1409.5439 [hep-ph], and updates at http://www.nu-fit.org.

Hamann, J., S. Hannestad, G. G. Raffelt, I. Tamborra, and Y. Y. Wong (2010). Cosmology seeking friendship with sterile neutrinos. *Phys.Rev.Lett. 105*, 181301, arXiv:1006.5276 [hep-ph].

Hambye, T. (2012). Leptogenesis: beyond the minimal type I seesaw scenario. *New J.Phys. 14*, 125014, arXiv:1212.2888 [hep-ph].

Haxton, W., R. Hamish Robertson, and A. M. Serenelli (2013). Solar Neutrinos: Status and Prospects. *Ann.Rev.Astron.Astrophys. 51*, 21–61, arXiv:1208.5723 [astro-ph.SR].

Hayes, A., J. Friar, G. Garvey, G. Jungman, and G. Jonkmans (2014). Systematic Uncertainties in the Analysis of the Reactor Neutrino Anomaly. *Phys.Rev.Lett. 112*, 202501, arXiv:1309.4146 [nucl-th].

Heeck, J. and H. Zhang (2013). Exotic Charges, Multicomponent Dark Matter and Light Sterile Neutrinos. *JHEP 1305*, 164, arXiv:1211.0538 [hep-ph].

Hinshaw, G. et al. (2013). Nine-Year Wilkinson Microwave Anisotropy Probe (WMAP) Observations: Cosmological Parameter Results. *Astrophys.J.Suppl. 208*, 19, arXiv:1212.5226 [astro-ph.CO].

Hisano, J., T. Moroi, K. Tobe, and M. Yamaguchi (1996). Lepton flavor violation via right-handed neutrino Yukawa couplings in supersymmetric standard model. *Phys.Rev. D53*, 2442–2459, arXiv:hep-ph/9510309 [hep-ph].

Huber, P. (2011). On the determination of anti-neutrino spectra from nuclear reactors. *Phys.Rev. C84*, 024617, arXiv:1106.0687 [hep-ph].

Ibanez, L. E. and A. M. Uranga (2012). *String theory and particle physics: an introduction to string phenomenology*. Cambridge: Cambridge Univ. Press.

Ishimori, H., T. Kobayashi, H. Ohki, Y. Shimizu, H. Okada, et al. (2010). Non-Abelian Discrete Symmetries in Particle Physics. *Prog.Theor.Phys.Suppl. 183*, 1–163, arXiv:1003.3552 [hep-th].

Kajiyama, Y., M. Raidal, and A. Strumia (2007). The Golden ratio prediction for the solar neutrino mixing. *Phys.Rev. D76*, 117301, arXiv:0705.4559 [hep-ph].

Katz, U. and C. Spiering (2012). High-Energy Neutrino Astrophysics: Status and Perspectives. *Prog.Part.Nucl.Phys. 67*, 651–704, arXiv:1111.0507 [astro-ph.HE].

Kayser, B., J. Kopp, R. H. Roberston, and P. Vogel (2010). On a theory of neutrino oscillations with entanglement. *Phys.Rev. D82*, 093003, arXiv:1006.2372 [hep-ph].

Kearns, E. et al. (2013). Hyper-Kamiokande Physics Opportunities. arXiv:1309.0184 [hep-ex].

King, S. F., A. Merle, S. Morisi, Y. Shimizu, and M. Tanimoto (2014). Neutrino Mass and Mixing: from Theory to Experiment. *New J.Phys. 16*, 045018, arXiv:1402.4271 [hep-ph].

Kopp, J., P. A. N. Machado, M. Maltoni, and T. Schwetz (2013). Sterile Neutrino Oscillations: The Global Picture. *JHEP 1305*, 050, arXiv:1303.3011 [hep-ph].

Krauss, L. M. and S. Tremaine (1988). Test of the Weak Equivalence Principle for Neutrinos and Photons. *Phys.Rev.Lett. 60*, 176.

Kusenko, A. (2009). Sterile neutrinos: The Dark side of the light fermions. *Phys.Rept. 481*, 1–28, arXiv:0906.2968 [hep-ph].

Langacker, P. (2012). Neutrino Masses from the Top Down. *Ann.Rev.Nucl.Part.Sci. 62*, 215–235, arXiv:1112.5992 [hep-ph].

Lasserre, T. (2014). Light Sterile Neutrinos in Particle Physics: Experimental Status. *Phys.Dark Univ. 4*, 81–85, arXiv:1404.7352 [hep-ex].

Lesgourgues, J., G. Mangano, G. Miele, and S. Pastor (2013). *Neutrino cosmology*. Cambridge: Cambridge Univ. Press.

Lesgourgues, J. and S. Pastor (2012). Neutrino mass from Cosmology. *Adv.High Energy Phys. 2012*, 608515, arXiv:1212.6154 [hep-ph].

Long, A. J., C. Lunardini, and E. Sabancilar (2014). Detecting non-relativistic cosmic neutrinos by capture on tritium: phenomenology and physics potential. *JCAP 1408*, 038, arXiv:1405.7654 [hep-ph].

Longo, M. J. (1988). New Precision Tests of the Einstein Equivalence Principle From SN1987A. *Phys.Rev.Lett. 60*, 173.

Lu, X. and H. Murayama (2014). Neutrino Mass Anarchy and the Universe. *JHEP 1408*, 101, arXiv:1405.0547 [hep-ph].

Ludhova, L. and S. Zavatarelli (2013). Studying the Earth with Geoneutrinos. arXiv:1310.3961 [hep-ex].

Ma, E. (2009). Neutrino Mass: Mechanisms and Models. arXiv:0905.0221 [hep-ph].

Mention, G., M. Fechner, T. Lasserre, T. Mueller, D. Lhuillier, et al. (2011). The Reactor Antineutrino Anomaly. *Phys.Rev. D83*, 073006, arXiv:1101.2755 [hep-ex].

Merle, A. (2013). keV Neutrino Model Building. *Int.J.Mod.Phys. D22*, 1330020, arXiv:1302.2625 [hep-ph].

Mirizzi, A., G. Mangano, N. Saviano, E. Borriello, C. Giunti, et al. (2013). The strongest bounds on active-sterile neutrino mixing after Planck data. *Phys.Lett. B726*, 8–14, arXiv:1303.5368 [astro-ph.CO].

Ohlsson, T. (2013). Status of non-standard neutrino interactions. *Rept.Prog.Phys. 76*, 044201, arXiv:1209.2710 [hep-ph].

Olive, K. A. et al. (2014). Review of Particle Physics (RPP). *Chin.Phys. C38*, 090001, http://pdg.lbl.gov.

Palazzo, A. (2013). Phenomenology of light sterile neutrinos: a brief review. *Mod.Phys.Lett. A28*, 1330004, arXiv:1302.1102 [hep-ph].

Qian, X. and W. Wang (2014). Reactor neutrino experiments: θ_{13} and beyond. *Mod.Phys.Lett. A29*, 1430016, arXiv:1405.7217 [hep-ex].

Ramond, P. (2010). *Group theory: a physicist's survey*. Cambridge: Cambridge Univ. Press.

Renshaw, A. et al. (2014). First Indication of Terrestrial Matter Effects on Solar Neutrino Oscillation. *Phys.Rev.Lett. 112*, 091805, arXiv:1312.5176 [hep-ex].

Ringwald, A. (2009). Prospects for the direct detection of the cosmic neutrino background. *Nucl.Phys. A827*, 501C–506C, arXiv:0901.1529 [astro-ph.CO].

Rodejohann, W. (2011). Neutrino-less Double Beta Decay and Particle Physics. *Int.J.Mod.Phys. E20*, 1833–1930, arXiv:1106.1334 [hep-ph].

Sayre, J., S. Wiesenfeldt, and S. Willenbrock (2005). Sterile neutrinos and global symmetries. *Phys.Rev. D72*, 015001, arXiv:hep-ph/0504198 [hep-ph].

Scholberg, K. (2012). Supernova Neutrino Detection. *Ann.Rev.Nucl.Part.Sci. 62*, 81–103, arXiv:1205.6003 [astro-ph.IM].

Sekiya, H. (2013). Solar neutrino analysis of Super-Kamiokande. arXiv:1307.3686.

Steigman, G. (2012). Neutrinos And Big Bang Nucleosynthesis. *Adv.High Energy Phys. 2012*, 268321, arXiv:1208.0032 [hep-ph].

Tegmark, M., A. Vilenkin, and L. Pogosian (2005). Anthropic predictions for neutrino masses. *Phys.Rev. D71*, 103523, arXiv:astro-ph/0304536 [astro-ph].

Turck-Chieze, S. and S. Couvidat (2011). Solar neutrinos, helioseismology and the solar internal dynamics. *Rept.Prog.Phys. 74*, 086901, arXiv:1009.0852 [astro-ph.SR].

Valle, J. W. F. and J. C. Romao (2014). *Neutrinos in high energy and astroparticle physics*. Weinheim: Wiley-VCH.

Vergados, J., H. Ejiri, and F. Simkovic (2012). Theory of Neutrinoless Double Beta Decay. *Rept.Prog.Phys. 75*, 106301, arXiv:1205.0649 [hep-ph].

Vissani, F. (1998). Do experiments suggest a hierarchy problem? *Phys.Rev. D57*, 7027–7030, arXiv:hep-ph/9709409 [hep-ph].

Weinberg, S. (1962). Universal Neutrino Degeneracy. *Phys.Rev. 128*, 1457–1473.

Weinberg, S. (2013). Goldstone Bosons as Fractional Cosmic Neutrinos. *Phys.Rev.Lett. 110*(24), 241301, arXiv:1305.1971 [astro-ph.CO].

Witten, E. (2001). Lepton number and neutrino masses. *Nucl.Phys.Proc.Suppl. 91*, 3–8, arXiv:hep-ph/0006332 [hep-ph].

Wong, Y. Y. (2011). Neutrino mass in cosmology: status and prospects. *Ann.Rev.Nucl.Part.Sci. 61*, 69–98, arXiv:1111.1436 [astro-ph.CO].

Xing, Z.-Z. and S. Zhou (2011). *Neutrinos in particle physics, astronomy, and cosmology*. Advanced topics in science and technology in China. Hangzhou: Zhejiang Univ. Press.

Zhang, C., X. Qian, and P. Vogel (2013). Reactor Antineutrino Anomaly with known θ_{13}. *Phys.Rev. D87*(7), 073018, arXiv:1303.0900 [nucl-ex].

Zuber, K. (2012). *Neutrino physics; 2nd ed.* Series in high energy physics, cosmology, and gravitation. Boca Raton, FL: CRC Press.

CRC PRESS
Boca Raton Ann Arbor London Tokyo

Index

CRC PRESS
Boca Raton Ann Arbor London Tokyo